Mitochondrial protein assemblies:

Biogenesis of the cytochrome *c* oxidase and mitophagic signaling complexes

Dissertation

for the award of the degree "Doctor rerum naturalium"
at the Georg-August-Universität Göttingen
within the doctoral program "Molecular Biology"
of the Georg-August University School of Science (GAUSS)

Submitted by

Mariia Levchenko

from Kyiv, Ukraine

Göttingen, September 2015

Thesis Committee

Prof. Dr. Peter Rehling   Institute of Cellular Biochemistry
(Supervisor and first referee)   Georg-August University
                                      Göttingen, Germany

Prof. Dr. Blanche Schwappach   Institute of Molecular Biology
(Second referee)   Georg-August University
                                      Göttingen, Germany

Prof. Dr. Stefan Jakobs   Department of NanoBiophotonics
                                      Max Planck Institute for Biophysical Chemistry
                                      Göttingen, Germany

Further members of the Examination Board

Dr. Dieter Klopfenstein   Department of Biophysics
                                      Third Institute of Physics
                                      Göttingen, Germany

Prof. Dr. Wilfried Krammer   Department of Molecular Genetics
                                      Institute for Microbiology and Genetics
                                      Göttingen, Germany

PD. Dr. Jörg Stülke   Department of General Microbiology
                                      Institute for Microbiology and Genetics
                                      Göttingen, Germany

Date of oral examination: 02.12.2015

Herewith I declare, that I have prepared this thesis on my own and with no other sources and aids than quoted.

Mariia Levchenko

Göttingen, September 2015

''Science is like sex: sometimes something useful comes out, but that is not the reason we are doing it.''

Richard P. Feynman

Table of contents

List of figures

List of tables

List of abbreviations

AAA+	ATPases associated with a variety of cellular activities
ADP	Adenosine diphosphate
AIM	Atg8 family interacting motif
APS	Ammonium persulfate
ATP	Adenosine triphosphate
AVO	Antimycin A, valinomycin, oligomycin mixture
BLAST	Basic Local Alignment Search Tool
BSA	Bovine serum albumin
CCCP	Carbonyl cyanide m-chlorophenyl hydrazone
CK2	Casein kinase 2
CMA	Chaperone-mediated autophagy
COA	Cytochrome c oxidase assembly intermediate
CoQ	Ubiquinone
COX	Cytochrome c oxidase
CYT	Cytosolic
DAB	Diaminobenzidine
DDM	n-Dodecyl-b-D-maltoside
DMSO	Dimethyl sulfoxide
DTT	1,4-dithiothreitol
EDTA	Ethylene diamine tetraacetic acid
EGTA	Ethylene glycol tetraacetic acid
ER	Endoplasmic reticulum
ERMES	ER-mitochondria tethering complex
ETC	Electron transport chain
$FADH_2$	Flavin adenine dinucleotide
FT	Flow-through
GFP	Green fluorescent protein
GTP	Guanosine triphosphate
H_2DCFDA	2',7'-Dichlorodihydrofluorescein diacetate
HA	Hemagglutinin
HEPES	4-(2-hydroxyethyl)-1-piperazineethanesulfonic acid

HRP	Horseradish peroxidase
IM	Inner mitochondrial membrane
IMS	Intermembrane space
In	Input
IPTG	Isopropyl β-D-1-thiogalactopyranoside
KAN	Kanamycin
kDa	Kilodaltons
LB	Lysogeny broth
LiAc	Lithium acetate
LIR	LC3 interacting region
MAPK	Mitogen-activated protein kinase
MDH	Malate dehydrogenase
MELAS	Mitochondrial encephalomyopathy, lactic acidosis, and stroke-like episodes
MOPS	Morpholinopropanesulfonic acid
MPP	Matrix processing peptidase
mtDNA	Mitochondrial DNA
MWCO	Molecular weight cut-off
NADH	Nicotinamide adenine dinucleotide
NAT	Nourseothricin
OCR	Oxygen consumption rate
OM	Outer mitochondrial membrane
ORF	Open reading frame
OXPHOS	Oxidative phosphorylation
P	Pellet
PAM	Presequence translocase associated motor
PAP	Peroxidase anti-peroxidase antibody
PAS	Phagophore assembly site
PBS	Phosphate buffered saline
PCR	Polymerase chain reaction
PE	Phosphatidylethanolamine
PEG	Polyethylene glycol
PI	Preimmune serum
PI3K	Phosphatidylinositol 3-kinase
PI3P	Phosphatidylinositol 3-phosphate

PK	Proteinase K
PKA	Protein kinase A
PMSF	Phenylmethanesulfonyluoride
PS	Presequence
PVDF	Polyvinylidene fluoride
ROS	Reactive oxygen species
S	Supernatant
SAM	Sorting and assembly machinery
SD-N	Nitrogen starvation medium
SDS	Sodium dodecyl sulfate
SEM	Standard error of the mean
SM	Synthetic medium
T	Total
TBS	Tris buffered saline
TBST	Tris buffered saline with Tween-20
TCA	Trichloroacetic acid
TEMED	Tetramethylethylenediamine
TEV	Tobacco etch virus
TIM23	Presequence translocase of the inner membrane
TM	Transmembrane span
TMD	Transmembrane domain
TOM	Translocase of the outer membrane
TOR	Target of rapamycin
TX-100	Triton X-100
Ub	Ubiquitination.
UTR	Untranslated region
UV	Ultra violet
WT	Wild type
YNB	Yeast nitrogen base without amino acids
YPAD	YPD with adenine
YPD	Yeast extract, peptone, glucose
YPG	Yeast extract, peptone, glycerol
YPL	Yeast extract, peptone, lactate
$\Delta\psi$	Membrane potential across the inner membrane

Abstract

Mitochondrial physiology requires a constant balance between biosynthesis and degradation events. This thesis addresses both mitochondrial biogenesis, exemplified by cytochrome c oxidase assembly, and mitochondrial removal in the course of mitophagy.

The cytochrome c oxidase is the terminal enzyme of the respiratory chain. It assembles in a complicated pathway from nuclear- and mitochondria-encoded subunits. Together with other respiratory chain complexes the cytochrome c oxidase is included into supercomplexes. These oligomeric structures are implicated in efficient electron transfer and increased stability of their constituents.

The first aim of this thesis was to address the role of an uncharacterized protein Cox26 in supercomplex biogenesis. I have identified Cox26 as a novel cytochrome c oxidase subunit that associates with respiratory chain supercomplexes. I discovered that Cox26 is required for efficient formation of supercomplexes and cytochrome c oxidase. Cox26 is expendable for catalytic activity of individual respiratory complexes and mitochondrial respiration.

Abnormal biogenesis of the respiratory chain compromises cellular energy metabolism and leads to mitochondrial damage. Defective mitochondria have to be selectively removed in the course of mitophagy. Mitophagy receptors on mitochondrial surface provide the basis for such selectivity.

Thus, the second goal of my project was to understand how yeast mitophagy receptor Atg32 governs mitochondrial recognition by the mitophagic machinery. I found that Atg32 is included into a mitochondrial complex, which dissociates during mitophagy. Atg32 is subsequently modified and delivered to the vacuole, presumably together with its cargo. Unaltered receptor is digested by an undetermined protease, possibly preventing excessive mitochondrial degradation.

1   Introduction

1.1   Mitochondrial structure and function

Mitochondria are cellular organelles of symbiotic ancestry that constitute a control hub of cellular life, stress and death. They arose through an endosymbiotic event between an α-proteobacterium and a pre-eukaryotic host. The mitochondrial evolutionary origin impacts their structure and physiology (Margulis, 1975; Poole and Gribaldo, 2014).

Mitochondria are divided into four subcompartments, defined by two membranes (outer – OM, and inner – IM) encompassing the organelle. The outer membrane and the intermembrane space (IMS) are host-derived, while the inner membrane and the matrix space are of symbiont origin. The OM contains unselective channels and protein translocation machinery (TOM and SAM complex). Various other organelles, such as the endoplasmic reticulum (ER), the lysosomes, and the peroxisomes form contact sites with the mitochondrial OM required for ion and lipid exchange (Klecker and Westermann, 2014; Klecker et al., 2014; Mattiazzi et al., 2015). The IM is impermeable to ions and metabolites and creates a diffusion barrier, necessary to establish chemical gradients across the membrane. It forms multiple invaginations – cristae, which increase the surface area and result in functional specialization of the membrane (Zerbes et al., 2012).

Mitochondria are crucial for many fundamental processes in eukaryotic cells. They house a number of metabolic pathways, including the citric acid cycle and the β-oxidation system of fatty acids, as well as parts of amino acid, pyrimidine, and lipid biosynthesis pathways. Mitochondria are essential for metal metabolism, specifically for heme and iron-sulfur clusters production (Lill and Mühlenhoff, 2008). In addition, mitochondria play a role in redox regulation, apoptosis, and calcium homeostasis (Venditti et al., 2013; Li and Dewson, 2015; Finkel et al., 2015). However, mitochondria are most noted for their role in cellular energy metabolism. In mammals, the majority of the cellular energy needs are covered by the mitochondrial oxidative phosphorylation (OXPHOS).

1.2   Oxidative phosphorylation and the respiratory chain

OXPHOS involves series of redox reactions, where electron transfer from donors to acceptors is coupled to proton pumping across the inner mitochondrial membrane. The

OXPHOS machinery consists of five protein complexes localized in the IM. Four oxido-reductases constitute the mitochondrial respiratory chain, or electron transport chain (ETC). These include the NADH dehydrogenase (complex I), the succinate dehydrogenase (complex II), the cytochrome c reductase (complex III), and the cytochrome c oxidase (complex IV or COX). Proton pumping by ETC generates the electrochemical gradient, composed of a membrane potential ($\Delta\psi$) and a pH gradient across the inner membrane. This gradient is used by F_1F_o ATP synthase (complex V) for adenosine triphosphate (ATP) synthesis (Mitchell and Moyle, 1968). Reduced equivalents NADH and $FADH_2$ are fed into the ETC through complex I or complex II, respectively. Ubiquinone (CoQ), a lipophilic mobile carrier in the inner mitochondrial membrane, shuttles electrons from both complexes to the cytochrome c reductase. The latter supplies electrons to the cytochrome c oxidase via another electron carrier – cytochrome c, a heme-containing polypeptide. Molecular oxygen, O_2, is the terminal electron acceptor. It becomes reduced by complex IV to form two water molecules. Proton pumping occurs at three of the four ETC complexes, namely complex I, III, and IV (Figure 1).
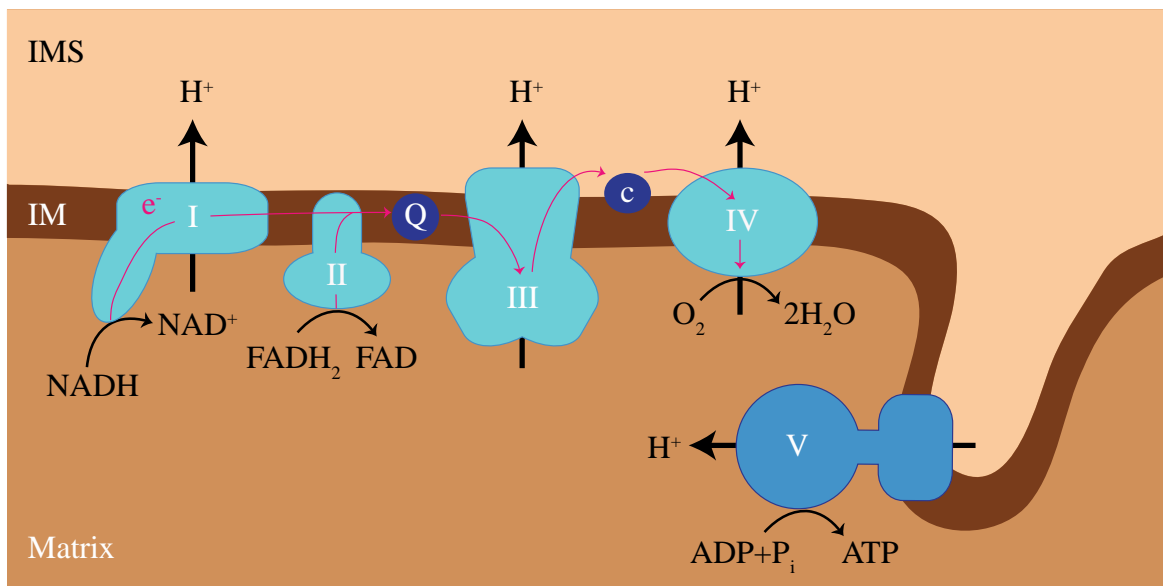
Fig. 1 Schematic representation of the OXPHOS system. Oxidative phosphorylation is carried out by enzyme complexes of the respiratory chain and the F_1F_o ATP synthase. The latter uses the proton gradient generated by complexes I, III, and IV to synthesize ATP. The respiratory chain complexes transfer electrons from NADH and $FADH_2$ to molecular oxygen with the help of mobile electron carriers: ubiquinone (Q), and cytochrome c (c). *S. cerevisiae* lack complex I which is instead represented by three single enzymes. IMS – intermembrane space, IM – inner mitochondrial membrane.

1.3 The respiratory chain is organized in supercomplexes

Evidence for an orderly organization of the respiratory chain came with the isolation of supercomplexes – stable associations of respiratory complexes (Schägger and Pfeiffer, 2000; Cruciat et al., 2000). Supercomplexes are found in bacterial and mitochondrial membranes of many eukaryotic species (Berry and Trumpower, 1985; Schägger and Pfeiffer, 2000; Eubel et al., 2003; Schägger et al., 2004; Stroh et al., 2004).

The respiratory complexes are thought to exist in free and supercomplex-associated states within the mitochondrial membrane and thus can switch between them to accommodate cellular metabolic needs (Schägger and Pfeiffer, 2000; Cruciat et al., 2000; Acin-Perez et al., 2008; Lapuente- Brun et al., 2013). Complex III forms a dimer (III_2) that stably interacts with the complex I in mammalian and plant mitochondria (Schägger and Pfeiffer, 2000; Dudkina et al., 2005). Numerous copies of complex IV associate with the supercomplexes (Figure 2.A), forming a single functional unit termed respirasome (Schägger and Pfeiffer, 2000; Schägger, 2001; Eubel et al., 2004). In *S. cerevisiae* complex I is represented by three single NADH dehydrogenases that lack proton translocation activity (Luttik et al., 1998; Small and McAlister-Henn, 1998; Velazquez and Pardo, 2001). Hence, supercomplexes in yeast consist of a complex III dimer bound to one or two copies of complex IV, noted as III_2IV and III_2IV_2 (Figure 2.B) (Schägger and Pfeiffer, 2000).

A

B
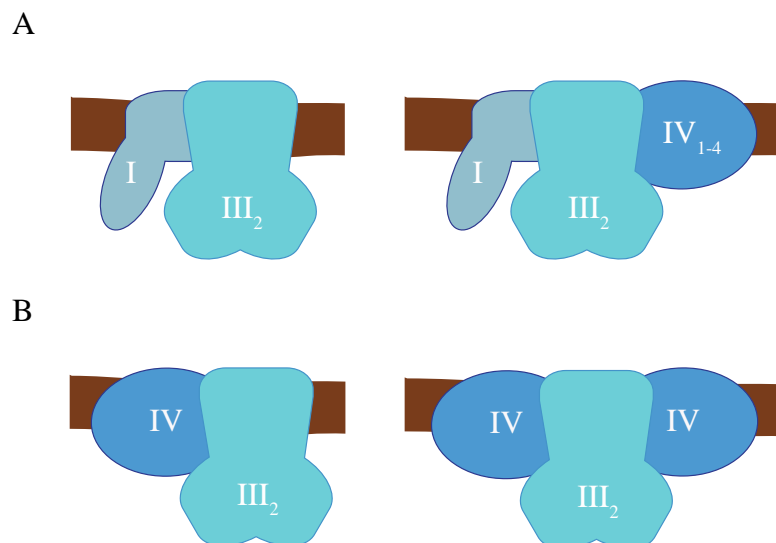
Fig. 2 Models of the respiratory chain supercomplexes. Exemplified supercomplexes of mammalian mitochondria (A), and mitochondria of *S. cerevisiae* (B).

In addition to supercomplexes of the respiratory chain, the F_1F_o ATP synthase forms homo-oligomerizes in the mitochondria (Arnold et al., 1998; Wittig and Schägger, 2008). It exists in both monomeric (V) and dimeric (V_2) forms, with the latter being vital for cristae formation and membrane curvature (Paumard et al., 2002; Zick et al., 2009).

Supercomplex organization of the respiratory chain is thought to fulfill a number of functions in the organelle. Supercomplexes could impact assembly and stability of respiratory complexes, thus providing a regulatory pathway for respiration. It was shown that stability of OXPHOS components is affected by mutations in subunits of other respiratory complexes (Acin-Perez et al., 2004; Diaz et al., 2006; Li et al., 2007). However other studies disprove this notion, as the loss of either complex III or IV in yeast did not alter the levels of the other complex (Schägger and Pfeiffer, 2000). Supercomplexes limit the generation of reactive oxygen species (ROS) due to electron leak from the ETC (Maranzana et al., 2013; Ghelli et al., 2013). Finally, higher organization of the respiratory chain could provide enhanced catalysis due to substrate channeling – direct transfer of the redox intermediate between the active sites of the respiratory enzymes. This hypothesis is supported by increased electron transfer rates of the I-III$_2$ supercomplex compared to the individual complexes, flux control of electron transfer, kinetic properties of isolated supercomplexes, and reduced distances for the mobile electron carriers between the complexes (Boumans et al., 1998; Schägger and Pfeiffer, 2000; Acin-Perez et al., 2008; Lenaz and Genova, 2010; Althoff et al., 2011).

1.4   Biogenesis of the respiratory chain

Components of the respiratory chain are heterogeneous in their genetic origin. Due to their endosymbiotic origin mitochondria contain their own genome (mitochondrial DNA – mtDNA), as well as a full translation system for protein synthesis. Although the majority of genetic information was transferred to the host nucleus in the course of evolution, catalytic subunits of the OXPHOS machinery are commonly encoded by the mtDNA (Adams and Palmer, 2003; Bowles et al., 2007; Wallace, 2007). Thus mitochondria have to cope with an intricate transport pathway that allows delivery of the nuclear-encoded proteins into the organelle. More than 99% of the mitochondrial proteins, along with metabolites and essential factors are imported from the cytosol with the help of specialized translocation machinery (Sickmann et al., 2003; Dudek et al., 2013; Schulz et al., 2015).

Protein targeting to various mitochondrial compartments is achieved due to a variety of sorting signals encoded in the protein sequence.

1.4.1 Import of the nuclear-encoded subunits

The majority of mitochondria-targeted proteins enter the organelle through the translocase of the outer membrane, the TOM complex (Endo and Yamano, 2010). Inner membrane proteins with an N-terminal presequence are imported with the help of the TIM23 complex (Vögtle et al., 2009). The presequence is a positively charged amphipatic α-helix (Heijne, 1986). Presequence-containing proteins without hydrophobic sorting signals are targeted to the matrix. The presence of a sorting signal leads to an import arrest and a lateral release of the polypeptide into the IM (van Loon and Schatz, 1987; Glick et al., 1992). Presequence translocation across the inner membrane requires the membrane potential (Martin et al., 1991). The import of precursors into the matrix is ATP-dependent and is driven by the presequence translocase associated motor – PAM (Figure 3). After import, the presequence is cleaved by the matrix processing peptidase MPP, resulting in precursor maturation (Luciano and Geli, 1996; Vögtle et al., 2009).

1.4.2 Synthesis and insertion of the mitochondria-encoded subunits

Together with tRNAs and rRNAs the mitochondrial genome encodes 13 proteins in human and 8 in the yeast *S. cerevisiae*. Mitochondrial translation occurs on membrane-bound ribosomes to facilitate co-translational protein insertion (Watson, 1972; Vogel et al., 2006; Ott and Herrmann, 2010). Export of the mitochondria-encoded proteins into the inner membrane is mediated by the conserved Oxa1 protein (Figure 3) (Bonnefoy et al., 1994; Altamura et al., 1996; Hell et al., 2001). It promotes IMS export of hydrophilic domains as well as integration of the transmembrane spans into the lipid bilayer (He and Fox, 1997; Hell et al., 1997; 2001). Oxa1 kinetically couples membrane insertion and mitochondrial translation due to its ribosome-binding domain (Szyrach et al., 2003; Jia et al., 2003; 2009; Haque et al., 2010). Two other ribosome-binding proteins of the inner membrane, Mba1 and Mdm38, cooperate with Oxa1 to promote protein export in yeast (Preuss et al., 2001; Ott et al., 2006; Frazier et al., 2006; Lupo et al., 2011).
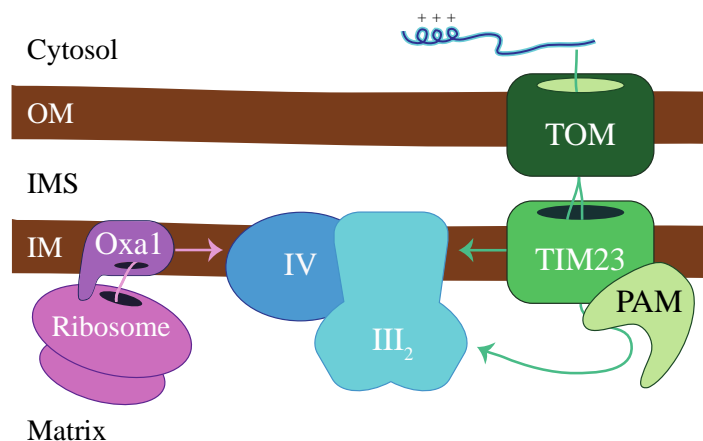
Fig. 3 Biogenesis of respiratory chain components. Precursor proteins synthesized in the cytosol take different import routes depending on their final destination. Translocase of the outer membrane (TOM) is an entry gate for all presequence-containing proteins, which are further passed to the translocase of the inner membrane 23 (TIM23). Later on, precursors are either transported into the matrix with the help of the presequence translocase-associated motor (PAM), or are laterally released into the inner membrane due to a hydrophobic sorting signal present in their sequence. Mitochondria-encoded proteins are inserted by the Oxa1 insertase in a co-translational manner. OM and IM – outer and inner mitochondrial membrane. IMS – intermembrane space.

1.4.3 Assembly of the respiratory chain

Assembly of nuclear- and mitochondria-encoded subunits into the respiratory complexes has to be coordinated with insertion of hemes and cofactors that form the catalytic cores. Specific pathways are required for assembly of each respiratory complex. Within the scope of this thesis I will focus on the assembly of the cytochrome *c* oxidase (COX) – the terminal enzyme of the respiratory chain that transfers electrons from reduced cytochrome *c* to molecular oxygen.

In yeast *S. cerevisiae* mature cytochrome *c* oxidase is composed of 11 subunits, based on homology modeling with bovine COX structure (Tsukihara et al., 1996). Mitochondria-encoded Cox1, Cox2, and Cox3 constitute the catalytic core of the enzyme and are highly conserved in all respiring organisms (Castresana et al., 1994). The Cox1 and Cox2 harbor prosthetic groups necessary for the electron transfer (Tsukihara et al., 1995), while Cox3 is a part of the structural core, possibly involved in modulation of oxygen access, or coordination of proton pumping (Brunori et al., 1987, Riistama et al., 1996; Hosler, 2004). The nuclear-encoded subunits surrounding the core (Cox4, Cox5a/b, Cox6, Cox7, Cox8, Cox9, Cox12, and Cox13 in yeast) are required for the assembly and stability of the enzyme, protection from the ROS and regulation of the catalytic activity (Dowhan et al.,

1985; Wright et al., 1986; Aggeler and Capaldi, 1990; Taanman and Capaldi, 1993; Fontanesi et al., 2006). Additional COX subunits, such as Rcf1 and Rcf2, have recently been described (Vukotic et al., 2012; Strogolova et al., 2012; Chen et al., 2012). COX contains four redox-active centers (two copper centers and two heme a moieties) and several metal ions with yet unknown functions (Tsukihara et al., 1995).

COX assembles in a modular fashion with separate pathways involved in Cox1, Cox2, and Cox3 biogenesis (Figure 4) (McStay et al., 2013). The starting point of assembly is the Cox1 protein (Nijtmans et al., 1998; Tiranti et al., 2000; Stiburek et al., 2005). Cox1 translation requires activator proteins, Pet309 and Mss51, that recognize the 5'-UTR of the COX1 mRNA and promote translation initiation (Decoster et al., 1990; Manthey et al., 1995; Perez-Martinez et al., 2003; Towpik, 2005). After co-translational membrane insertion by Oxa1, Cox1 associates with the assembly factors Cox14 and Coa3, forming an early assembly intermediate – COA complex (Glerum et al., 1995; Barrientos et al., 2004; Mick et al., 2010). This interaction stabilizes Cox1 and prevents its degradation. It also poses a negative regulatory loop on Cox1 translation by Mss51 sequestration (Perez-Martinez et al., 2003; Barrientos et al., 2004; Mick et al., 2007; Perez-Martinez et al., 2009; Mick et al., 2010). As assembly progresses, other factors, such as Coa1 and Shy1, are recruited to the COA, while Mss51 is released (Mick et al., 2007; Pierrel et al., 2007; Mick et al., 2011). Hemes and metal cofactors are incorporated into the catalytic core prior to or together with the first nuclear-encoded subunits, Cox5a and Cox6, both of which form a separate complex (Stiburek et al., 2005). The Cox1-Cox5a-Cox6 intermediate associates with the Cox2 protein after its maturation (Tiranti et al., 2000). In yeast, Cox2 is synthesized as a precursor (pCox2) that has to be processed and metallated after Oxa1-mediated export (Schneider et al., 1991; Nunnari et al., 1993; Herrmann et al., 1995; Rentzsch et al., 1999; Jan et al., 2000). During pCox2 maturation it is chaperoned by Cox20 protein that keeps it in assembly-competent state (Hell et al., 2000; Preuss et al., 2001). Cox2 binding to the Cox1-Cox5a-Cox6 intermediate occurs prior to, or directly after the addition of the Cox3 subunit (Horan et al., 2005). Cox3 assembly progresses through several intermediates possibly involving Cox4, Cox7 and Cox13 (Su et al., 2013). Cox7 was reported to form a complex with Cox8 and Cox9 prior to their incorporation into the holoenzyme (Church et al., 2005). Cox12 and Cox13 are the last structural subunits that join the assembly (LaMarche et al., 1992; Taanman and Capaldi, 1993; Vukotic et al., 2012). Cox13 assembly additionally requires Rcf1 (Vukotic et al., 2012).
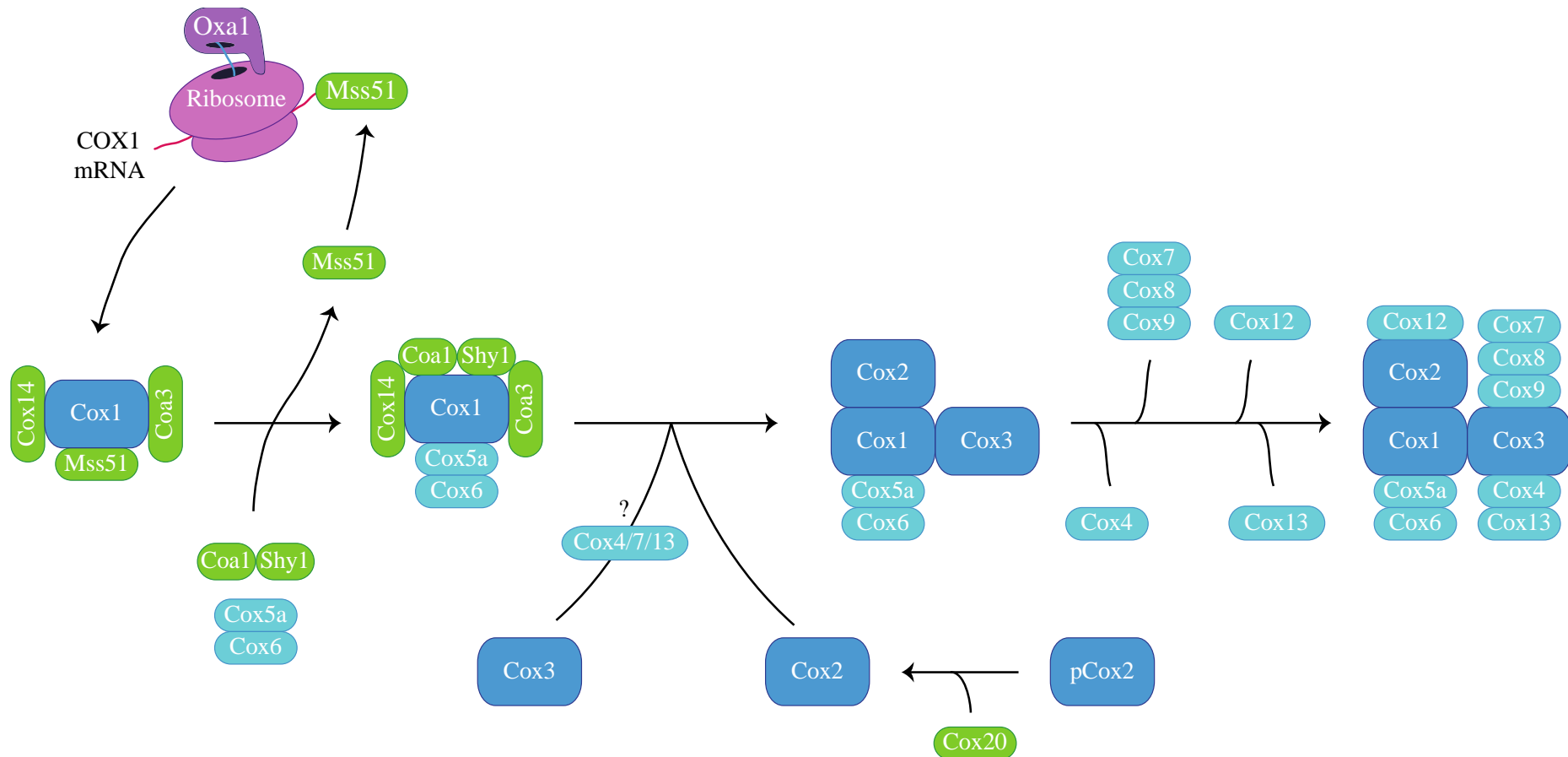
Fig. 4 Assembly line of the cytochrome *c* oxidase in *S. cerevisiae*. The mature enzyme assembles from three modules, each containing a mitochondria-encoded subunit (Cox1, Cox2 and Cox3, deep blue), with nuclear-encoded subunits (shown in light blue) joining in a linear fashion. Formation of the cytochrome *c* oxidase (COX) requires specific assembly factors (depicted in green) that are involved in several essential processes, such as translation, processing and membrane insertion of the COX subunits, as well as synthesis and incorporation of cofactors.

1.5   The respiratory chain defects lead to mitochondrial disorders

OXPHOS biogenesis has to be precisely regulated, since inefficient respiratory chain formation can compromise energy metabolism in the cell. Mitochondrial dysfunction is implicated in various metabolic disorders, cancer, and neurodegenerative diseases, as well as in the aging process (Johannsen and Ravussin, 2009). It primarily affects high energy-demand tissues, such as skeletal muscle, heart, liver and brain.

Genetic alterations in both nuclear and mitochondrial genomes can contribute to mitochondrial pathology (Area-Gomez and Schon, 2014). About 15% of disease-related mutations reside in the mtDNA, resulting in maternally inherited syndromes, such as MELAS – mitochondrial encephalomyopathy, lactic acidosis, and stroke-like episodes (Pavlakis et al., 1984; DiMauro and Davidzon, 2005; Davis and Sue, 2011). A mitochondrial theory of ageing suggests age-dependent accumulation of somatic mtDNA mutations to cause respiratory chain defects, impaired ATP synthesis, and decline in cellular energy metabolism (Harman, 1972; Barja, 2014). A vast number of mitochondrial disorders originate from mutations in genes coding for assembly factors of the OXPHOS system (Diaz et al., 2011). Leigh syndrome, an infantile subacute necrotizing encephalomyopathy, is caused by defective OXPHOS system, as a result of mutations in COX assembly factors (Tiranti et al., 1998; Zhu et al., 1998; Pequignot et al., 2001; Zhang et al., 2007a). Additionally, defects in protein import, organellar dynamics, apoptosis, or mitochondrial metabolism can lead to mitochondrial pathologies (DiMauro and Schon, 2008).

Mitochondrial dysfunction poses yet another danger. The lack of functional respiratory chain complexes, and COX in particular, leads to accumulation of high-energy electrons, resulting in elevated ROS levels. The assembly intermediates themselves can catalyze ROS production due to extremely reactive heme moieties, as well as active metal centers (Khalimonchuk et al., 2007). ROS can damage multiple macromolecules in the cell including DNA, proteins and lipids. To prevent increased ROS formation, the protein synthesis and the heme biogenesis are tightly regulated, while the unassembled ETC subunits are rapidly degraded (Forsburg and Guarente, 1989; Barros and Tzagoloff, 2002; Tatsuta and Langer, 2008). Mitochondrial ROS levels can also be modulated by various

antioxidants, as well as uncoupling proteins, which mediate proton leakage (Venditti et al., 2013). However, if the organelle becomes damaged, additional mechanisms are required to maintain a healthy mitochondrial population.

1.6 Mitochondrial quality control

Cells exploit a number of quality control systems to prevent mitochondrial malfunction. The cytosolic proteasomal system together with mitochondrial proteases constitutes the first line of cellular defense. The proteasome degrades mistargeted mitochondrial proteins (Radke et al., 2008; Livnat-Levanon and Glickman, 2011), as well as damaged proteins of the outer mitochondrial membrane (Karbowski and Youle, 2011). Mitochondrial proteases, such as Lon and AAA+ family proteases (ATPases associated with a variety of cellular activities), fulfill a number of different functions. Besides their conventional role in the degradation of oxidized and misfolded mitochondrial proteins, they also degrade non-assembled complex subunits and act as processing peptidases, which control protein stability (Quiros et al., 2015).

In addition to the proteolytic protein removal, mitochondrial fission and fusion contributes to the quality control. Mitochondria in the cell are integrated into a dynamic functional reticulum that is governed by dynamin-like GTPases in the mitochondrial inner and outer membrane (Lackner, 2014). Intact mitochondrial dynamics is crucial for health and development, as mice knockouts of fusion and fission factors are embryonic lethal, and mutations in these factors lead to a number of human disorders (Chan, 2012). Fission and fusion ensure non-random segregation of malfunctioning mitochondria during cell division, facilitating their retention or removal from the mother cell (Vevea et al., 2014). Fusion allows mitochondrial content mixing to complement pathogenic mtDNA mutations (Gilkerson et al., 2008), while fission enables the discrimination and removal of damaged organelles (Sathananthan and Trounson, 2000).

However, membrane potential loss resulting from severe mitochondrial damage impairs mitochondrial fusion. Ongoing fission events then lead to fragmentation of the mitochondrial network (Ishihara et al., 2003). This is an important prerequisite for the mitochondria-specific form of autophagy, termed mitophagy, which represents another form of mitochondrial quality control. During mitophagy, fragmented mitochondria are

sequestered into autophagosomal vesicles and transported to the lysosome for degradation (Wei et al., 2015).

Finally, if all previous steps of quality control fail, stressed cells undergo apoptosis. The apoptosis is a programmed cell death pathway, carried out by specific cysteine proteases, or caspases (Kerr et al., 1972; Thornberry, 1997). Mitochondria are central players in apoptotic signaling and execution (Li and Dewson, 2015). Apoptotic stimuli result in a pore formation at the mitochondrial membranes, governed by the pro- and anti-apoptotic Bcl-2 family proteins. This in turn allows release of pro-apoptotic proteins, such as cytochrome *c*, into the cytosol to promote caspase activation (Jurgensmeier et al., 1998; Narita et al., 1998; Shimizu et al., 1998; Cory and Adams 2002).

1.7 Mitophagy mechanisms

Among different mitochondrial quality control systems, mitophagy represents a bulk degradation pathway, capable of clearing entire organelles rather than a subset of proteins.

Mitophagy is a selective form of autophagy, an evolutionarily conserved cellular degradation pathway. Autophagy occurs ubiquitously in eukaryotic cells and is implicated in various processes, such as cellular development and differentiation, innate and adaptive immunity, cancer and aging (Mizushima, 2005). Autophagy combines different pathways for lysosomal degradation of cytosolic substrates and organelles. A bulk, non-specific autophagy is a typical cell response to nutrient starvation (Takeshige et al., 1992). On the contrary, selective autophagy clears superfluous or damaged organelles, as in the case of mitochondrial (mitophagy) or peroxisomal (pexophagy) degradation. Selective autophagy utilizes the core autophagic machinery for packaging and delivery of the cargo, together with specific receptors necessary for substrate recognition (Johansen and Lamark, 2011; Suzuki, 2013). Genetic screens for defects in autophagy pathway in the yeast *Saccharomyces cerevisiae* have identified more than 30 autophagy-related (ATG) genes (Tsukada and Ohsumi, 1993; Thumm et al., 1994; Klionsky et al., 2003).

1.7.1 Autophagic machinery

There are three major classes of autophagy: chaperone-mediated autophagy (CMA), micro- and macroautophagy (Nakatogawa et al., 2009). The CMA involves chaperone-mediated translocation of various substrates across the lysosomal membrane for degradation (Kon

and Cuervo, 2010). During microautophagy, portions of the cytoplasm are directly engulfed by invaginations of the lysosomal membrane (Li et al., 2012). Macroautophagy (further referred to as autophagy) is the most prominent autophagy type, involving generation of double membrane vesicles − autophagosomes, which deliver their cargo to the lysosomes (Klionsky and Codogno, 2013).

Autophagy starts with the formation of a phagophore, an isolation membrane that surrounds a portion of the cytoplasm, or an organelle. The phagophore is produced at a specific position in the cell, termed phagophore assembly site (PAS), which serves as a recruitment platform for autophagy components. The phagophore expands and fuses to generate an autophagosomal vesicle. Autophagosomes are targeted to the lysosome or vacuole, where hydrolytic degradation takes place (Figure 5) (Mizushima et al., 2011).

Nutrient starvation, especially in the form of amino acid depletion, is a prominent inducer of autophagy. Under nutrient-rich conditions TOR (target of rapamycin) kinase represses autophagy in yeast and mammals by phosphorylating components of the Atg1 kinase complex (Noda and Ohsumi, 1998; Kamada et al., 2000). The Atg1 complex is a starting point of autophagic signaling. It consists of the Atg1 kinase and its regulatory subunit Atg13, together with other accessory proteins (Matsuura et al., 1997; Straub et al., 1997; Funakoshi et al., 1997; Kabeya et al., 2005). TOR prevents Atg13 from binding Atg1, and starvation removes this restriction (Kamada et al., 2000). Additionally, a TOR inhibitor rapamycin can be used to induce autophagy in the absence of starvation (Heitman et al., 1991). The Atg1 complex acts as a scaffold for assembly of downstream components and is required for activation of the phosphatidylinositol 3-kinase (PI3K) complex (Abeliovich et al., 2003; Cheong et al., 2008). The PI3K complex is directed to the PAS by Atg14, where it generates phosphatidylinositol 3-phosphate (PI3P). PI3P serves as a recruitment platform for the PI3P-binding proteins implicated in membrane trafficking and phagophore expansion (Kametaka et al., 1998; Kihara et al., 2001; Obara et al., 2006; Krick et al., 2008; Vergne and Deretic, 2010; Burman and Ktistakis, 2010).
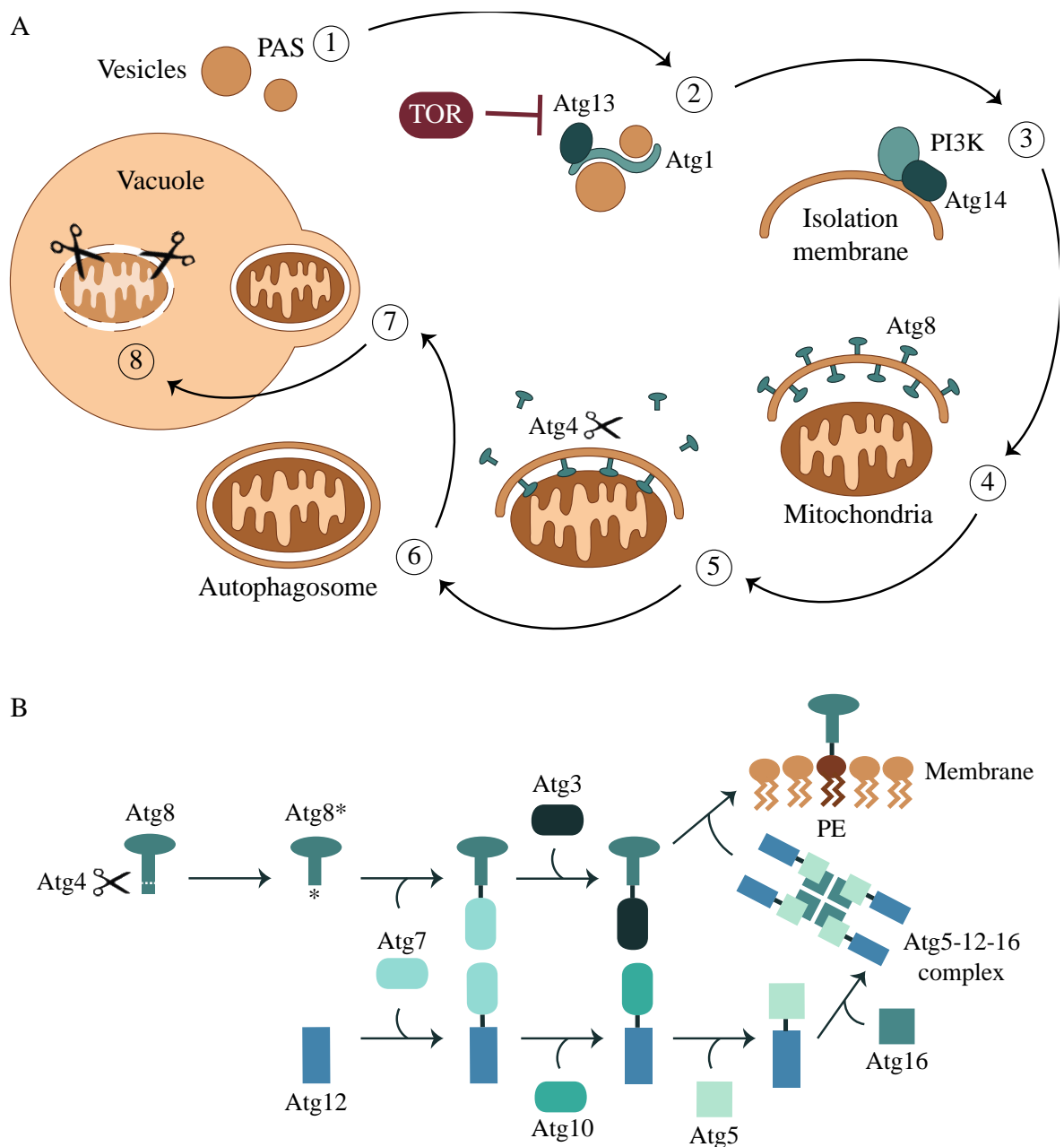
Fig. 5 Summary of the cellular autophagic process. Morphological steps **(A)** and Atg8-conjugation **(B)** are shown schematically and are summarized in the text. Atg8* depicts activated Atg8 after its cleavage by Atg4 protease. PAS – pre-autophagosomal structure, TOR – target of rapamycin, PI3K – phosphatidylinositol 3-kinase, PE - phosphatidylethanolamine. Numbers indicate different steps of the process.

Two ubiquitin-like conjugation systems take part in membrane elongation and determine its curvature (Nakatogawa et al., 2013). Atg12 is covalently linked to a target protein, Atg5, by the action of Atg7 and Atg10. The Atg12-Atg5 conjugate forms an oligomeric complex with Atg16. This new complex then promotes the lipidation of Atg8 (homolog of mammalian LC3) in a second ubiquitin-like reaction (Mizushima et al., 1998; Mizushima et al., 1999; Kuma et al., 2002; Hanada et al., 2007; Noda et al., 2013; Sakoh-Nakatogawa

et al., 2013). Atg8 is first processed by the Atg4 protease, activated by Atg7 and conjugated by Atg3 to phosphatidylethanolamine (PE) on the autophagosomal membrane (Kirisako et al., 2000; Ichimura et al., 2000; Kim et al., 2001). Lipidated Atg8 is required for cargo recognition during selective autophagy and determines the size of the autophagosomal vesicle (Noda et al., 2008; Xie et al., 2008; Knorr et al., 2012; Knorr et al., 2014). After autophagosome completion, Atg8 is removed from the outer surface of the autophagosome by a second Atg4 cleavage. This process appears to be important for disassembly of the autophagic machinery and subsequent fusion with the lysosome (Kirisako et al., 2000; Nakatogawa et al., 2007). Once in the lysosome, the autophagosomal membrane must be lysed by the Atg15 lipase, and the cargo is degraded by various hydrolases (Teter et al., 2001; Epple et al., 2001).

1.7.2 Mitophagy in human

Mitophagy can eliminate both malfunctioning and healthy mitochondria, the latter being important for mitochondria removal during development and differentiation (Ney, 2015). A central role in the damage-induced mitophagy has been assigned to the PINK1 and Parkin proteins. Mutations in both genes are linked to the autosomal recessive forms of Parkinson's disease, leading to the accumulation of defective mitochondria and death of dopaminergic neurons in the substantia nigra (Kitada et al., 1998; Valente et al., 2004).

PINK1 is a mitochondrial protein kinase, which is imported in a membrane potential ($\Delta\psi$)-dependent manner and cleaved by PARL protease, resulting in PINK1 degradation (Silvestri et al., 2005; Jin et al. 2010; Deas et al., 2011; Meissner et al., 2011; Yamano and Youle, 2013). Mitochondrial depolarization inhibits PINK1 import and leads to PINK1 accumulation on the outer mitochondrial membrane (Narendra et al. 2010). Stabilized PINK1 recruits Parkin to the mitochondria (Narendra et al. 2008; Narendra et al. 2010). Parkin is a cytosolic ubiquitin ligase that exists in an auto-inhibited form (Caulfield et al., 2015). PINK1 phosphorylates Parkin, leading to its activation and ubiquitination of target proteins on the OM (Kondapalli et al., 2012; Sarraf et al., 2013). Depending on the linkage of the attached ubiquitin chain, Parkin substrates are either degraded by the proteasome, or serve to recruit autophagic adaptor proteins, such as p62 (Geisler et al., 2010; Chan et al., 2011; Ordureau et al., 2014; Cunningham et al., 2015). These adaptors interact with the LC3 protein on the autophagosomal surface, thereby docking mitochondria at the autophagosome (Figure 6) (Geisler et al., 2010; Okatsu et al., 2010).
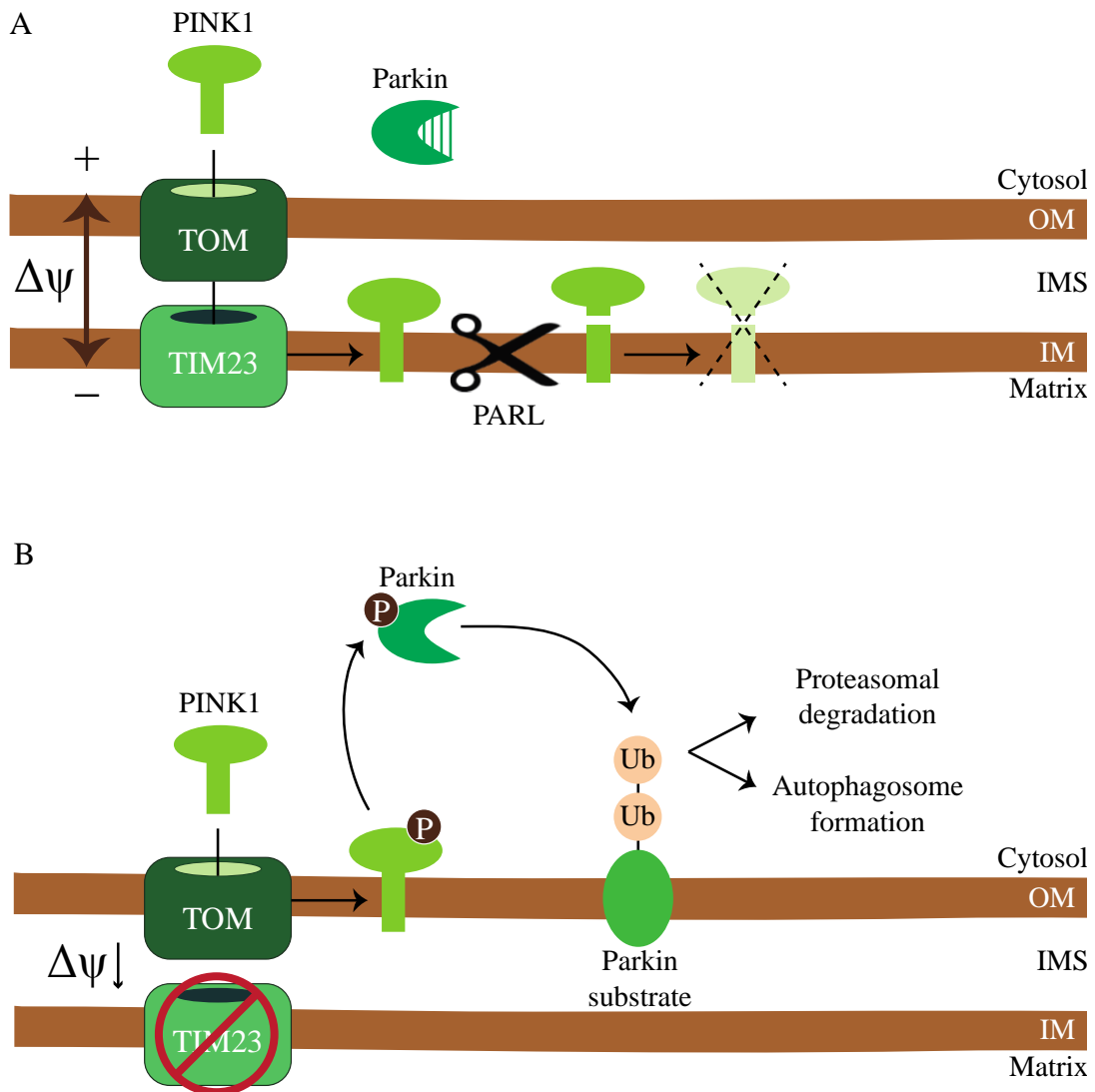
Fig. 6 Mechanism of PINK-Parkin mediated mitophagy. (A) Under physiological conditions PINK1 kinase is imported into the mitochondria by the TIM23 complex, cleaved by PARL protease and subsequently degraded. Ubiquitin ligase Parkin remains in the cytosol in an auto-inhibited form. **(B)** If the membrane potential is decreased import of PINK1 via the TIM23 complex is blocked and PINK1 accumulates on the outer mitochondrial membrane, leading to its auto-phosphorylation and Parkin recruitment. Parkin is phosphorylated by PINK, leading to its activation. Active Parkin promotes ubiquitination of various substrates, resulting in their degradation or recruitment of autophagic adaptors, necessary for the autophagosome formation. OM – outer mitochondrial membrane, IMS – intermembrane space, IM – inner mitochondrial membrane, $\Delta\psi$ – membrane potential, P – phosphorylation, Ub – ubiquitination.

In contrast to the damage-induced mitophagy, programmed mitophagy eliminates healthy mitochondria during development and cell differentiation. Nix, a protein of the outer mitochondrial membrane, is a mitophagy receptor involved in reticulocyte maturation (Schweers et al., 2007; Zhang et al., 2008; Novak et al., 2010). Notably, NIX can also stimulate mitophagy upon membrane depolarization, providing an alternative mitophagic

16

pathway (Ding et al., 2010). The Nix homolog, Bnip3 protein, was shown to mediate mitophagy in hypoxic cells by disrupting the interaction between an autophagy inductor Beclin 1 and its inhibitor, Bcl-2 (Bellot et al., 2009). FUNDC1 is another mitochondrial receptor for hypoxia-induced mitophagy (Liu et al., 2012).

1.7.3 Mitophagy in yeast *Saccharomyces cerevisiae*

In *S. cerevisiae* mitophagy serves various purposes, including quality control, steady-state turnover, and adaptation to environmental changes. Damage-induced mitophagy can be triggered by defects in mitochondrial protein turnover, F_1F_o ATP synthase assembly, K^+/Na^+ exchange, or mtDNA replication (Campbell and Thorsness, 1998; Priault et al., 2005; Nowikovsky et al., 2007; Zhang et al. 2007b). In contrast to the mammalian systems, dissipation of the mitochondrial membrane potential ($\Delta\psi$) by carbonyl cyanide *m*-chlorophenyl hydrazone (CCCP) does not result in mitophagy in yeast (Kissova et al., 2004; Kanki et al., 2009a; Mendl et al., 2011).

Yeast growth on non-fermentable carbon sources results in mitochondrial proliferation. Surplus mitochondria are subsequently recycled by mitophagy either during stationary phase or upon nitrogen starvation (Kissova et al., 2004; Tal et al., 2007; Kanki and Klionsky, 2008; Kanki et al., 2009a; Okamoto et al., 2009; Mendl et al., 2011). Mitochondrial turnover in aged or starved yeast cells can provide necessary nutrients and decrease deleterious ROS production. Impaired mitochondrial degradation during stationary phase leads to oxidative damage and decreased cell viability (Tal et al., 2007; Journo et al., 2009). Similarly, if mitophagy is restrained during starvation, non-degraded mitochondria produce excess ROS, leading to mitochondrial damage and loss of mtDNA (Suzuki et al., 2011; Kurihara et al., 2012). In the case of starvation reduced amino acid pool results in lower expression of the ROS scavenger proteins and subsequent mitochondrial damage. Accordingly, N-acetylcysteine treatment increases glutathione levels and prevents starvation-induced mitophagy (Deffieu et al., 2009; Kissova and Camougrand, 2009).

Mitochondria appear to regulate their own mitophagic degradation. For instance, respiratory deficiency due to mtDNA loss or inhibition of respiratory chain components can compromise autophagy during nitrogen starvation (Graef and Nunnari, 2011). On the other hand, mitophagy requires functional mitochondrial dynamics. Changes in organellar

morphology, caused by impaired mitochondrial bioenergetics, can help to distinguish defective organelles and ensure their selective removal. For example, reduced ATP levels in the matrix affect processing of the mitochondrial fusion factor Mgm1, resulting in mitochondrial fragmentation (Herlan et al., 2004). The role of mitochondrial fission in mitophagy remains controversial. Fission could provide a segregation mechanism to separate damaged components from the healthy mitochondrial network. Accordingly, mitochondrial fission factor Dnm1 was identified as a positive mitophagy regulator (Nowikovsky et al., 2007; Kanki et al., 2009a; Mao et al., 2013; Bernhardt et al., 2015). However, according to several studies, deletion of fission machinery components does not affect mitophagy (Okamoto et al., 2009; Mendl et al., 2011). Finally, efficient mitophagy requires a contact between mitochondria and the ER via the ER-mitochondria tethering complex (ERMES). The absence of ER-mitochondrial junctions leads to the accumulation of immature mitophagosomes due to disrupted lipid exchange between the organelles. The expression of artificial membrane tethers rescues mitophagy defects in cells lacking ERMES complexes (Böckler and Westermann, 2014).

Post-translational protein modifications, including protein phosphorylation, are implicated in mitophagy regulation. A stress response factor Whi2 controls mitochondrial degradation by modulating protein kinase A (PKA) signaling pathway (Mendl et al., 2011). Furthermore, two mitogen-activated protein kinases (MAPK), Slt2 and Hog1, are involved in mitophagy. Hog1 together with its upstream kinase Pbs2 affects phosphorylation of the yeast mitophagy receptor Atg32 (Aoki et al., 2011). In Slt2-deficient cells mitochondrial recruitment to the PAS is disturbed (Mao et al., 2011). Moreover, mitochondrial protein phosphatase Aup1, localized in the intermembrane space, is important for stationary phase mitophagy (Tal et al., 2007). Aup1 regulates mitophagy by coordinating the retrograde signaling pathway, a cellular mechanism that couples mitochondrial stress to changes in nuclear gene expression (Journo et al., 2009).

Recently it was shown that ubiquitination plays a role in mitophagy regulation in yeast. The Ubp3-Bre5 deubiquitination complex was found to inhibit mitophagy while promoting other types of autophagy. During mitophagy Ubp3-Bre5 complex components dynamically translocate from the cytosol to mitochondria and in their absence mitophagy rate is drastically increased (Baxter et al., 2005; Kraft et al., 2008; Müller et al., 2015).

1.7.4 Yeast mitophagy receptors

Mitochondrial association with the autophagic machinery requires the presence of mitophagy receptors on the mitochondrial surface. The mitochondrial outer membrane protein Uth1 was shown to function in starvation-induced mitochondrial removal (Kissova et al., 2004). This gene was not found in screens for mitophagy components, and another study proved Uth1 to be fully dispensable for mitophagy (Kanki et al., 2009a; Okamoto et al., 2009; Welter et al., 2013). Mitochondrial removal in stationary phase requires Atg33, a mitochondrial outer membrane protein found by a genetic screen for yeast mutants defective in mitophagy (Kanki et al., 2009a). Recently, Atg32 was identified as a mitophagy receptor in yeast, essential for all modes of mitophagy induction (Kanki et al., 2009b; Okamoto et al., 2009).

Atg32 is a 59-kDa protein of the outer mitochondrial membrane. It contains a single transmembrane domain with its N- and C-termini in the cytosol and the intermembrane space (IMS) respectively (Kanki et al., 2009b; Okamoto et al., 2009). During initial steps of mitophagy Atg32 interacts with Atg11, an adaptor protein for selective autophagy (Kanki et al., 2009b; Suzuki, 2013). The Atg32-Atg11 complex recruits Dnm1 to mitochondria undergoing mitophagy, thereby promoting mitochondrial fission (Mao et al., 2013). Atg11 then transports its cargo to the PAS, where Atg32 binds the autophagosome component Atg8 (Kanki et al., 2009b; Okamoto et al., 2009). This interaction ensures mitochondrial docking at the autophagosome, and destines the mitochondria for degradation. Atg32 is then recruited to the vacuole along with the mitochondria, and is subsequently degraded in mitophagy-dependent and independent manner (Figure 7) (Okamoto et al., 2009; Kanki et al., 2009b).

Interaction of Atg32 with both Atg8 and Atg11 is significantly increased during mitophagy, although it does not depend on other autophagy components (Kondo-Okamoto et al., 2012). Atg11 binding requires a SSD/EXSEE/DE motif, conserved among yeast homologs of Atg32 (Aoki et al., 2011; Kondo-Okamoto et al., 2012). Atg32 interaction with Atg8 requires a conserved WXXL consensus sequence, termed Atg8 family interacting motif (AIM) in yeast or LC3 interacting region (LIR) in mammals. Mutations in this region reduce Atg32 binding to Atg8, resulting in mitophagy defect (Okamoto et al., 2009; Kondo-Okamoto et al., 2012).
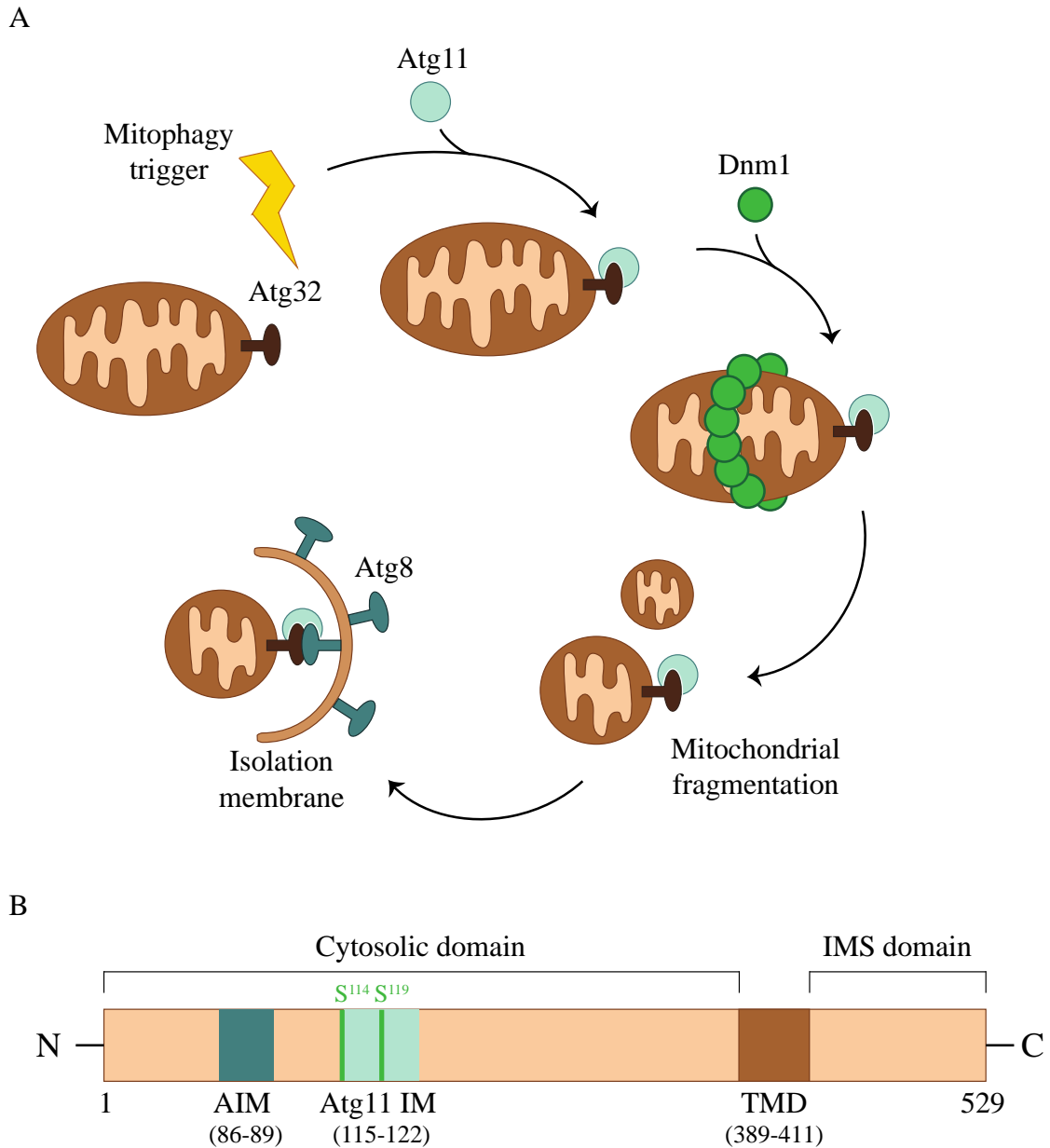
Fig. 7 Atg32 as a yeast mitophagy receptor. (A) Mechanism of Atg32-mediated mitophagy. Atg32 is modified in response to a mitophagy trigger and can subsequently recruit Atg11, adaptor protein for selective autophagy. Atg32-Atg11 complex promotes mitochondrial fragmentation through its interaction with fission factor Dnm1. Both Atg32 and Atg11 interact with Atg8 tethered to the isolation membrane, thus docking mitochondria at the autophagosome. **(B)** Schematic representation of the Atg32 domain structure. AIM – Atg8 interacting motif, Atg11 IM – Atg11 interacting motif, TMD – transmembrane domain. Numbers indicate amino acid residues.

Post-translational modifications regulate Atg32-mediated mitophagy. The cytosolic domain of Atg32 is phosphorylated on two serine residues, Ser[114] and Ser[119], by Casein kinase 2 (CK2) upon mitophagy induction (Aoki et al., 2011; Kanki et al., 2013). Ser[114] phosphorylation stabilizes the Atg32-Atg11 interaction, thus promoting mitophagy, however it is dispensable for Atg8 binding (Aoki et al., 2011). In addition, proteolytic

processing of the C-terminus of Atg32 by mitochondrial Yme1 protease enhances the interaction between Atg32 and Atg11. C-terminal tagging blocks Atg32 cleavage and hinders mitochondrial degradation, suggesting that the IMS domain of Atg32 negatively regulates mitophagy (Wang et al., 2013).

Recently, Bcl-2-like protein 13 (Bcl2-L-13) has been identified as an Atg32 homolog in mammals. Bcl2-L-13 is expressed in all tissues and localizes to mitochondria. It contains two WXXL motifs for LC3 (Atg8 homolog) binding. Bcl2-L-13 induces mitochondrial fragmentation and mitophagy in mammalian cells independent from Parkin, and can trigger mitophagy in Atg32-deficient yeast cells (Murakawa et al., 2015).

1.8   Project aims

Mitochondria are complex organelles that are constantly recycled by the cell in response to environmental changes. Diverse protein machineries orchestrate mitochondrial biogenesis and degradation. Often formation of mitochondrial protein complexes is interconnected, as can be illustrated by the respiratory chain biogenesis. Complexes of the electron transport chain together form higher oligomeric structures, known as respirasomes or supercomplexes. These supramolecular assemblies are important for efficient electron transfer, decreased ROS production, and stabilization of individual complexes. In the last years several new supercomplex-associated factors were described in yeast *Saccharomyces cerevisiae*. For example, a novel protein termed Cox26 was specifically co-purified with supercomplexes. However, its physiological function with regard to mitochondrial respiration was not addressed. Hence, the first aim of this study was to determine Cox26 role by biochemical and functional analysis of this protein, as well as by characterization of its deletion mutant.

Notably, improper biogenesis of the respiratory chain can lead to higher ROS load and thus to increased mitochondrial damage. Malfunctioning mitochondria need to be removed from the healthy network by mitophagy to maintain cellular homeostasis. Nonetheless, the mechanism that provides selective recognition of damaged mitochondria is not well understood. Mitophagy requires a specific receptor on the mitochondrial surface, which interacts with the components of the autophagic machinery. In yeast, Atg32 protein was identified as mitophagy receptor. It is plausible that mitophagy triggers formation of mitochondrial receptor signaling complexes. Therefore, this project aimed to determine Atg32 interaction profile and to assess its alterations upon various mitophagy-inducing conditions. Identification of the novel players in the mitophagic signaling cascade would provide insights into general mechanisms of mitophagy regulation, and allow better understanding of how mitophagic stimuli are sensed and transduced by the mitochondrial mitophagy receptor.

2 Materials and Methods

2.1 Materials

2.1.1 Chemicals and manufacturers

Laboratory equipment, kit systems, and common and specific reagents used in this study were purchased from the companies listed in the Table 1. List of chemicals is given in the Table 2.

Table 1 Companies information.

Company name	City	Country
Adobe Systems	San Jose	USA
Affymetrix	Santa Clara	USA
Agfa	Mortsel	Belgium
AppliChem	Darmstadt	Germany
Applied Precision	Issaquah	USA
Avestin	Mannheim	Germany
BD	New Jersey	USA
Beckman Coulter	Pasadena	USA
Bio-Rad	München	Germany
BioChemica	Billingham	UK
Biomatters Ltd	Auckland	New Zealand
Biometra	Göttingen	Germany
Calbiochem	Darmstadt	Germany
Dianova	Hamburg	Germany
Eppendorf	Hamburg	Germany
Epson	Suwa	Japan
Fermentas	Waltham	USA
Fluka	Taufkirchen	Germany
Foma Bohemia	Hradec Kralove	Czech Republic
FujiFilm	Tokyo	Japan

GE Healthcare	Buckinghamshire	UK
Greiner Bio-One	Solingen	Germany
Gilson	Limburg an der Lahn	Germany
Grano Vita	Radolfzell	Germany
Hartmann Analytic	Braunschweig	Germany
Heat Systems-Ultrasonics	Billingham	UK
Heidolph	Schwabach	Germany
Heinemann Labortechnik	Duderstadt	Germany
Hitachi High Technologies	Tokyo	Japan
Invitrogen	Waltham	USA
LABalance	New Jersey	USA
LC Laboratories	Woburn	USA
Life Technologies	Carlsbad	USA
Merck	Darmstadt	Germany
Metabion	Martinsried	Germany
Millipore	Darmstadt	Germany
MoBiTec	Göttingen	Germany
MP Biomedicals	Eschwege	Germany
Nacalai Tesque	Kyoto	Japan
New Brunswick Scientific	Hamburg	Germany
Novagen	Darmstadt	Germany
OROBOROS Instruments	Innsbruck	Austria
PAA	Buckinghamshire	UK
PEQLAB Biotechnologie	Erlangen	Germany
Promega	Manheim	Germany
Qiagen	Venlo	Netherlands
Retsch	Haan	Germany
Roche	Manheim	Germany
Roth	Karlsruhe	Germany
Sarstedt	Nümbrecht	Germany
Sartorius AG	Göttingen	Germany
Scientific Industries	New York	USA

Scie-Plas	Holliston	USA
Seqlab	Göttingen	Germany
Serva	Heidelberg	Germany
Sigma-Aldrich	Taufkirchen	Germany
Stratagene	Santa Clara	USA
Systec	Lohfelden	Germany
Thermo Scientific	Waltham	USA
Varian	Palo Alto	USA
Werner BioAgents	Jena-Cospeda	Germany
Xylem Group	New York	USA

Table 2 List of chemicals and their suppliers.

Chemical	Supplier
[^{35}S]-L-methionine	Hartmann Analytic
2-mercaptoethanol (β-mercaptoethanol)	Sigma-Aldrich
6-aminocaproic acid	Sigma-Aldrich
Acetic acid	Roth
Acetone	AppliChem or Merk
Acrylamide/bisacrylamide (37.5:1) solution (Rotiphorese® Gel 30)	Roth
Acrylamide, 4x crystallized	Roth
Adenine hemisulfate salt	Sigma-Aldrich
ADP (adenosine-5'-diphosphate)	Sigma-Aldrich
Agarose NEEO ultra-quality	Roth
Ammonium acetate (NH$_4$Ac)	Merck
Ammonium persulfate	Roth
Ampicillin	AppliChem
Antimycin A	Sigma-Aldrich
ATP (adenosine-5'-triphosphate)	Roche
Bacto^{TM} Agar	BD
Bacto^{TM} Peptone	BD

Bacto™ Tryptone	BD
Bacto Yeast Extract	BD
N,N'-Methylene bisacrylamide	Roth
Bis-Tris	AppliChem
Bovine serum albumin (BSA) fatty acid free	Sigma-Aldrich
Bromophenol Blue	Merck
Calcium chloride ($CaCl_2$) dihydrate	Roth
cOmplete, EDTA-free protease inhibitor tablet	Roche
Coomassie Brilliant Blue G-250	Serva
Coomassie Brilliant Blue R-250	Serva
Creatine kinase	Roche
Creatine phosphate	Roche
CSM-HIS	MP Biomedicals
Cytochrome *c* from bovine heart	Sigma-Aldrich
Diaminobenzidine (DAB)	Sigma-Aldrich
DDM (n-Dodecyl-b-D-maltoside)	Sigma-Aldrich
2',7'-Dichlorodihydrofluorescein diacetate (H_2DCFDA)	Invitrogen
Digitonin	Calbiochem
DMSO (dimethylsulfoxide)	AppliChem
DNase I	Roche
DTT (1,4-dithiothreitol)	Roth
EDTA (ethylene diamine tetraacetic acid)	Roth
EGTA *(ethylene glycol tetraacetic acid)*	Sigma-Aldrich
Ethanol	Roth
Ethidium bromide 0.07%	AppliChem
Galactose, D(+)	Roth
Geneticin 418 Sulfate (G418)	PAA
Glucose, D(+)	Roth
Glycerol	Sigma-Aldrich
Glycine	Roth
HEPES (4-(2-hydroxyethyl)-1-piperazineethanesulfonic acid)	Roth
Herring sperm DNA	Promega

L-Histidine	Serva
Hydrochloric acid (HCl) 37%	Roth
Hydrogen peroxide solution	Sigma-Aldrich
IgG from bovine serum	Bio-Rad
IgG from human serum	Sigma-Aldrich
Imidazole	Merck
IPTG (Isopropyl β-D-1-thiogalactopyranoside)	Roth
L(+)-Lactic acid	AppliChem
Lead (II) nitrate ($Pb(NO_3)_2$)	Merck
L-Leucine	Serva
Lithium acetate (LiAc)	AppliChem
L-Lysine	Serva
Lysozyme from chicken egg white	Sigma-Aldrich
Mannitol, D(+)	Roth
Magnesium chloride ($MgCl_2$) heptahydrate	Merck
Magnesium sulfate ($MgSO_4$) heptahydrate	Roth
Manganese (II) chloride ($MnCl_2$) tetrahydrate	Roth
Methanol	Roth
L-Methionine	Roth
Milk powder	Grano Vita
MOPS (morpholinopropanesulfonic acid)	Sigma-Aldrich
NADH (nicotinamide adenine dinucleotide)	Roche
Nourseothricin	Werner BioAgents
Oligomycine	Sigma-Aldrich
OrangeG	Sigma-Aldrich
Oxaloacetic acid	Sigma-Aldrich
PEG-4000 (polyethylene glycol 4000)	Merck
PMSF (phenylmethanesulfonyluoride)	Roth
Potassium acetate (KAc)	Merck
Potassium chloride (KCl)	Roth
Potassium cyanide (KCN)	Sigma-Aldrich
Potassium dihydrogen phosphate (KH_2PO_4)	Merck

Di-potassium hydrogen phosphate (K_2HPO_4)	Roth
Potassium hydroxid (KOH)	Roth
Proteinase K	Roche
Rapamycin	LC Laboratories
Rubidium chloride (RbCl)	Roth
Saccharose	Roth
SDS (sodium dodecyl sulfate)	Serva
Sodium chloride (NaCl)	Roth
Sodium hydroxide (NaOH)	Roth
Sodium bicarbonate (Na_2CO_3)	Sigma-Aldrich
Sodium dithionite	Fluka
Sodium hydrogen carbonate ($NaHCO_3$)	Merck
di-Sodium hydrogen phosphate (Na_2HPO_4)	AppliChem
Sorbitol	Roth
Sulfuric acid (H_2SO_4)	Merck
TCA (trichloroacetic acid)	Merck
TEMED (tetramethylethylenediamine)	Roth
Tricine	Roth
Tris (tris(hydroxymethyl)aminomethane)	Roth
Triton X-100	Sigma-Aldrich
L-Tryptophan	AppliChem
Tween-20	Roth
Uracil	Sigma-Aldrich
Urea	Roth
Valinomycine	Sigma-Aldrich
Yeast nitrogen base without amino acids (YNB)	BD

2.1.2 Kits and disposals

Disposals and commercial kits used in this study together with suppliers are listed in Table 3. Kits were used and stored according to the manufacturers' instructions.

Table 3 Kits and disposals.

Product	Supplier
Amicon® Ultra-4 centrifugal filter unit 10K MWCO	Millipore
Blotting paper	Heinemann Labortechnik
CELLSTAR® Centrifuge Tubes 15 ml, 50 ml	Geiner Bio-One
Cyanogen bromide activated Sepharose 4B	GE Healthcare
ECL Plus Western Blotting Detection Reagent	GE Healthcare
Fast Digest restriction enzymes	Fermentas
Flexi® Rabbit Reticulocyte Lysate System	Promega
GeneRuler DNA Ladder Mix	Fermentas
High molecular weight calibration kit	GE Healthcare
High Pure PCR Template Preparation Kit	Roche
HisTrap Desalting 5 ml column	GE Healthcare
HisTrap HP 1 ml column	GE Healthcare
Immobilon-P Transfer membrane (PVDF)	Millipore
KOD Hot Start DNA Polymerase	Novagen
MEDIX X-ray films	FOMA BOHEMIA
Microtube 1.5 ml and 2.0 ml	Sarstedt
Minisart syringe filters	Sartorius AG
MitoTracker® Orange CMTMRos	Life Technologies
Ni-NTA agarose	Qiagen
Pierce® ECL Western Blotting substrate	Thermo Scientific
Pipette tips 10 μl, 200 μl, and 1 ml	Sarstedt
Rapid DNA Ligation Kit	Thermo Scientific
Resourse S column 5 ml	GE Healthcare
Roti-Quant® reagent	Roth
SnakeSkin™ dialysis tubing 7K MWCO	Life Technologies
Spin columns Mobicol „classic"	MoBiTec
SP6 mMESSAGE mMACHINE® Kit	Life Technologies
TNT® SP6 Quick coupled Transcription/Translation System	Promega

Unstained SDS PAGE Protein Marker (6.5 – 200 kDa)	Serva
USB® Taq DNA Polymerase	Affymetrix
Wizard® Plus SV Gel and PCR DNA Purification System	Promega
Wizard® Plus SV Minipreps DNA Purification System	Promega
Zymolyase®-20T enzyme (20,000 U/g)	Nacalai Tesque

2.1.3 Equipment

Table 4 Equipment.

Product	Model	Supplier
Electrophoresis and blotting	EPS 601 power supply	GE Healthcare
	Mini-PROTEAN® 3 Cell	Bio-Rad
	Mini-Sub® Cell GT Cell	Bio-Rad
	PowerPac™ HC Power Supply	Bio-Rad
	SE 600 Ruby Standard system	GE Healthcare
	Semi Dry Blotting Chamber	PEQLAB Biotechnologie
FPLC equipment	ÄKTA Purifier 10	GE Healthcare
	Superose™ 6 10/300 GL	GE Healthcare
Centrifuges	OptimaTMDX-XP	Beckman Coulter
	Sorvall RC 12BP	Thermo Scientific
	Sorvall® RC6 Plus	Thermo Scientific
	12-MC	Beckman Coulter
	5415R	Eppendorf
	5417R	Eppendorf
	5424	Eppendorf
	5804R	Eppendorf
Rotors	A-4-44	Eppendorf
	F45-24-11	Eppendorf
	F45-30-11	Eppendorf
	FA-45-24-11	Eppendorf
	Sorvall® F10S- 6x500Y	Thermo Scientific
	Sorvall® F14S- 6x250Y	Thermo Scientific

Rotors	Sorvall® H-12000	Thermo Scientific
	Sorvall® SS-34	Thermo Scientific
	TLA-55	Beckman Coulter
Scanners	Autoradiography storage phosphor screen	GE Healthcare
	BioPhotometer	Eppendorf
	Cary® 50 UV-Vis spectrophotometer	Varian
	Curix 60 processor	Agfa
	Perfection V750 Pro scanner	Epson
	F-7000 fluorescence spectrophotometer	Hitachi High Technologies
	GeneQuant^{TM} 1300 Spectrophotometer	GE Healthcare
	iMark^{TM} microplate absorbance reader	Bio-Rad
	LAS 1000	FujiFilm
	NanoVue^{TM} Spectrophotometer	GE Healthcare
	Starion FLA-9000	FujiFilm
	Storm 820 Phosphorimager	GE Healthcare
	UVsolo TS transilluminator	Biometra
Other	Autoclave Systec DX-200	Systec
	Balance BP 3100P	Sartorius
	CryoMill	Retsch
	DeltaVision microscope Olympus IX71	Applied Precision
	Electronic Digital Balance Kern ABJ 220-4M	LABalance
	EmulsiFlex C5	Avestin
	Excella® E10 platform shaker	New Brunswick Scientific
	G25 Shaker Incubator	New Brunswick Scientific
	Innova® 44 Incubator shaker	New Brunswick Scientific
	Magnetic Stirrer MR 3001	Heidolph
	Milli-Q-Water purification system	Millipore
	Oxygraph 2k	OROBOROS Instruments
	pH-meter	Xylem Group

Other	Pipettes	Gilson
	Potter S glass-Teflon Homogenizer	Sartorius AG
	Sonicator Cell Disruptor W-220F	Heat Systems-Ultrasonics
	Termomixer Comfort	Eppendorf
	TPersonal 48 thermocycler	Biometra
	Vortex-Genie 2	Scientific Industries
	Vacuum gel drier	Scie-Plas

2.1.4 Software

List of software used for data analysis, image processing, and data documentation is given in Table 5.

Table 5 Software.

Software	Company
Adobe Illustrator CS6	Adobe
Adobe Photoshop CS6	Adobe
Genious Pro 5.3.6	Biomatters Ltd
ImageQuant TL Software	GE Healthcare
SoftWoRx 3.5.1	Applied Precision

2.1.5 Buffers and solutions

Refer to Table 6 for buffer recipes. All buffers were prepared using Milli-Q deionized water and analytical grade chemicals.

Table 6 Buffers and solutions.

Buffer	Composition
Acetate buffer	0.5 M NH_4Ac/acetic acid pH 3.5
Activity assay buffer complex III	40 mM KPi pH 7.4, 0.02% bovine heart cytochrome c, 0.5 mM NADH, 10 mM KCN
Activity assay buffer complex IV	40 mM KPi pH 7.4, 0.02% reduced bovine heart cytochrome c

Activity assay buffer MDH	0.1 M KPi pH 7.4, 0.1 mM NADH, 0.2 mM oxaloacetate
Agarose gel solution	1% agarose, TAE buffer
AVO mix	1 mM antimycin A, 0.1 mM valinomycin, 2 mM oligomycin in ethanol
Blocking solution	5%-10% milk powder in TBST
Blotting buffer	25 mM Tris, 192 mM glycine, 10% ethanol
BN acrylamide	48% acrylamide, 1.5% bis-acrylamide
BN anode buffer	50 mM Bis-Tris/HCl pH 7.0
BN clear cathode buffer	50 mM tricine, 15 mM Bis-Tris
BN blue cathode buffer	50 mM tricine, 15 mM Bis-Tris, 0.2% Coomassie Brilliant Blue G-250
BN gel buffer	67 mM 6-aminocaproic acid, 50 mM Bis-Tris/HCl pH 7.0
BN loading buffer	0.5% Coomassie Brilliant Blue G-250, 50 mM 6-aminocaproic acid, 10 mM Bis-Tris/HCl pH 7.0
BN solubilization buffer	20 mM Tris/HCl, 60 mM NaCl, 10% glycerol, 1 mM EDTA, 1mM PMSF with 1% digitonin or 0.6% DDM
Carbonate buffer	100 mM Na_2CO_3/$NaHCO_3$ pH 10.8
Carrier DNA	Herring sperm DNA (10 mg/ml) in TE buffer
Coomassie destaining solution	30% ethanol, 10% acetic acid
Coomassie staining solution	0.25% Coomassie Brilliant Blue R-250, 40% ethanol, 10% acetic acid
Digitonin stock solution	5% digitonin in H_2O
DDM stock solution	5% DDM in H_2O
DNA loading dye	10% saccharose, 0.25% OrangeG
DTT buffer	10 mM DTT, 100 mM Tris/H_2SO_4 pH 9.4
E. coli cracking buffer	20 mM Tris/HCl pH 7.4, 50 mM NaCl, 5 mM imidazole, 1 mM $MgCl_2$, 1 mM PMSF, 0.1 mg/ml lysozyme, 0.01 mg/ml DNase I, cOmplete, EDTA-free protease inhibitor tablet
Equilibration solution complex IV	50 mM KPi buffer pH 7.4

Equilibration solution complex V	270 mM glycine, 35 mM Tris/HCl pH 8.3
EM buffer	1 mM EDTA, 10 mM MOPS/KOH pH 7.2
Homogenization buffer	0.6 M sorbitol, 1 mM EDTA, 0.2% fatty acid free BSA, 1 mM PMSF, 10 mM Tris/HCl pH 7.4
HisTrap buffer	50 mM NaCl, 5 mM imidazole, 20 mM Tris/HCl pH 7.4
Import buffer	3% BSA, 250 mM saccharose, 80 mM KCl, 5 mM $MgCl_2$, 2 mM KH_2PO_4, 5 mM methionine, 5 mM ATP, 5 mM NADH, 10 mM MOPS/KOH pH 7.2 with or without 6.25 mM creatin phosphate and 125 µg/ml creatin kinase
MAS buffer	70 mM saccharose, 220 mM mannitol, 5 mM $MgCl_2$, 1 mM EGTA, 10 mM KH_2PO_4, 2 mM HEPES/KOH pH 7.4
MonoS buffer	50 mM NaCl, 20 mM Tris/HCl pH 7.4
PMSF stock	0.2 M PMSF in ethanol
Phosphate buffer saline (PBS)	137 mM NaCl, 2.7 mM KCl, 10 mM Na_2HPO_4, 1.8 mM KH_2PO_4/HCl pH 7.4
Potassium phosphate (KPi) buffer	80.2% K_2HPO_4, 19.8% KH_2PO_4
Rapamycin stock solution	1mg/ml rapamycin in DMSO
Reduced cytochrome c	1% cytochrome c, 50 mM KPi, 0.12% sodium dithionite
Resolving gel (SDS PAGE)	10-16% acrylamide (Rotiphorese® Gel 30), 0.05% TEMED, 0.1% APS, 0.1% SDS, 386 mM Tris/HCl pH 8.8
Resolving gel (Urea PAGE)	17.5% acrylamide, 0.23% bis-acrylamide, 5.4 M urea, 8 mM NaCl, 0.09% SDS, 0.1% APS, 0.05% TEMED, 684 mM Tris/HCl pH 8.8
ROS assay buffer	0.1% Triton X-100, 150 mM NaCl, 20 mM Tris/HCl pH 7.4
SDS loading buffer	10% glycerol, 2% SDS, 0.01% bromophenole blue, 1% β-mercaptoethanol, 60 mM Tris/HCl pH 6.8
SDS running buffer	25 mM Tris, 192 mM glycine, 0.1% SDS
SEM buffer	250 mM saccharose, 1 mM EDTA, 10 mM MOPS/KOH pH 7.2

Stacking gel (SDS PAGE)	4% arylamide, 0.1% SDS, 0.1% APS, 0.05% TEMED, 80 mM Tris/HCl pH 6.8
Stacking gel (Urea PAGE)	5.4% arylamide, 0.07% bis-acrylamide, 0.12% SDS, 3.33 M urea, 0.1% APS, 0.05% TEMED, 109 mM Tris/HCl pH 6.8
Staining solition complex IV	50 mM KPi pH 7.4, 0.5 mg/ml DAB, 1 mg/ml reduced cytochrome c
Staining solition complex V	270 mM glycine, 35 mM Tris/HCl pH 8.3, 8 mM ATP, 14 mM $MgSO_4$, 0.2% $Pb(NO_3)_2$
Solubilization buffer (mitochondria)	100 mM NaCl, 5% glycerol, 0.5 mM EDTA, 1mM PMSF 20 mM Tris/HCl pH 7.4 with 1% digitonin or 0.6% DDM
Solubilization buffer (yeast powder)	150 mM NaCl, 10% glycerol, 0.1 mM EDTA, 1mM PMSF, 1% digitonin, cOmplete, EDTA-free protease inhibitor tablet, 1% DNase I, 20 mM Tris/HCl pH 7.5
TAE buffer	2 mM EDTA, 40 mM Tris/acetic acid pH 8.0
TBS (Tris-Buffered Saline)	150 mM NaCl, 50 mM Tris/HCl pH 7.5
TBST (TBS and Tween-20)	150 mM NaCl, 0.05% Tween-20, 50 mM Tris/HCl pH 7.5
TCA solution	100% TCA in water
TE buffer	1 mM EDTA, 10 mM Tris/HCl pH 8.0
TfB1 buffer	30 mM KAc, 100 mM RbCl, 10 mM $CaCl_2$, 50 mM $MnCl_2$, 15% glycerol/acetic acid pH 5.8
TfB2 buffer	10mM RbCl, 75 mM $CaCl_2$, 15% glycerol, 10 mM MOPS/KOH pH 6.5
Urea PAGE acrylamide	60% acrylamide, 0.8% bis-acrylamide in H_2O
Urea PAGE running buffer	50 mM Tris, 192 mM glycine, 0.1% SDS
Washing buffer (mitochondria)	100 mM NaCl, 5% glycerol, 0.5 mM EDTA, 1mM PMSF 20 mM Tris/HCl pH 7.4 with 0.3% digitonin or 0.6% DDM
Washing buffer (yeast powder)	300 mM NaCl, 10% glycerol, 0.1 mM EDTA, 1mM PMSF, 1% digitonin, cOmplete, EDTA-free protease inhibitor tablet, 20 mM Tris/HCl pH 7.5
Yeast cell lysis solution	255 mM NaOH, 1% β-mercaptoethanol

Yeast cracking buffer for DNA extraction	0.2 M LiAc, 1% SDS
Yeast transformation solution	0.1 M LiAc, 40% PEG-4000 in water, filter sterilized
Zymolyase buffer	1.2 M sorbitol, 20 mM KPi buffer

2.1.6 Media

Refer to Table 7 for medium recipes. All media were prepared using Milli-Q deionized water and analytical grade chemicals.

Table 7 Media composition.

Medium	Composition
Lysogeny broth (LB)	0.5% yeast extract, 1% tryptone, 1% NaCl
LB agar medium	0.5% yeast extract, 1% tryptone, 1% NaCl, 1.5% agar
LB cryo storage medium	0.5% yeast extract, 1% tryptone, 1% NaCl, 15% glycerol
Nitrogen starvation medium (SD-N)	0.67% YNB without amino acids, 2% glucose
Synthetic drop-out medium	0.67% YNB, 0.07% single dropout mixture (CSM)
Synthetic complete medium	0.67% yeast nitrogen base without aminoacids (YNB), 0.2% adenine hemisulfate, 0.2% L-histidine, 0.3% L-leucine, 0.3% L-lysine, 0.2% L-methionine, 0.2% L-tryptophan, 0.2% uracil, filter sterilized
YP medium	1% yeast extract, 2% peptone
YPAD (2x)	2% yeast extract, 4% peptone, 4% glucose, 0.008% adenine hemisulfate
YP agar medium	1% yeast extract, 2% peptone, 2.5% agar
YPD cryo storage medium	1% yeast extract, 2% peptone, 2% glucose, 0.3% adenine hemisulfate, 15% glycerol

2.1.7 Antibodies

Primary polyclonal antibodies were produced by injecting antigen (synthetic peptide or purified proteins) into rabbits. For detection of HA tag or FLAG tag corresponding mouse monoclonal antibodies were used (Sigma-Aldrich). Collected serum was diluted in 5% blocking solution (1:100 − 1:2000). Secondary goat anti-rabbit or anti-mouse antibodies coupled with horseradish peroxidase (HRP) (Dianova) were used at 1:10,000 dilution in blocking solution. Peroxidase Anti-Peroxidase Soluble Complex antibody (Sigma-Aldrich) was used for detection of ZZ tag.

2.1.8 Microorganisms

E. coli strains for cloning and protein expression are listed in Table 8.

Table 8 Bacterial strains.

Strain	Genotype	Reference
XL1-Blue	*recA1 endA1 gyrA96 thi-1 hsdR17 supE44 relA1 lac* [F′ *proAB lacI^{q}ZΔM15* Tn*10* (Tet^r)]	Stratagene
Rosetta(DE3)pLysS	F$^-$ *ompT hsdS*$_B$(r$_B^-$ m$_B^-$) *gal dcm* (DE3) pLysSRARE (Cam^R)	Novagen

Saccharomyces cerevisiae wild-type strains and their derivatives are listed in Table 9. Yeast strains used in this study are derivatives of *S. cerevisiae* strains YPH499 (Sikorski and Hieter, 1989), BY4741 (Euroscarf), and WCG4a (Hilt et al. 1993). Cox4^{ZZ}, *cyt1Δ*, *cox4Δ, cox13Δ, rcf1Δ*, and *rcf2Δ* were described previously (Vukotic et al., 2012; Frazier et al., 2006). Gene deletions were achieved by homologues recombination of HIS3MX6, KANMX6, or NATMX6 cassettes into the corresponding loci. In *rcf1Δ* and *cox26Δ* strains KANMX6 disruption cassette was removed upon Cre recombinase expression leaving a single loxP site at the chromosomal locus (Güldener et al., 1996). Generation of tagged strains was performed by PCR-based chromosomal integration (Longtine et al., 1998; Knop et al., 1999; Janke et al., 2004). If the tag was incorporated at the N-terminus of the protein, *NOP1* or *GAL1* promoters (*NOP1pr* or *GAL1pr*) were used to drive protein expression. Atg32 tagging and *PEP4* deletion in autophagy mutants were done in corresponding mutant strains from the Euroscarf collection.

Table 9 Yeast strains.

Strain	Genotype	Reference
YPH499	MATa *ade2-101; his3-Δ200; leu2-Δ1; ura3-52; trp1-Δ63; lys2-801*	Sikorski and Hieter, 1989
rcf2Δ	YPH499 *rcf2Δ::HIS3*	Vukotic et al., 2012
rcf1Δ	YPH499 *rcf1Δ*::loxP	Vukotic et al., 2012
cyt1Δ	YPH499 *cyt1Δ::HIS3*	Frazier thesis
cox4Δ	YPH499 *cox4Δ::HIS3*	Frazier et al., 2006
cox13Δ	YPH499 *cox13Δ::HIS3*	Vukotic et al., 2012
Cox4^{ZZ}	YPH499 *cox4::COX4*-TEV-ProA- His$_7$-*HIS3*	Vukotic et al., 2012
Cox26^{GFP}	YPH499 *cox26::COX26*-GFP-*kanMX4*	M. Deckers
Cox26^{FLAG}	YPH499 *cox26::COX26*-FLAG-*HIS3*	M. Deckers
Cox26^{ZZ}	YPH499 *cox26::COX26*-TEV-ProA- His$_7$-*HIS3*	M. Deckers
cox26Δ	YPH499 *cox26Δ*::loxP	M. Deckers
atg32Δ	YPH499 *atg32Δ::HIS3*	This study
Atg32^{ZZ}	YPH499 *atg32::ATG32*-TEV-ProA-His$_7$-*HIS3*	J. Dudek
^{ZZ}Atg32	YPH499 *atg32::HIS3-NOP1pr*-His$_7$-ProA-TEV-*ATG32*	J. Dudek
^{ZZ}Atg32$_{IMS}$	YPH499 *atg32::HIS3-NOP1pr*-His$_7$-ProA-TEV-*ATG32*(382-529)	J. Dudek
^{HA}Atg32	YPH499 *atg32::HIS3-GAL1pr*-HA$_3$-*ATG32*	J. Dudek
^{HA}Atg32$_{IMS}$	YPH499 *atg32::HIS3-GAL1pr*-HA$_3$-*ATG32*(382-529)	J. Dudek

BY4741	MATa *his3Δ1; leu2Δ0; met15Δ0; ura3Δ0*	Euroscarf
atg32Δ	BY4741 *atg32Δ::kanMX4*	Euroscarf
^{ZZ}Atg32	BY4741 *atg32::HIS3-NOP1pr*-His$_7$-ProA-TEV-*ATG32*	This study
^{ZZ}Atg32 *pep4Δ*	BY4741 *pep4Δ::kanMX4; atg32::HIS3-NOP1pr*-His$_7$-ProA-TEV-*ATG32*	This study
^{ZZ}Atg32 *pep4Δ atg1Δ*	BY4741 *pep4Δ::natMX6; atg1Δ::kanMX4; atg32::HIS3-NOP1pr*-His$_7$-ProA-TEV-*ATG32*	This study
^{ZZ}Atg32 *pep4Δ atg3Δ*	BY4741 *pep4Δ::*natMX6; *atg3Δ::kanMX4; atg32::HIS3-NOP1pr*-His$_7$-ProA-TEV-*ATG32*	This study
^{ZZ}Atg32 *pep4Δ atg4Δ*	BY4741 *pep4Δ::*natMX6; *atg4Δ::kanMX4; atg32::HIS3-NOP1pr*-His$_7$-ProA-TEV-*ATG32*	This study
^{ZZ}Atg32 *pep4Δ atg5Δ*	BY4741 *pep4Δ::*natMX6; *atg5Δ::kanMX4; atg32::HIS3-NOP1pr*-His$_7$-ProA-TEV-*ATG32*	This study
^{ZZ}Atg32 *pep4Δ atg7Δ*	BY4741 *pep4Δ::*natMX6; *atg7Δ::kanMX4; atg32::HIS3-NOP1pr*-His$_7$-ProA-TEV-*ATG32*	This study
^{ZZ}Atg32 *pep4Δ atg8Δ*	BY4741 *pep4Δ::*natMX6; *atg8Δ::kanMX4; atg32::HIS3-NOP1pr*-His$_7$-ProA-TEV-*ATG32*	This study
^{ZZ}Atg32 *pep4Δ atg10Δ*	BY4741 *pep4Δ::*natMX6; *atg10Δ::kanMX4; atg32::HIS3-NOP1pr*-His$_7$-ProA-TEV-*ATG32*	This study
^{ZZ}Atg32 *pep4Δ atg12Δ*	BY4741 *pep4Δ::*natMX6; *atg12Δ::kanMX4; atg32::HIS3-NOP1pr*-His$_7$-ProA-TEV-*ATG32*	This study

[ZZ]Atg32 *pep4Δ atg13Δ*	BY4741 *pep4Δ::*natMX6; *atg13Δ::kanMX4*; *atg32::HIS3-NOP1pr-*His₇-ProA-TEV-*ATG32*	This study
[ZZ]Atg32 *pep4Δ atg14Δ*	BY4741 *pep4Δ::natMX6; atg14Δ::kanMX4;* *atg32::HIS3-NOP1pr-*His₇-ProA-TEV-*ATG32*	This study
[ZZ]Atg32 *pep4Δ atg15Δ*	BY4741 *pep4Δ::natMX6; atg15Δ::kanMX4*; *atg32::HIS3-NOP1pr-*His₇-ProA-TEV-*ATG32*	This study
[ZZ]Atg32 *pep4Δ atg16Δ*	BY4741 *pep4Δ::natMX6; atg16Δ::kanMX4*; *atg32::HIS3-NOP1pr-*His₇-ProA-TEV-*ATG32*	This study
[ZZ]Atg32[IMS]	BY4741 *atg32::HIS3-NOP1pr-*His₇-ProA-TEV-*ATG32*(382-529)	This study
[ZZ]Atg32[IMS] *pep4Δ*	BY4741 *pep4Δ::kanMX4; atg32::HIS3-NOP1pr-*His₇-ProA-TEV-*ATG32*(382-529)	This study
[ZZ]Atg32[IMS] *pep4Δ atg11Δ*	BY4741 *pep4Δ::kanMX4; atg11Δ::natMX6; atg32::HIS3-NOP1pr-*His₇-ProA-TEV-*ATG32*(382-529)	This study
WCG4a	MATα *his3-11; 15 leu2-3; 112 ura3*	Hilt et al. 1993
[ZZ]Atg32	WCG4a *atg32::HIS3-NOP1pr-*His₇-ProA-TEV-*ATG32*	This study
[ZZ]Atg32 *pep4Δ*	WCG4a *pep4Δ::kanMX4*; *atg32::HIS3-NOP1pr-*His₇-ProA-TEV-*ATG32*	This study
[ZZ]Atg32 *atg11Δ*	WCG4a *atg11Δ::natMX6*; *atg32::HIS3-NOP1pr-*His₇-ProA-TEV-*ATG32*	This study
[ZZ]Atg32 *pep4Δ atg11Δ*	WCG4a *pep4Δ::kanMX4; atg11Δ::natMX6; atg32::HIS3-NOP1pr-*His₇-ProA-TEV-*ATG32*	This study
[ZZ]Atg32 *pre1-1 pre2-2*	WCG4a *pre1-1*; *pre2-2*; *atg32::HIS3-NOP1pr-*His₇-ProA-TEV-ATG32	This study

2.1.9 Oligonucleotides and plasmids

Oligonucleotides used in this study were produced by Metabion and are listed in Table 10.

Table 10 Oligonucleotides.

Primer	Sequence	Purpose
pJD16	5'AGAAGAGAATTCTCGATTTAGGTGACACTATAGAATACGCCGCCGCCATGGTTTTGGAATACCAACAAAGGG3'	pML1 cloning
pJD17	5'ATAAGAGTCGACTTACAATAGAATATAACCCAGTGCCAAAATCCG3'	pML1 cloning
pMVP72	5'GATCGATTTAGGTGACACTATAGATGTTTAGACAGTG3'	Cox13 lysate
pMVP73	5'TTAATCGTCGTGCTCGATGTGCCTG3'	Cox13 lysate
pOMD19	5'GGATTTAGGTGACACTATAGAATACGAATTCATGTCACGCATGCCATCTAGT3'	Rcf1 lysate
pOMD20	5'AAGCTTCTCGAGTTACTTCTTTCCAAGCTTATTTTC3'	Rcf1 lysate
pOMD22	5'GGATTTAGGTGACACTATAGAATACGAATTCATGTTCTTCAGCCA3'	Cox26 lysate
pOMD445	5'CGAAGCTTTTACATCATCATCTCGAGTGCTTTTCTTG3'	Cox26 lysate
pML37	5'GTGACCTAGTATTTAATCCAAATAAAATTCAAACAAAAACCAAAACTAACATGCGTACGCTGCAGGTCGAC3'	*PEP4* deletion
pML38	5'CTAGATGGCAGAAAAGGATAGGGCGGAGAAGTAAGAAAAGTTTAGCTCAATCGATGAATTCGAGCTCG3'	*PEP4* deletion
pML31	5'TACTGTTGTTGTTCGGAAAGTACTTCTTTTATTTTCTTTTATACATCATGCGTACGCTGCAGGTCGAC3'	*ATG11* deletion
pML32	5'GATACATAATTAAAATCTTGTCATTTGTGACAAACGTTTAGCACTGTTCAATCGATGAATTCGAGCTCG3'	*ATG11* deletion
pML07	5'GAAGTCCTAATCACAAAAGCAAAAAAAATCTGCCAGGAACAGTAAACATATGCGTACGCTGCAGGTCGAC3'	*ATG32* deletion
pML08	5'GTAAAAAGTGAGTAGGAACGTGTATGTTTGTGTATATTGGAAAAAGGTTAATCGATGAATTCGAGCTCG3'	*ATG32* deletion
pJD12	5'TTTGACAATTTTTCTTATCAGTTGTGACTTCTCTTATCGATAAGCAATATTGAAGTCCTAGGAATACGAATTCGAGCTC3'	*ATG32* N-terminal tagging
pJD13	5'AGGTGGCATGCTTTTAGATGAGGATCCTTTACCTTCCCTTTGTTGGTATTCCAAAACCATCACGTCACTCATACCCTGA3'	*ATG32* N-terminal tagging

pJD41	5'GAAATGCCCCAAGTGAACCAGCTCGTGAAGAACTTCT GCTTCTTCACGTCACTCATACCCTGA3'	*ATG32* N-terminal truncation

All plasmids generated for this study are listed in Table 11. pTNT[TM] vector (Promega), pGEM®-4Z vector (Promega), and pETDuet[TM]-1 vector (Novagen) were used for cloning. Plasmids were propagated in *E. coli* XL1-Blue cells.

Table 11 Plasmids.

Plasmid	Backbone	Insert	Purpose	Reference
pYM2.1	–	–	C-terminal FLAG tag	D. Mick
pYM10			C-terminal TEV-ProA-His$_7$ tag	Knop et al., 1999
p1417	–	–	N-terminal TEV-ProA-His$_7$ tag with NOP1 promoter	N. Wiedemann
pFA6a-NATMX6	–	–	Gene deletion NAT^R marker	Janke et al., 2004
pFA6a-HIS3MX6	–	–	Gene deletion HIS3 marker	Longtine et al., 1998
C21	pTNT	*COX5a*	Cox5a lysate	Rehling lab
pML1	pGEM-4Z	*ATG32*	Atg32 lysate	This study
pJD51	pETDuet-1	*ATG32*(1-343)-His$_{10}$	Atg32$_{CYT}$ expression in *E. coli*	J. Dudek

2.2   Methods

2.2.1 Handling of biological material

2.2.1.1 Cultivation of *Escherichia coli*

E. coli were grown according to standart protocols (Sambrook and Russel, 2001). *E. coli* strains BL21, XL1-Blue and Rosetta(DE3)pLysS were cultivated at 37°C in liquid LB medium with vigoruos shaking (220 rpm). For solid media preparation 1.5% agar was added to the medium prior to autoclaving. To select for plasmids containing Amp^R marker, LB was supplemented with 0.1 g/L ampicillin. Liquid cultures were inoculated with biomass from solid medium or from pre-culture with 1:100 to 1:1000 dilutions. Growth of *E. coli* was monitored by measuring optical density at 600 nm (OD_{600}; OD_{600} of 1 ~ $8x10^8$ cells/ml). For long-term storage cryostocks were prepared by adding 15% sterile glycerol to the liquid *E. coli* culture and freezing the mixture at -80°C.

2.2.1.2 Preparation of chemically competent *E. coli* cells

Competent *E.coli* were prepared according to the RbCl method (Hanahan, 1983). In brief, a liquid pre-culture was inoculated with cryostock material and propagated overnight. Pre-culture was diluted 1:100 and grown until OD_{600} reached 0.6, corresponding to mid-log phase. Cells were chilled on ice for 15 min and harvested by centrifugation at 5,000 rcf for 10 min at 4°C. Pellet was re-suspended in 100 ml/g cold TfB1 buffer and incubated on ice for 15 min. Cells were pelleted as previously described and re-suspended in 20 ml/g cold TfB2 buffer. For storage 100 µl aliquotes of competent cells were flash-frozen in liquid nitrogen and kept at -80°C.

2.2.1.3 Transformation of *E. coli*

For transformation 100 µl of competent cells were thawed on ice, mixed with 200 ng of plasmid DNA or 10 µl ligation reaction, and incubated 20 min on ice. *E. coli* were heat-shoked at 42°C for 45 sec and left to recover on ice for 2 min. 1 ml LB medium was added to the cells and the culture was grown for 1 hour at 37°C under strong agitation. Cells were pelleted for 5 min at 1,000 rcf, plated on solid LB medium with antibiotic for selection, and grown at 37°C until single colonies were visible.

2.2.1.4 Cultivation of Saccharomyces cerevisiae

Yeast *Saccharomyces cerevisiae* were grown according to standart procedures (Curran and Bugeja, 2006). Media compositions are listed in Table 7. All media and solutions used for yeast handling were either autoclaved or filter-sterilized. Solid medium plates were prepared by adding 2.5% agar to the liquid medium prior to autoclaving. Yeast were plated on solid medium from cryostocks and grown for 2-3 days at 30°C. Liquid cultures were inoculated from plates or a pre-culture (1:10 or 1:20) and incubated at 30°C while shaking (220 rpm). Cell growth was monitored by OD_{600} measurements (OD_{600} of $1 \sim 1 \times 10^7$ cells/ml). In general rich YP medium was used for yeast cultivation. Antibiotic resistant strains were grown on solid YP media with 0.2 g/L geneticin or 0.1 g/L nourseothricin added after the autoclaving. Synthetic medium (SM) lacking the appropriate metabolite was used to select for genetic markers and propagate strains containing plasmids. Full synthetic medium was used to culture cells for microscopy studies. All media were supplemented with 2% glucose (YPD), 2% galactose (YPGal), 3% glycerol (YPG), or 3% lactate (YPL, pH 5.0 with NaOH) as fermentable (glucose, galactose) or non-fermentable (glycerol, lactate) carbon sourse. For GAL1 promoter induction 2% galactose was added to the medium. Yeast cryostocks were prepared by re-suspending biomass from solid medium in 1 ml YPD medium with 0.3% adenine hemisulfate and 15% glycerol. Cryo vials were frozen and stored at -80°C.

2.2.1.5 Mitophagy induction

Mitophagy was induced with different stimuli as previously described (Kissova et al., 2004; Kanki and Klionsky, 2008; Aoki et al., 2011). For starvation-induced mitophagy yeast were cultured in liquid non-fermentable medium until OD_{600} reached 2-4, and either washed once with sterile water, and incubated in nitrogen starvation medium supplemented with glucose for 2-6 hours, or directly treated with rapamycin at concentration of 1 μg/ml medium for indicated time periods. Post-log phase mitophagy was triggered by culturing yeast in YPL medium for 36-72 hours.

2.2.1.6 *S. cerevisiae* growth test

Growth rates of yeast strains were compared in a dilution assay. An overnight preculture in YPD medium was used to inoculate a fresh culture, which was propagated until it reached an OD600 of 0.8, corresponding to mid-log phase. Cells were pelleted at 1,000 rcf, 5 min,

washed once with sterile water and diluted in water to an OD_{600} of 0.3. Serial 10-fold dilutions of yeast cells were prepared (0.3 to 0.0003 OD_{600}) and 5 µl of each dilution was spotted on solid YP medium plates with fermentable (YPD) and non-fermentable (YPG) carbon sourse. Plates were incubated at various temperatures (24°C, 30°C, or 37°C) for 2-4 days. To address H_2O_2 sensitivity of the mutants, corresponding yeast strains were cultured in YPD medium until reaching an OD600 of 1. Cultures were treated with various concentrations of 30% stock H_2O_2 solution for 2 hours at 30°C while shaking. Serial dilutions prepared as described above were plated onto solid YPD medium incubated for 2 days at 30°C. For documentation plates were scanned with Perfection V750 Pro scanner.

2.2.1.7 *S.cerevisiae* transformation

Competent yeast cells were prepared with lithium acetate/PEG method as descibed in literature (Gietz and Schiestl, 2007) with some modifications. *S. cerevisiae* were precultured overnight in 2x YPD with 0.6% adenine hemisulfate (YPAD), diluted to OD_{600} of 0.1 next day and grown until OD_{600} of 1-1.5. Cells were harvested at 1,000 rcf, 5 min, washed once with sterile water, and with sterile 0.1 M LiAc. Cell pellet from 50 ml culture was re-suspended in 2 ml of 0.1 M LiAc and aliquoted at 100 µl. Competent cells were frozen at -80°C or used directly for transformation procedure.

To transform competent cells herring sperm (carrier) DNA was denatured for 5 min at 95°C and rapidly cooled on ice. Cells were incubated with 120 µg of carrier DNA together with 200 ng plasmid DNA or 2 µg of purified PCR product at 30°C for 30 min with agitation (700 rpm). Afterwards 600 µl of yeast transformation solution was added and the cells were grown at 30°C for 90 min while shaking vigorously (1,400 rpm). Yeast were heat-shocked for 15 min at 42°C after adding 68 µl of DMSO to the mixture. Cells were harvested by centrifugation at 1,000 rcf for 2 min, re-suspended in sterile 1.2 M sorbitol, plated onto appropriate selection medium, and grown for 2-3 days at 30°C. When antibiotics were used as selection markers, cells were grown for additional 4 hours at 30°C in 2x YPAD medium prior to plating. Single colonies were picked and transferred to fresh plates for a second selection round. Integration of exogenous DNA was confirmed by colony PCR (section 2.2.3.2) or at the protein level by Western blotting of yeast whole cell extracts (section 2.2.2.2).

2.2.2 Cellular assays

2.2.2.1 Preparation of cryo powder from yeast cells

Yeast cells were grown as described in 2.2.1.4. If necessary, mitophagy was induced as described in 2.2.1.5. For grinding cells were pelleted at 7,000 rcf for 15 min at 18°C, washed once with sterile water, once with solubilization buffer for yeast powder without detergent, and all liquid was removed. Cell pellet was then transferred to a syringe and pressed into a container with liquid nitrogen. Frozen cells were then ground with CryoMill in a 50 ml grinding jar with a 25 mm ball for 20 min at 25 Hz. Prepared powder was stored at -80°C until further use.

2.2.2.2 Cell extracts of *S. cerevisiae*

Whole cell extracts were prepared as descibed (Yaffe and Schatz, 1984). Yeast were grown in appropriate liquid medium and biomass corresponding to 3 OD_{600} was taken for analysis. Cells were pelleted for 5 min at 4,000 rcf and re-suspended in yeast cell lysis solution. Mixture was incubated for 10 min on ice and 15% TCA was added for protein precipitation. After additional 10 min on ice precipitate was spun down at 16,000 rcf for 2 min at 4°C. Pellet was taken up into 50 µl of SDS loading buffer containing 0.1 M Tris (pH 11.5) for neutralization. Samples were boiled for 5 min at 95°C prior to SDS-PAGE loading.

2.2.2.3 Subcellular fractionation and mitochondrial isolation

Mitochondrial isolation from yeast cells was performed according to published protocols (Meisinger et al., 2006). Yeast were grown in appropriate liquid medium as described in 2.2.1.4 until OD_{600} reached 1.5 – 2. Typically to promote mitochondrial proliferation non-fermentable medium containing 3% glycerol was used. Respiratory-deficient strains were cultured in fermentable medium with 2% galactose. Yeast cells were then harvested at 7,000 rcf for 15 min at 18°C, washed once with sterile water and incubated in 2 ml/g yeast pellet of DTT buffer for 30 min at 30°C with mild agitation (90 rpm). Following DTT treatment, cells were pelleted at 3,000 rcf for 10 min at 18°C, washed once with 1.2 M sorbitol and re-supended in 7 ml/g yeast pellet of zymolyase buffer supplemented with 4 mg/g yeast pellet of Zymolyase®-20T enzyme to digest the cell wall and convert cells to spheroplasts. Zymolyase treatment was done for 60 min at 30°C with mild agitation (90

rpm). Spheroplasts were collected at 1,600 rcf for 10 min at 18°C and washed once with zymolyase buffer without enzyme. Subsequently, cell pellet was placed on ice and re-suspended in 7 ml/g yeast weight of ice-cold homogenization buffer. Plasma membrane was disrupted with 20 strokes in Potter S homogenizer at 700 rpm. Mitochondria were isolated by differential centrifugation. First centrifugation step at 1,600 rcf for 5 min at 4°C followed by the second step at 3000 rcf for 10 min at 4°C pelleted unopened cells, cellular debris, and nuclei. Mitochondria were sedimented after centrifugation at 17,500 rcf for 15 min at 4°C. Obtained mitochondrial pellet was washed with SEM buffer with 1 mM PMSF and re-suspended in 200 µl/g yeast pellet of SEM buffer. Protein concentration was determined by Bradford assay and mitochondrial suspension was adjusted to 10 mg/ml with SEM buffer. Mitochondria were aliquoted into single-use aliquots, flash frozen in liquid nitrogen, and stored at -80°C.

2.2.2.4 Fluorescent microscopy for protein localization analysis

Microscopy analysis of yeast cells was done according to previous publications (Alkhaja et al., 2012). Proteins tagged with GFP were visualized by in vivo fluorescent microscopy using a DeltaVision microscope. Yeast cells were cultured in full synthetic medium supplemented with glycerol to OD_{600} of 1-2 as described in section 2.2.1.4. Mitochondria were additionally stained with 0.2 µg/ml MitoTracker® Orange CMTMRos during 15 min incubation at 30°C. Cells were then directly used for microscopy with FITC and TRITC filters used to detect fluorescence of GFP and MitoTracker dye respectively. Whole cells were visualized with differential interference contrast microscopy. Collected images were deconvoluted with softWoRx.

2.2.3 Molecular biology methods

2.2.3.1 DNA isolation from *E. coli*

Plasmids were isolated from 5 ml overnight culture of *E. coli* inoculated with a single colony after transformation or from the cryostock. DNA isolation was carried with Wizard® Plus SV Minipreps DNA Purification System according to manufacturer's instruction. Concentration of isolated DNA was measured with a NanoVue spectrophotometer monitoring the absorbance at 260 nm. DNA solution was stored in water at -20°C.

2.2.3.2 Genomic DNA isolation from *S. cerevisiae*

Genomic DNA was isolated from 200 µl yeast culture grown until $OD_{600}=1.5$ in YPD medium. Cells were pelleted at 3,000 rcf for 5 min, re-suspended in 200 µl PBS, and treated with 5 µg Zymolyase®-20T for 30 min at 37°C. DNA isolation was done with High Pure PCR Template Preparation Kit, according to manufacturer's specifications. DNA was stored in elution buffer at -20°C. For quick genotyping (colony PCR) DNA was extracted as described previously (Looke et al., 2011). One yeast colony was re-suspended in 100 µl yeast cracking buffer for DNA extraction and incubated for 10 min at 70°C. Sample was mixed with 300 µl of 100% ethanol and vortexed. DNA and cell debris were pelleted for 3 min at 15,000 rcf and the pellet was washed with 300 µl of 70% ethanol. Residual ethanol was removed by drying the sample for 20 min at 30°C and the pellet was dissolved in 100 µl dH_2O. Cell debris was pelleted as described above. For subsequent PCR 1 µl was used as a template.

2.2.3.3 Polymerase chain reaction (PCR)

DNA fragments for molecular cloning and yeast transformation were amplified with KOD Hot Start DNA polymerase according to manufacturer's instructions. For amplification of integration cassettes containing natMX6 resistance marker 2-4% DMSO and 0.1% Triton X-100 were added to the reaction. To check for genomic integration DNA was amplified with USB® Taq DNA Polymerase following manufacturer's protocol. PCR products were then analyzed by agarose gel electrophoresis (section 2.2.3.5). For purification Wizard® SV Gel and PCR Clean-Up System was used according to manufacturer's specifications.

2.2.3.4 Enzymatic manipulation of DNA

Cloning was done according to published protocols (Sambrook and Russel, 2001). Plasmid DNA and PCR products were digested with Fast Digest restriction enzymes following manufacturer's specifications. DNA fragments were analyzed by agarose gel electrophoresis and extracted from the gel using Wizard® SV Gel and PCR Clean-Up System. Digested plasmid and insert were mixed at a 1:2 ratio and ligated with a Rapid DNA Ligation Kit for 1 hour at 22°C. Cloned constructs were verified by analytical restriction and sequencing.

2.2.3.5 Agarose gel electrophoresis

Agarose gel electrophoresis was used for DNA visualization and purification. Gel solution was heated until the agarose dissolved. Ethidium bromide (1 µg/ml) was added to the cooled gel solution and the gel was left to solidify. DNA samples were mixed with 4x DNA loading dye. Electrophoresis was done in TAE buffer at 120 V in Mini-Sub® Cell GT system. GeneRuler DNA Ladder Mix was used as a standard. DNA was visualized upon UV exposure using UVsolo TS transilluminator. If necessary, DNA fragments were excized from the gel for purification.

2.2.3.6 DNA Sequencing

Sequencing of DNA was done by Seqlab according to comany's instructions. Sequencing data was analyzed with Geneious Pro 5.3.6.

2.2.4 Biochemical methods

2.2.4.1 Determination of protein concentration

Protein concentration was determined using Bradford assay (Bradford, 1976) using Roti®-Quant reagent according to manufacturers instructions. For mitochondrial protein determination bovine IgG was used as a standard to establish a calibration curve. Mitochondrial suspension in SEM buffer was diluted 1:10 with water. For the measurement 5, 10, and 20 µl of mitochondrial dilution were used. Standard and mitochondrial samples were incubated for 5 min at 25°C in 2 ml of 1x Roti®-Quant reagent. Absorbance at 595 nm was measured with Eppendorf® BioPhotometer. Protein concentration was calculated based on the calibration curve.

Concentration of purified recombinant proteins was determined with Bio-Rad protein assay using BSA as a protein standard. Standard and samples were re-suspended in 800 µl of water and 200 µl of 5x Roti®-Quant reagent was added to the mixture. After incubation at 25°C for 5 min, 100 µl of the mixture was pipetted in duplicate into a 96-well plate. Absorbance at 595 nm was measured with iMark™ microplate absorbance reader. Protein concentration was calculated based on the calibration curve.

2.2.4.2 Affinity chromatography

Protein complexes carrying ZZ tag (Chen et al., 2006) were isolated using IgG affinity chromatography method (Nilsson et al., 1987; Rehling et al., 2003).

For complex purification isolated yeast mitochondria were defrosted on ice, re-isolated by centrifugation at 16,100 rcf for 10 min at 4°C and re-suspended in solubilization buffer for mitochondria with appropriate detergent (1% digitonin or 0.6% DDM) at 1 mg/ml by pipetting (20 times). Yeast powder prepared with cryo grinding (section 2.2.2.1) was solubilized at 0.1 mg/ml in solubilization buffer for yeast powder. After 30 min incubation on ice unsolubilized material was removed by centrifugation at 16,100 rcf for 15 min at 4°C. Input sample was taken after solubilization. Solubilized sample was mixed with affinity matrix at various concentrations to ensure maximal depletion.

IgG affinity matrix was made by coupling cyanogen bromide activated Sepharose 4B to human IgG according to manufacturer's instructions. IgG sepharose was washed twice with acetate buffer, twice with 2x solubilization buffer, and once with 1x solubilization buffer with appropriate detergent prior to binding. Washing was done in spin columns Mobicol „classic" at 100 g for 1 min at 4°C with 10 bed volumes of buffer.

After binding for 90 min at 4°C with mild agitation, unbound fraction was removed, and the resin was washed 10 times with corresponding washing buffer as described above.

For SDS PAGE analysis bound proteins were eluted with 2x bed volume of 1x SDS loading buffer without β-mercaptoethanol. Alternatively beads were incubated with 0.1 M glycine/HCl pH 2.8 for 5 min at 25°C. Elution was done for 2 min at 200 g at 25°C. Low pH of the glycin elution was neutralized with 0.1 M Tris base.

Native protein complexes were released from the resin upon ZZ tag cleavage with 0.4 mg/ml tobacco etch virus (TEV) protease (self-made). Cleavage was done at 4°C overnight. TEV protease carrying a polyhistidine tag was removed after 60 min incubation at 4°C with Ni-NTA resin pre-equilibrated with wash buffer. The cleaved native complexes were eluted by centrifugation at 4°C for 2 min at 100 g and subsequently analysed by SDS or BN PAGE.

2.2.4.3 SDS PAGE

Denaturing protein electrophoresis, originally developed by Laemmli (1970), was performed using polyacrylamide gels with 0.1% SDS (SDS PAGE), to separate proteins of interest according to their molecular weight (Chakavarti and Chakavarti, 2008). Gels were prepared with 30% acrylamide stock solution. For stacking 4% polyacrylamide gel buffered with Tris/HCl pH 6.8 was used. Resolving gels of different percentages (8-16%), depending on molecular weight of the proteins to be separated, were buffered with Tris/HCl pH 8.8. Both sections of the gel were polymerized with 0.1% ammonium persulfate and 0.05% TEMED. Prior to gel loading protein samples were mixed with 4x SDS loading buffer and boiled for 5 min at 95°C. Mini-PROTEAN Tetra cell or custom-made gel chambers were used for gel running. Electrophoresis was performed in SDS PAGE running buffer at 30 mA/gel. To estimate protein molecular weight, Serva Unstained SDS PAGE Protein Marker (6.5 – 200 kDa) was used as a standard.

2.2.4.4 Urea SDS PAGE

To increase protein separation in low molecular range (5 – 15 kDa) urea was added to SDS PAGE gels (Summer et al., 2009). Resolving gel and stacking gel were polymerized as described for SDS PAGE. Urea PAGE running buffer was used for electrophoresis. Electrophoresis conditions were similar to SDS PAGE. Urea containing gels were run at 50 mA/gel.

2.2.4.5 BN PAGE

Native protein complexes were separated using Blue Native polyacrylamide gel electrophoresis (BN PAGE) as previously described (Schägger and von Jagow, 1991; Wittig et al., 2006). Gradient gels of desired percentage with 4% stacking gel were prepared in a SE 600 Ruby Standard gel system (GE Healthcare) using custom-made gradient mixer. Gel solutions were prepared with BN acrylamide and BN gel buffer. 20% glycerol was added to the higher percentage gel solution. Solubilized mitochondria (section 2.2.5.2) or purified protein complexes mixed with 10x BN loading buffer were loaded on the gel. BN anode and BN cathode buffer were used for electrophoresis. BN cathode buffer was supplemented with 0.02% Coomassie Brilliant Blue G-250 (blue cathode buffer) or was used directly (clear cathode buffer). Electrophoresis was done at 600 V and 15 mA/gel at 4°C. To increase subsequent blotting and enzymatic staining efficiency blue cathode

buffer was replaced by clear cathode buffer after samples had entered the resolving gel. This step was omitted if the gel was later stained with Coomassie (section 2.2.4.8). High molecular weight calibration kit was used as a marker to estimate molecular weigth of protein complexes.

2.2.4.6 Western blotting

After separation by gel electrophoresis proteins were transferred to polyvinylidene fluoride (PVDF) membranes by semi-dry blotting (Gallagher et al., 2004). Membranes were activated upon brief incubation in methanol and soaked in blotting buffer together with the blotting paper. Membrane was assembled beneath the gel, between the three layers of blotting paper. Transfer was done at 250 mA for 2 hours.

2.2.4.7 Immunodecoration

Immunodecoration was done according to standard procedures (Gallagher et al., 2004). After the transfer the membrane was stained with Coomassie staining solution (section 2.2.4.8) to visualize protein bands and marker. Membrane was cut to decorate for proteins of various sizes and Coomassie dye was removed with methanol. For immunodecoration the membrane was briefly rinsed with TBST and incubated in blocking solution for 1-2 hours at room temperature or at 4°C overnight. Afterwards, the membrane was decorated with primary antibodies diluted in blocking solution (1:200-1:2,000) for 1 hour at room temperature or at 4°C overnight. The blot was washed 3x for 10 min with TBST buffer and decorated with secondary antibodies coupled with HRP (1:10,000 in blocking solution) for 1 hour. After washing the membrane as described, the signals were detected after incubation with Pierce® ECL Western Blotting substrate on MEDIX X-ray films. After exposure films were developed with Curix 60 processor. For detection of ZZ tag Peroxidase Anti-Peroxidase Soluble Complex antibody, diluted 1:500 in blocking solution, was used as a primary antibody, and no secondary antibody was applied.

2.2.4.8 Coomassie staining

Proteins in polyacrylamide gels and on PVDF membranes were visualized with Coomassie staining solution after incubation for 1 min (membranes) or 2 hours (gels). Background staining was removed with Coomassie destaining solution until protein bands became clearly visible. Membranes were dried to label the molecular weight marker and destained

completely with methanol. Polyacrylamide gels were placed on two sheets of blotting paper and covered with a plastic bag. Drying was done for 2 hours at 65°C with a vacuum gel drier.

2.2.4.9 In-gel enzyme activity staining

The catalytic activities of mitochondrial OXPHOS complexes were visualized after BN PAGE according to published protocols (Wittig et al., 2007). Gel stripes were cut after the run, equilibrated in the corresponding buffer (equilibration solution for complex IV or complex V) for 15 min, and stained at 25°C with the staining solution until the colored complexes became visible.

2.2.5 Assays with purified mitochondria

2.2.5.1 Steady state analysis

To analyze mitochondrial protein levels by SDS PAGE, isolated yeast mitochondria were pelleted at 16,100 rcf for 10 min at 4°C and re-suspended in 1x SDS loading buffer at 1 mg/ml. Mitochondrial dilutions were prepared to load identical volumes per gel lane.

2.2.5.2 Solubilization of mitochondria for BN-PAGE

Mitochondrial samples for BN PAGE were prepared according to published procedure (Dekker et al., 1997). Isolated yeast mitochondria were defrosted on ice, re-isolated by centrifugation at 16,100 rcf for 10 min at 4°C and re-suspended in BN solubilization buffer with appropriate detergent (1% digitonin or 0.6% DDM) at 1 mg/ml by pipetting (20 times). After 15 min incubation on ice unsolubilized material was removed by centrifugation at 16,100 rcf for 10 min at 4°C. Cleared supernatant was then mixed with BN loading buffer.

2.2.5.3 Submitochondrial protein localization

To assess protein association with mitochondrial membranes carbonate extraction was performed as described (Fujiki et al., 1982; Mick et al., 2007). Isolated mitochondria were treated with carbonate buffer at 0.5 mg/ml to release proteins periferally bound to the membrane. Alternatively mitochondria were solubilized in SEM buffer with 0.4 M KCl and 0.1% Triton X-100. After 20 min incubation on ice sample of the input was taken and

the rest was subjected to centrifugation at 100,000 rcf in a TLA-55 rotor for 1 hour at 4°C to separate soluble proteins from membrane fraction. Pellets were re-suspended in SEM buffer and proteins from all fractions were precipitated with 15% TCA for 1 hour on ice. The precipitate was pelleted at 16,000 rcf for 30 min at 4°C. Pellets were dissolved in SDS loading buffer and analyzed by SDS PAGE and immunoblotting.

Mitochondrial protein localization was determined in a proteinase K protection assay (Mick et al., 2007). Isolated mitochondria were left intact, converted to mitoplasts, or lysed with detergent. Intact mitochondria were re-suspended in 1 mg/ml SEM buffer. Mitoplasts were generated by osmotic swelling to disrupt the outer membrane. Swelling was done in 1 mg/ml EM buffer after thorough re-suspension (20 times). Alternatively after swelling mitoplasts were treated with 0.2% Triton X-100. After 20 min incubation on ice samples were split and treated with increasing concentrations of proteinase K (0, 100, 200 μg/ml) for 10 min on ice. Proteinase K was inhibited with 2 mM PMSF for 10 min at 4°C, and the samples were precipitated with 15% TCA for 1 hour on ice with subsequent centrifugation at 16,100 rcf for 30 min at 4°C. Pellets were dissolved in SDS loading buffer with 2 mM PMSF and analyzed by SDS PAGE and Western blotting.

2.2.5.4 Synthesis of radiolabelled proteins and their import into isolated mitochondria

For the *in vitro* protein synthesis mRNA was synthesized with SP6 mMESSAGE mMACHINE® Kit according to the manufacturer's instructions. PCR products amplified from yeast genomic DNA served as templates for transcription reaction. SP6 polymerase binding site was introduced with the forward primer. For Cox26 transcription three C-terminal methionine residues were added to the template with the reverse primer. The open reading frame of *ATG32* was cloned into pGEM®-4Z vector under control of SP6 promoter for RNA synthesis. In this case plasmid DNA directly served as a template.

Proteins of interest were translated in the presence of [^{35}S] methionine from synthesized mRNA using Flexi® Rabbit Reticulocyte Lysate System according to manufacturer's instructions. Cox5a lysate was produced with the TnT® SP6 Quick Coupled Transcription/Translation System using *COX5A* ORF in a pTNT^{TM} vector, as a template. Translation reaction was started by addition of [^{35}S] methionine (4 μCi/μl). After incubation at 30°C for 90 min the reaction was quenched with 16 mM cold methionine for 2 min and 0.5 M saccharose was added to the lysate prior to storage at -80°C.

Radiolabeled proteins were imported into mitochondria according to published procedures (Wiedemann et al., 2006). Isolated yeast mitochondria were re-suspended in 1 mg/ml import buffer. If import reactions longer that 15 min were performed, 6.25 mM creatin phosphate and 125 µg/ml creatin kinase were added as the energy regeneration system (Wrobel et al., 2013). In control samples membrane potential was dissipated with 1% AVO mix. Import reaction took place at 25°C with mild agitation after addition of 10% lysate for indicated time points. Import was stopped with 1% AVO mix on ice. After the import, if not indicated otherwise, mitochondria were treated with 0.1 mg/ml Proteinase K (PK) for 10 min on ice to digest unimported precursor. PK was inhibited by addition of 2 mM PMSF for 10 min on ice. Mitochondria were re-isolated by centrifugation at 16,100 rcf for 10 min at 4°C, and washed twice with SEM buffer supplemented with 2 mM PMSF. Prepared samples were then re-suspended in 1 mg/ml SDS loading buffer for SDS PAGE analysis, or solubilized for BN PAGE as described in section 2.2.5.2. After run SDS and BN gels were stained with Coomassie, dried and exposed to Storage Phosphor screens for detection of radiolabeled proteins. Signals were detected with Storm 820 Gel Scanner. Quantification was done with the ImageQuant TL Software with rolling ball background substruction.

2.2.5.5 Mitochondrial oxygen consumption measurements

Oxygen consumption rates (OCR) were assessed in isolated yeast mitochondria with the Oxygraph 2k. Measurements were done at 30°C with stirring (750 rpm) with 10 µg of mitochondria in 2 ml MAS buffer. The state III respiration was induced afer addition of 1 mM NADH and 1 mM ADP (Barrientos et al., 2009). OCR was calculated using a 5 min slope and expressed as nmol/ml/min/mg of mitochondrial protein. The measurement was repeated 4 times and the mean values were taken.

2.2.5.6 Mitochondrial enzyme activity assays

Enzymatic activities of mitochondrial complexes were determined spectrophotometrically with Cary® 50 UV-Vis spectrophotometer as described previously (Vukotic et al., 2012). Malate dehydrogenase (MDH) activity was assesed as oxaloacetate dependent NADH oxidation at 340 nm with NADH extinction coefficient of 6.3 mM^{-1}cm^{-1}. The measurement was done in 1 ml MDH activity assay buffer after addition of 25 µg of mitochondria. Activity of NADH-cytochrome *c* reductase (complex III) and cytochrome c oxidase

(complex IV) was determined as the rate of cytochrome *c* reduction and oxidation, respectively. The measurement was done at 550 nm in 1 ml activity assay buffer. For oxidase activity cytochrome *c* was reduced with sodium dithionite. As an electron donor for the complex III 0.5 mM NADH was added to the buffer. The measurement was started upon addition of 50 µg of mitochondria. For the reductase activity measurement the mitochondria were treated with 10 mM KCN to inhibit complex IV activity. The extinction coefficient of reduced cytochrome *c* at 550 nm was 21.84 $mM^{-1}cm^{-1}$. The activity was determined as the rate of absorbance change. Each measurement was repeated five times and the mean values were taken.

2.2.5.7 Measurement of mitochondrial ROS production

Mitochondrial ROS production was assessed with 2',7'-dichlorodihydrofluorescein diacetate (H_2DCFDA), a compound that becomes fluorescent upon ROS oxidation (Giorgio et al., 2005). Fluorescence of 200 µM H_2DCFDA upon incubation with 100 µg of isolated yeast mitochondria was measured in 500 µl ROS assay buffer using F-7000 fluorescence spectrophotometer. Excitation and emission wavelength was set to 495 nm and 525 nm, respectively. Data was collected at 0.5 s intervals during 10 min.

2.2.6 Recombinant protein techniques

2.2.6.1 Recombinant protein expression in *E. coli*

Cytosolic domain of Atg32 (amino acids 1-343) under control of lacZ promoter in pETDuet^{TM}-1 vector was recombinantly expressed in *E. coli*. A C-terminal polyhistidine tag containing 10 histidine residues was inserted for downstream purification. Competent cells of Rosetta(DE3)pLysS strain were transformed with the obtained construct ($Atg32_{CYT}$-His_{10}) as described in section 2.2.1.3. For protein expression cultures propagated as described in section 2.2.1.1 were grown to OD_{600} of 0.5, and induced with 1 mM IPTG at 30°C for 4 hours under constant shaking. Cells were pelleted for 15 min at 4,000 rcf, washed once with H_2O and frozen at -20°C for storage.

2.2.6.2 Solubility test for recombinant proteins

For solubility check of recombinant proteins expressed in *E. coli*, 20 ml of culture before and after induction with IPTG was taken. Cells were pelleted for 5 min at 4,000 rcf, re-

suspended in 1 ml *E. coli* cracking buffer, and incubated at 4°C for 30 min with constant shaking. Cells were opened using Sonicator Cell Disruptor W-220F during three pulses of 30 sec with incubations on ice for 1 min between the pulses. Obtained sample was centrifuged at 16,000 rcf for 10 min at 4°C and divided into supernatant and pellet. The pellet was then re-suspended in 1 ml H$_2$O. Samples of 100 µl were taken for SDS PAGE analysis before (total), and after the centrifugation (soluble, pellet). Samples were mixed with 4x SDS loading buffer, and analyzed by SDS PAGE and Coomassie staining.

2.2.6.3 Preparation of E. coli lysates for protein purification

To lyse *E. coli* cells expressing the protein of interest, frozen cell pellet was re-suspended in 10 ml/g cracking buffer and the cells were opened with EmulsiFlex C5 at 1,000 bar. Passage was repeated three times until cell suspension became clear. Insoluble material was removed by centrifugation at 18,000 rcf for 20 min at 4°C, and the cleared supernatant was filtered through 0.2 µm cellulose acetate filters.

2.2.6.4 Metal affinity chromatography for purification of recombinant proteins

Recombinant proteins bearing histidin tag were purified with 1 ml HisTrap HP column using ÄKTA Purifier 10. Filtered cell lysate was loaded on the column at 0.5 ml/min flow rate. The column was equilibrated with 10 column volumes of HisTrap buffer prior to loading. The column with bound protein was washed with approximately 20 column volumes of HisTrap buffer until a stable base line of UV absorbance at 280 nm was reached. Proteins were eluted from the column with a 0-100% linear gradient of HisTrap buffer containing 500 mM imidazole at 1 ml/min flow rate. Peak fractions with highest UV absorbance at 280 nm were analyzed with SDS PAGE and Coomassie staining. The cleanest fractions were combined and dialyzed in the MonoS buffer stirring overnight at 4°C. For dialysis the elution fractions was transferred to 7K MWCO SnakeSkin™ dialysis tubing.

2.2.6.5 Ion exchange chromatography

For purification proteins were loaded on 5 ml Resourse S column, pre-equilibrated with MonoS buffer at the flow rate of 0.5 ml/min. The column was washed with 10 column volumes of MonoS buffer at 1 ml/min until the base line of UV absorbance at 280 nm was reached. Bound proteins were eluted in 10 column volumes with a 0-50% linear gradient of

MonoS buffer with 1 M NaCl. The buffer was then exchanged on a 5 ml HiTrap Desalting column to MonoS buffer. Fractions containing purified protein were analyzed by SDS PAGE and Coomassie staining for impurities, combined, and concetrated with Amicon® Ultra-4 centrifugal filter unit with 10 kDa MWCO according to manufacturers specifications. Protein concentration was measured with Bradford assay and 20% glycerol was added to the samples. After aliquoting the protein was flesh-frozen in liquid nitrogen and stored at -80°C.

2.2.7 Bioinformatics tools

Mitochondrial targeting signals were predicted using the MitoProt Server (Claros and Vincens, 1996). Protein transmembrane regions were predicted by TMpred (Hofmann and Stoffel, 1993). Molecular weight of proteins was calculated with Protein Molecular Weight (http://www.bioinformatics.org/sms/prot_mw.html) on the basis of a protein sequence. Homology search was done with nucleotide BLAST (Altschul et al., 1990).

3 Cox26 is a novel subunit of the yeast cytochrome *c* oxidase

3.1 Biogenesis of the respiratory supercomplexes

Although the composition of respiratory chain supercomplexes has been intensively studied, little is known about their biogenesis. Pulse-chase experiments suggest that the supercomplexes are established through direct interaction of respiratory chain complexes during their assembly (Acin-Perez et al., 2008). In human cells, sequential incorporation of supercomplex components was observed, starting with an intermediate of complex I, to which subunits and subassemblies of complexes III and IV are added. Integration of the complex I catalytic core finishes respirasome formation (Moreno-Lastres et al., 2012).

A search for specific supercomplex assembly factors lead to the discovery of the yeast Rcf1 and Rcf2 proteins that mediate supercomplex formation (Vukotic et al., 2012; Chen et al., 2012; Strogolova et al., 2012). A mammalian factor, SCAF1 protein, has also recently been identified (Lapuente-Brun et al., 2013). Another component required for supercomplex assembly and stability is cardiolipin, a hallmark phospholipid of the inner mitochondrial membrane (Zhang et al., 2002; Pfeiffer et al., 2003; Zhang et al., 2005; Brandner et al., 2005; McKenzie et al., 2006).

3.2 Identification of Cox26 as a novel protein associated with supercomplexes in yeast *Saccharomyces cerevisiae*

Recently, an uncharacterized protein, Cox26 (YDR119W-A), was described as a putative supercomplex component. Its supercomplex association was suggested based on co-migration studies using BN PAGE (Helbig et al., 2009) and proteomic analysis of isolated respirasomes (Vukotic et al., 2012). Since Cox26 function was not characterized in any of the previous studies, the goal of this thesis was to address its role with regard to supercomplex formation.

3.3 Cox26 is a mitochondrial inner membrane protein

3.3.1 Cox26 co-localizes with mitochondria

Cox26 was previously found in the mitochondrial proteome (Helbig et al., 2009). The protein consists of 66 amino acids with the calculated molecular mass of 7 kDa. A homology search using BLAST (NCBI) did not retrieve any promising candidates among mammal or fungal species. Cox26 sequence analysis using MitoProt (Claros and Vincens, 1996) suggested a putative presequence with a 99% probability. In addition, the protein contains a predicted transmembrane span deduced from the primary sequence (Figure 8).

Fig. 8 Schematic representation of the Cox26 protein. Numbers indicate amino acid residues; grey box represents the putative presequence (PS); black box represents the predicted transmembrane span (TM).

To confirm the mitochondrial localization of Cox26, its C-terminus was endogenously tagged with GFP. Mitochondria of the yeast strain expressing Cox26^{GFP} were stained with the fluorescent dye MitoTracker® Orange CM^{TM}Ros and the cells were analyzed by microscopy. The GFP signal could be superimposed with the stained mitochondrial membranes (Figure 9), indicating that Cox26 is targeted to mitochondria.
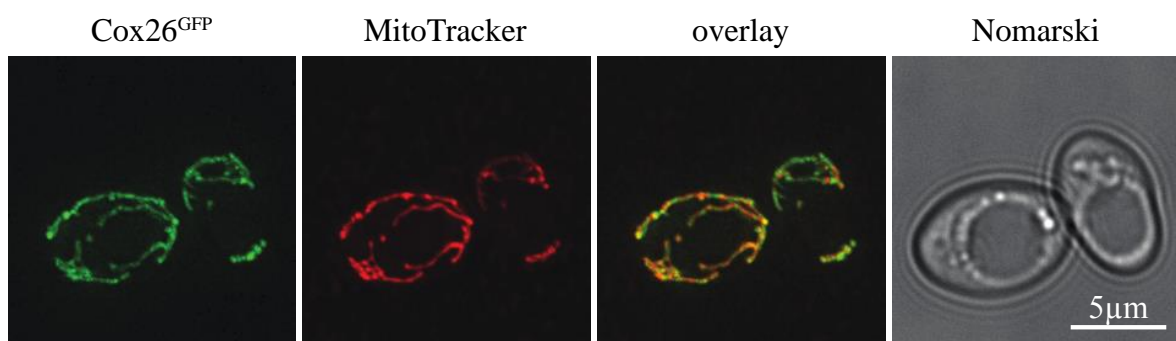

Fig. 9 Cox26 localizes to mitochondria. Yeast expressing Cox26^{GFP} were cultured to mid-log phase in synthetic medium containing 2% galactose. Mitochondria were visualized with the MitoTracker® Orange probe. Representative images were obtained by fluorescence microscopy. Microscopy analysis was performed by Dr. L. Juris in the Institute of Cellular Biochemistry, Göttingen.

3.3.2 Mitochondrial topology of Cox26

To confirm the membrane association of Cox26, it was chromosomally tagged with a C-terminal FLAG peptide. Mitochondria were subsequently isolated and subjected to carbonate extraction. Upon alkaline treatment, a peripheral inner membrane protein Tim44 detached from the membrane, and was recovered in the soluble fraction. In contrast, Cox26^{FLAG} remained in the pellet, similar to the integral inner membrane protein Tim21 (Figure 10.A).

To address the mitochondrial sub-localization of Cox26, protease protection experiments were performed. The FLAG tag on the C-terminus of Cox26 remained stable in intact mitochondria upon protease treatment, unlike Tom40, a protein of the outer mitochondrial membrane. However, Cox26 was degraded in mitoplasts after outer membrane disruption, similar to the inner membrane protein Tim21 (Figure 10.B). Finally, a matrix protein Tim44 could only be digested after solubilization with triton X-100 (Figure 10.B).
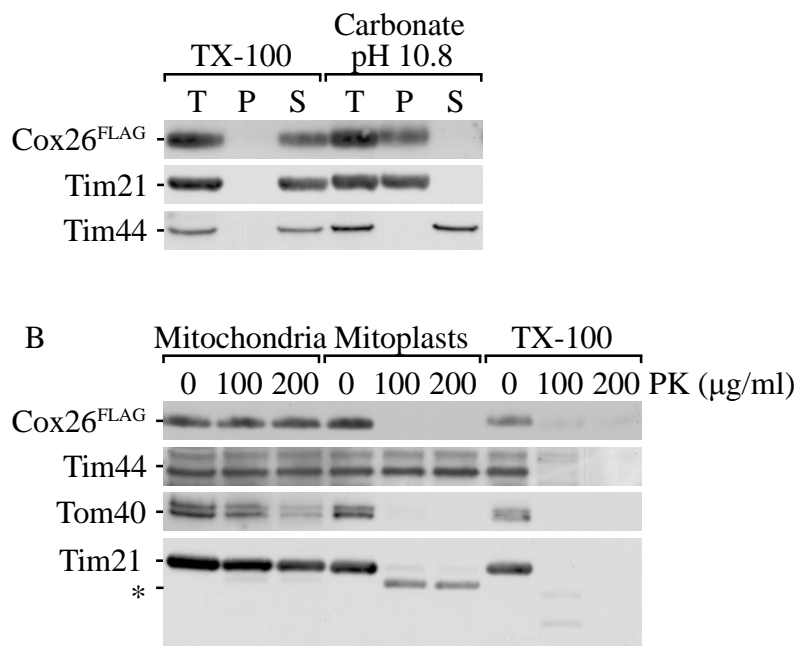

Fig. 10 Cox26 is an integral protein of the inner mitochondrial membrane. (A) Carbonate extraction of Cox26^{FLAG} mitochondria. Total (T), pellet (P), and supernatant (S) samples after extraction with carbonate buffer (pH 10.8) or solubilization with triton X-100 (TX-100) were analyzed by SDS PAGE and immunoblotting. **(B)** Submitochondrial localization of Cox26^{FLAG}. Intact, swollen (mitoplasts), or triton X-100 lysed (TX-100) mitochondria were treated with indicated amounts of proteinase K (PK). The asterisk (*) indicates a degradation product of Tim21.

In conclusion, Cox26 is an integral protein of the mitochondrial inner membrane, with its C-terminus exposed to the IMS, and the N-terminus localized to the matrix.

3.3.3 Import analysis of Cox26

Since Cox26 contains a predicted N-terminal presequence, its import into the mitochondria was assessed. The Cox26 protein was synthesized *in vitro* using rabbit reticulocyte lysate in the presence of $[^{35}S]$ methionine for radioactive labeling. The first and only methionine residue of Cox26 is presumably removed after translation, or as a result of presequence processing (Li and Chang, 1995; Yang et al., 1988). Hence, three additional methionine residues were added for labeling to the C-terminus of Cox26. The obtained construct was imported into isolated yeast mitochondria, followed by proteinase K (PK) treatment to remove non-imported precursor (Figure 11). An accumulation of radiolabeled protein with increasing import times could be observed, indicating protein translocation into the organelle. Import of Cox26 was independent of the membrane potential ($\Delta\psi$).
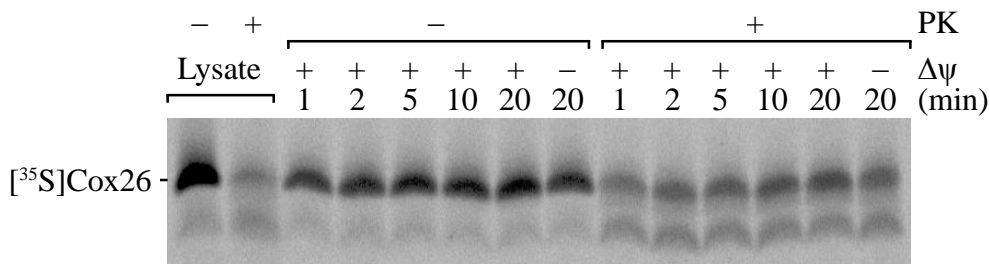
Fig. 11 Cox26 is imported into the mitochondria. Cox26 labeled with $[^{35}S]$ methionine was imported into isolated mitochondria for the indicated times in the presence or absence of membrane potential ($\Delta\psi$). After the import mitochondria were treated with proteinase K (PK) as indicated. Reticulocyte lysate with radiolabelled Cox26 protein was loaded as a control.

The presequence in precursor proteins is typically removed by the matrix processing peptidase (MPP), generating a faster-migrating mature form. After Cox26 import, no size shift due to presequence removal was detected, despite the predicted cleavage site. A smaller fragment was present after PK digestion, however it could also be found in the PK-treated lysate, indicating a PK-resistant form of the protein rather than a processing event.

3.4 Cox26 is associated with respiratory chain supercomplexes

3.4.1 Cox26 co-isolates supercomplex components

A proteomic approach identified Cox26 as a protein putatively associated with respiratory supercomplexes (Vukotic et al., 2012). To confirm the mass spectrometry results, Cox26 was chromosomally tagged with a C-terminal ZZ tag (Cox26^{ZZ}). Cox26^{ZZ}

was isolated together with its binding partners from digitonin-solubilized mitochondria using IgG affinity chromatography. Digitonin is a mild detergent that preserves even weak protein interactions within respirasomes. $Cox4^{ZZ}$, a structural subunit of the cytochrome *c* oxidase (COX), was used as a positive control. Eluates were then analyzed by SDS PAGE and Western blotting.

Subunits of complex III (Rip1, Qcr8), and complex IV (Cox1, Cox4, Cox5a, Cox13) were co-purified with $Cox26^{ZZ}$ in similar amounts, when compared to the $Cox4^{ZZ}$ isolation (Figure 12). At the same time Atp2, a component of F_1F_o ATP synthase, was not detected in the eluted fraction. This finding confirmed the interaction of Cox26 with respiratory chain supercomplex components.
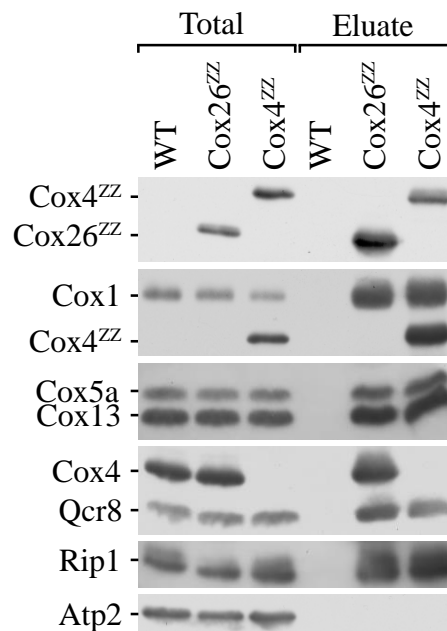

Fig. 12 Cox26 interacts with the supercomplexes. Complexes containing $Cox26^{ZZ}$ and $Cox4^{ZZ}$ were isolated from digitonin-solubilized mitochondria using IgG chromatography and analyzed by SDS PAGE and immunoblotting. Total (10%), eluate (100%).

3.4.2 Cox26 co-migrates with respiratory chain supercomplexes on BN PAGE

To analyze Cox26-containing complexes, $Cox26^{ZZ}$ mitochondria were solubilized with digitonin and subjected to BN PAGE and Western blotting. OXPHOS components were visualized using antibodies directed against complex III (Qcr8), complex IV (Cox4), and complex V (Atp5) subunits. $Cox26^{ZZ}$ was detected using the peroxidase anti-peroxidase (PAP) antibody. As a result, $Cox26^{ZZ}$ was present in two high molecular weight

assemblies, co-migrating with the supercomplexes (Figure 13). Supporting this observation, respirasomes in Cox26^{ZZ} mitochondria appeared shifted on BN PAGE when compared to the wild type, presumably due to the size difference caused by addition of the ZZ-tag.
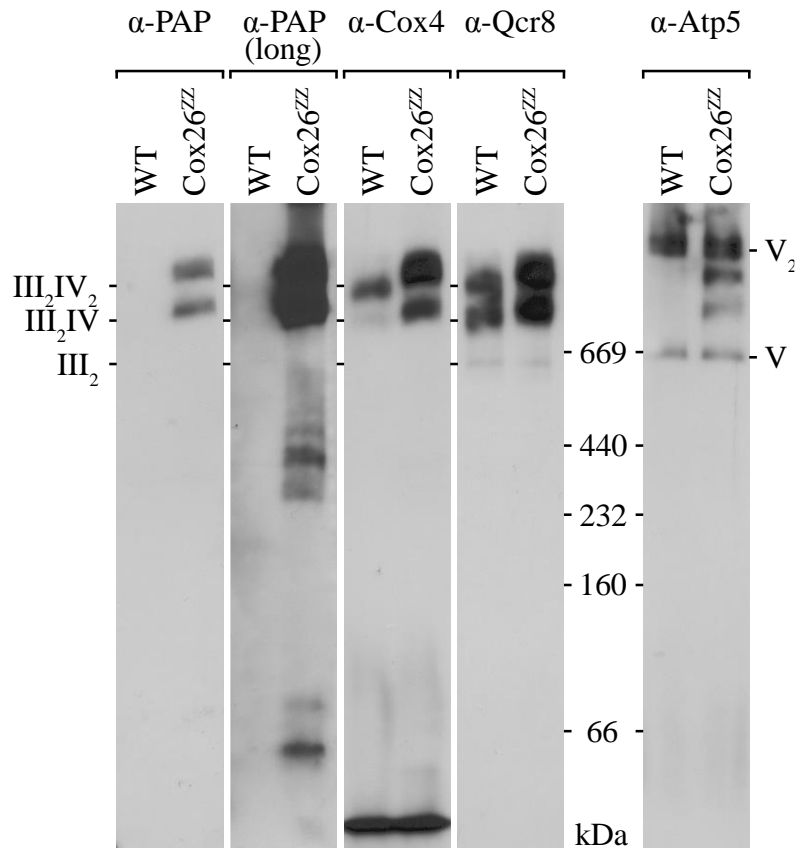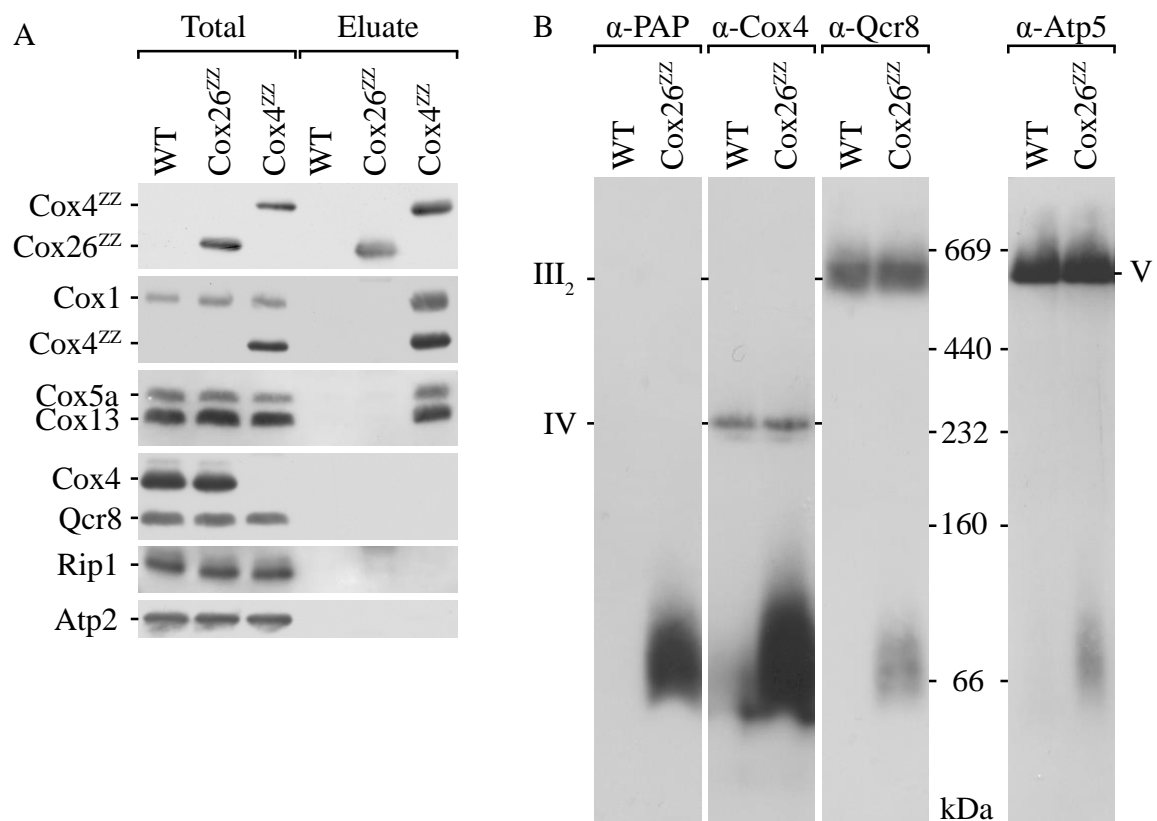

Fig. 13 Cox26 is a supercomplex component. Digitonin-solubilized wild type (WT) and Cox26^{ZZ} mitochondria were analyzed by BN PAGE and Western blotting.

After a long exposure, several complexes containing Cox26^{ZZ} could be observed between 230 and 440 kilodaltons (kDa). These complexes could correspond to the monomeric forms of complex IV (Vukotic et al., 2012), suggesting that Cox26 is a part of cytochrome *c* oxidase within the respirasomes. No complexes matching the dimer of complex III could be detected after PAP decoration. Moreover, the dimer did not appear shifted in size in the Cox26^{ZZ} strain, unlike the supercomplexes. This indicates that the Cox26 interaction with complex III components, detected previously (Figure 12), is mediated through association of complex III and complex IV in the supercomplexes.

3.5 Cox26 is a subunit of the cytochrome *c* oxidase (COX)

3.5.1 Cox26 dissociates from the respiratory chain upon DDM solubilization

To verify the association of Cox26 with cytochrome *c* oxidase, dodecylmaltoside (DDM) was used for mitochondrial solubilization. This detergent leads to dissociation of respirasomes into individual respiratory complexes (Schägger and Pfeiffer, 2000). Following solubilization, Cox26^{ZZ} was isolated and in these conditions no interaction of Cox26^{ZZ} with the components of complex III or complex IV was detected, although Cox4^{ZZ} retained its association with the COX. To support this observation, BN PAGE analysis of DDM-solubilized Cox26^{ZZ} mitochondria was performed. Intact complex IV monomer and complex III dimer could be seen on the gel, however Cox26^{ZZ} was not present in any high molecular weight assemblies (Figure 14).


Fig. 14 Cox26 is lost from the respiratory chain after solubilization with DDM. (A) Complexes containing Cox26^{ZZ} and Cox4^{ZZ} were isolated from DDM-solubilized mitochondria using IgG chromatography and analyzed by SDS PAGE and immunoblotting. Total (10%), eluate (100%). **(B)** DDM-solubilized wild type (WT) and Cox26^{ZZ} mitochondria were analyzed by BN PAGE and Western blotting.

This poses the question as to whether Cox26 is a supercomplex-specific subunit that does not interact with individual complexes, or whether DDM treatment releases Cox26 from the respiratory chain.

3.5.2 Cox26 isolates monomeric COX, but not the dimer of complex III

To confirm that Cox26 is primarily a COX subunit, Cox26-associated complexes were isolated from digitonin-solubilized $Cox26^{ZZ}$ mitochondria. Complexes were eluted natively from the IgG sepharose matrix by TEV protease treatment and analyzed by BN PAGE and Western blotting. Eluate fractions were decorated for subunits of complex III (Rip1) and complex IV (Cox1). $Cox26^{ZZ}$ was visualized in the input with a PAP antibody. After elution, untagged Cox26 could not be detected due to the lack of an antibody. Supercomplexes containing both Cox1 and Rip1 could be observed in the elution (Figure 15). They appeared to be shifted in size compared to the input samples due to the loss of ZZ-tag.
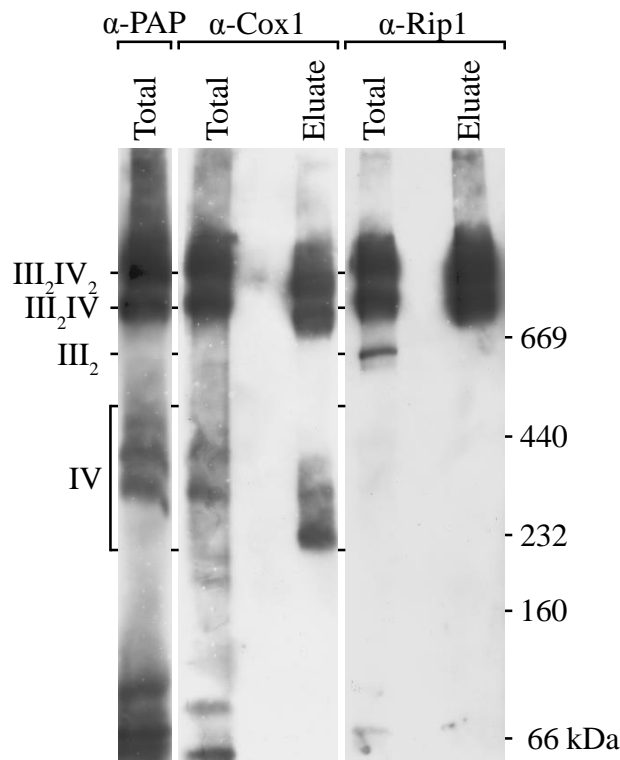
Fig. 15 Cox26 associates with cytochrome *c* oxidase within the supercomplexes. Complexes containing $Cox26^{ZZ}$ were isolated from digitonin-solubilized mitochondria using IgG chromatography and eluted natively upon cleavage with TEV protease. Total and elution samples were analyzed by BN PAGE and immunoblotting. Total (3%), eluate (100%).

In addition to the supercomplexes, Cox1 was also present in several complexes in the range of 220-440 kDa, which represent the monomeric forms of COX. However, the complex III dimer was not detected in the elution. This finding demonstrates that Cox26 directly associates with complex IV and not complex III within the respirasomes.

3.5.3 Cox26 assembly requires Cox4 but not the Cyt1 protein

To further support Cox26 association with complex IV, Cox26 assembly after import was monitored in mutant mitochondria. Complexes containing radiolabeled Cox26 were separated by BN PAGE and detected by autoradiography. For this experiment, mitochondria were isolated from either *cyt1Δ* or *cox4Δ* yeast strains. In the absence of Cyt1, complex III formation is abolished, while Cox4 absence prevents formation of mature complex IV.

In wild type mitochondria Cox26 assembles into two protein complexes of high molecular weight (Figure 16). These complexes correspond to respirasomes, as confirmed by Western blotting analysis using the Cox4 antibody. In contrast, Cox26 was present in two smaller complexes in the range of 230 to 440 kDa in the *cyt1Δ* mitochondria. These complexes co-migrate with the monomeric forms of complex IV, as visualized by Western blot analysis. Despite similar import efficiency, Cox26 assembly was abrogated in *cox4Δ* mitochondria. This proves that Cox26 is a part of the supercomplexes and a cytochrome *c* oxidase subunit in yeast.

### 3.5.4 Cox26 assembly does not require presence of the late COX subunits

Formation of the cytochrome *c* oxidase is an intricate process, during which COX components are incorporated in a sequential manner. To analyze at which point Cox26 joins the complex, the radiolabelled protein was imported into mutant mitochondria lacking COX subunits and mitochondrial complexes were analyzed by BN PAGE. Upon deletion of Cox4, the association of Cox26 with complex IV is abolished. Therefore, yeast strains deficient in Rcf1, Cox13, and Rcf2, which succeed Cox4 during cytochrome *c* oxidase assembly, were used in this experiment. These proteins are incorporated consecutively, with Rcf1 assembling first, followed by Cox13, and finally Rcf2 (Vukotic et al., 2012).
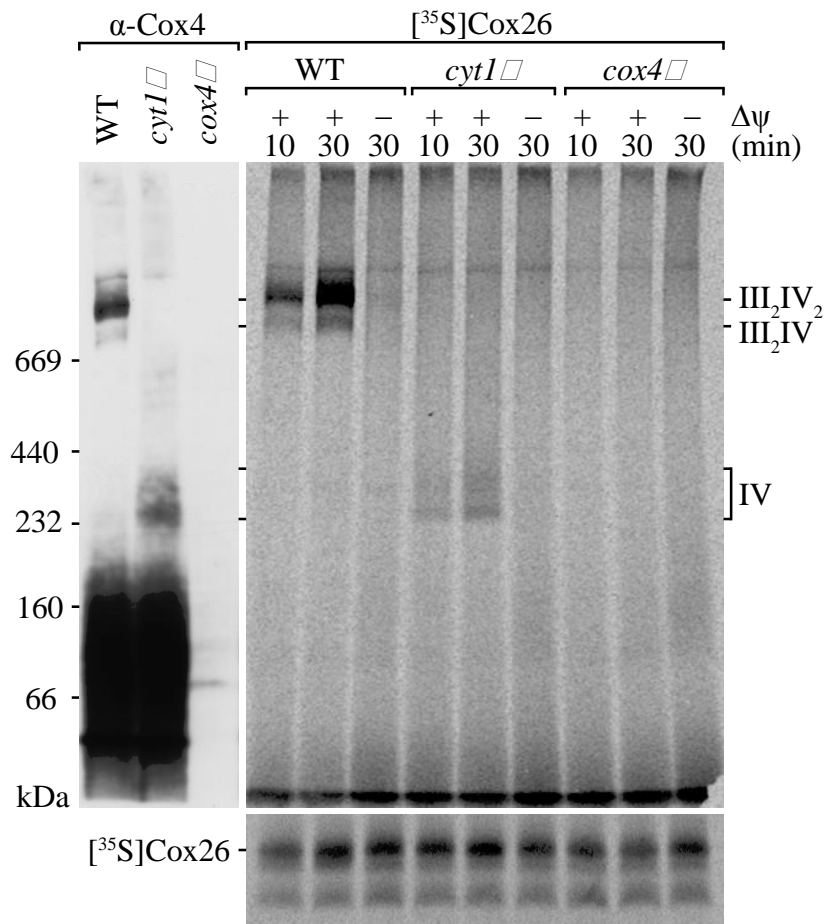
Fig. 16 Cox26 is a component of the cytochrome *c* oxidase. Radiolabeled Cox26 was imported into wild type (WT), *cyt1Δ*, and *cox4Δ* mitochondria in the presence or absence of membrane potential (Δψ) for indicated times. Samples were treated with Proteinase K (PK), solubilized in 1% digitonin buffer, and analyzed by BN PAGE and digital autoradiography. For comparison, solubilized mitochondria from corresponding strains were analyzed by BN PAGE, followed by western blotting and immunodecoration.

In the *rcf1Δ* background Cox26 was assembled with a wild type efficiency, however it showed a different complex distribution (Figure 17). This is due to the fact that Rcf1 is required for supercomplex formation, and there are less III_2IV_2 and more III_2IV complexes in the *rcf1Δ* mutant (Vukotic et al., 2012). Wild type-like assembly of Cox26 into the supercomplexes was observed in the Rcf2-deficient mutant. The absence of Cox13 resulted in a reduced incorporation of Cox26 into the respirasomes, but did not lead to a complete assembly block. Cox26 import levels were comparable in all tested strains, as can be inferred from the SDS PAGE analysis.

In conclusion, Cox26 is integrated into the supercomplex either prior to, or independent from Rcf1, Cox13, and Rcf2 proteins.
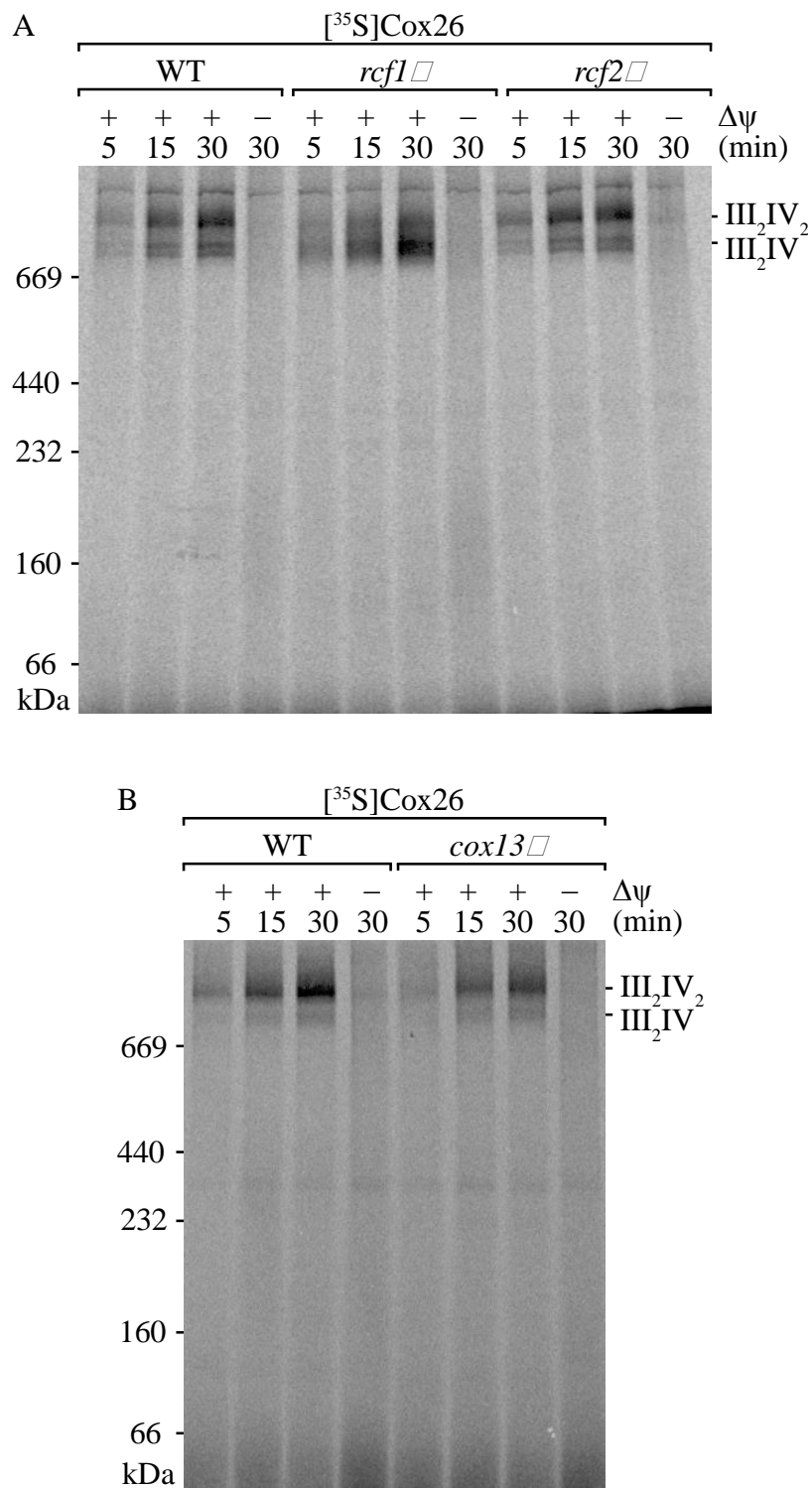
Fig. 17 Cox26 is incorporated into COX independent from Rcf1, Rcf2, and Cox13. Radiolabeled Cox26 was assembled **(A)** in wild type (WT), *rcf1Δ, rcf2Δ,* and **(B)** in *cox13Δ* mitochondria in the presence or absence of membrane potential ($\Delta\psi$) for the indicated times. Non-imported protein was removed with Proteinase K (PK), and mitochondria were solubilized in 1% digitonin buffer, and analyzed by BN PAGE and digital autoradiography.

3.6 Cox26 deletion affects supercomplex formation

3.6.1 *cox26Δ* mutant does not display a growth defect on non-fermentable medium

As Cox26 associates with the supercomplexes and is a part of the cytochrome *c* oxidase, the lack of Cox26 could affect oxidative phosphorylation. To characterize Cox26 function, a *COX26* deletion strain was generated. Dysfunction of the respiratory chain in yeast can result in a growth defect when cells are forced to respire. Thus, growth of the *cox26Δ* mutant was assessed on fermentable (YP Glucose) and non-fermentable (YP Glycerol) medium at various temperatures. As a control, a respiratory-deficient *cox4Δ* strain was used.

COX4 deletion resulted in the strong growth defect on non-fermentable media at all temperatures. However, the absence of Cox26 did not compromise respiratory growth in these conditions (Figure 18).
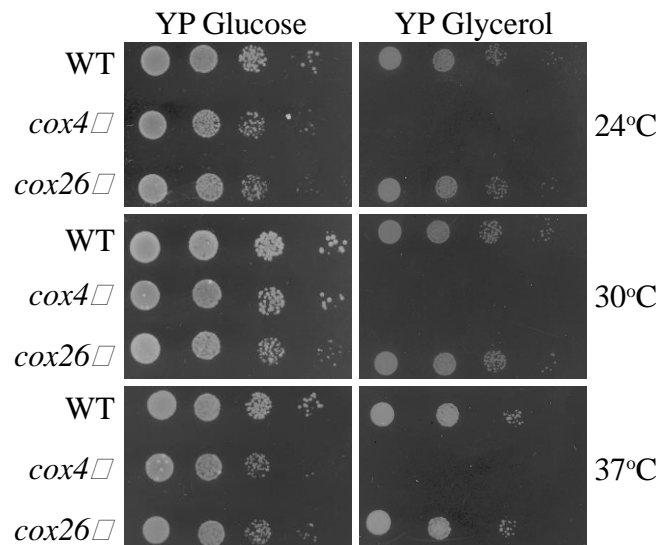

Fig. 18 Cox26 is not essential for respiratory growth in yeast. Wild type (WT), *cox4Δ*, and *cox26Δ* yeast cells were spotted in serial 10-fold dilutions on plates containing YP medium, supplemented with glucose or glycerol, and grown at the indicated temperatures for 2–5 days.

3.6.2 Mitochondrial protein levels remain unaltered in *cox26Δ*

To determine whether *COX26* deletion affects protein levels of respiratory chain supercomplex constituents, the steady state abundance of mitochondrial proteins in the

cox26Δ mutant was analyzed by SDS PAGE and immunoblotting. No significant differences between WT and *cox26Δ* mitochondria could be detected for any of the tested proteins (Figure 19).
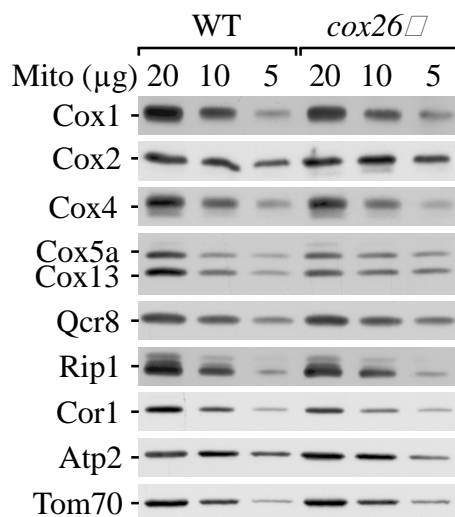

Fig. 19 Steady state protein levels of *cox26Δ* mitochondria are similar to wild type. Isolated wild type (WT) and *cox26Δ* mitochondria were subjected to SDS PAGE and analyzed by Western blotting.

3.6.3 BN PAGE analysis of *cox26Δ* mitochondria shows decreased levels of supercomplexes

Despite the fact that the steady state levels of supercomplex-associated proteins were not altered in the absence of Cox26, the protein could be important for supercomplex formation or stability. Thus, the supercomplex organization was analyzed in *cox26Δ* mitochondria by BN PAGE and immunoblotting. Indeed, the amount of III_2IV_2 complexes was lower in the absence of Cox26, as visualized using antibodies against complex IV (Cox1, Cox4) and complex III (Rip1, Qcr8) subunits (Figure 20.A). Simultaneously, accumulation of monomeric COX and free complex III_2 could be detected in the mutant strain. F_1F_o ATP synthase levels remained unaffected, as observed upon Atp5 decoration.

To test whether the decreased levels of supercomplexes were caused by the lack of individual respiratory complexes, a BN PAGE of DDM-solubilized mitochondria was performed. Immunoblotting did not reveal any significant alterations of complex III, complex IV, or complex V amounts between the wild type and *cox26Δ* mitochondria (Figure 20.B).
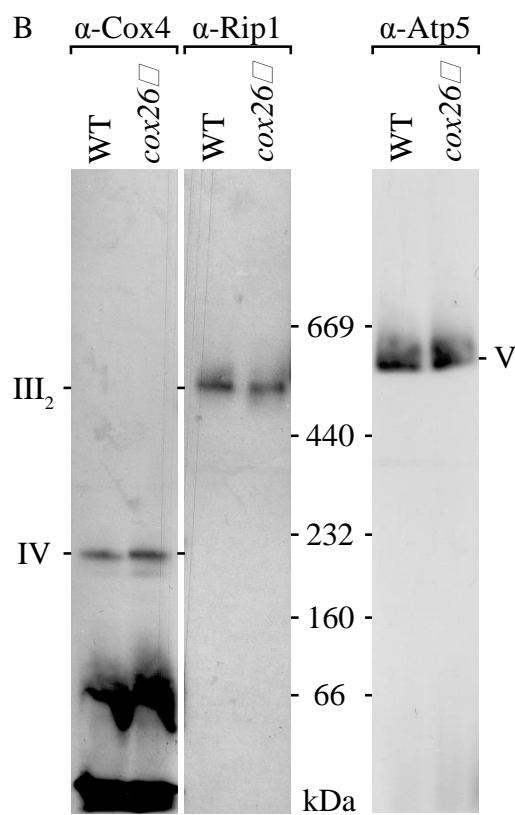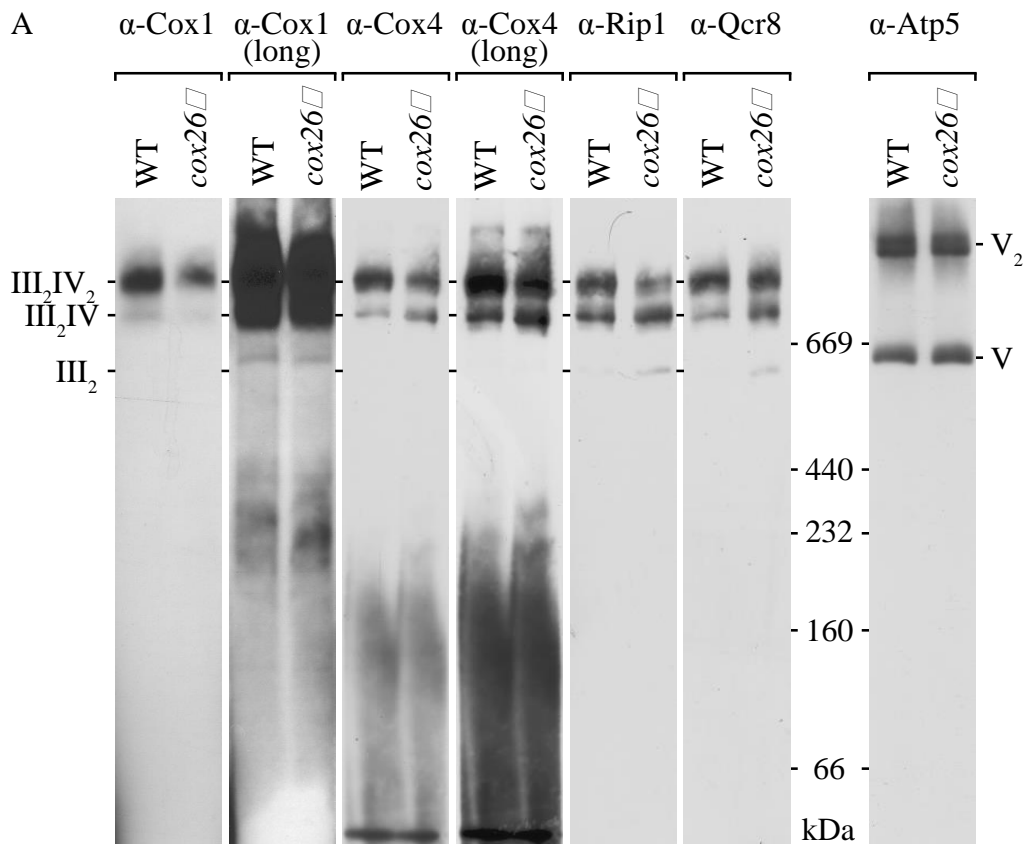
Fig. 20 *COX26* deletion leads to the loss of supercomplexes. (A) Digitonin- or **(B)** DDM-solubilized wild type (WT) and *cox26Δ* mitochondria analyzed by BN PAGE and immunoblotting.

3.6.4 Decreased supercomplex assembly and accumulation of COX in *cox26Δ* mitochondria

The loss of supercomplexes upon *COX26* deletion could be explained either by decreased stability or by inefficient production of the respirasomes. To monitor supercomplex biogenesis, assembly of radiolabeled Cox13 and Rcf1 after import was assessed by BN PAGE and autoradiography. Both Cox13 and Rcf1 are nuclear-encoded COX subunits that join the holo-enzyme at the late stage of COX maturation (Vukotic et al., 2012). Both Rcf1 and Cox13 were assembled to a lesser extent into the supercomplexes in the absence of Cox26, despite similar import efficiency (Figure 21). Interestingly, accumulation of Cox13 in low molecular weight complexes (250 – 400 kDa) was observed in *cox26Δ* mitochondria. These complexes could correspond to the mature monomeric COX or its sub-assemblies.
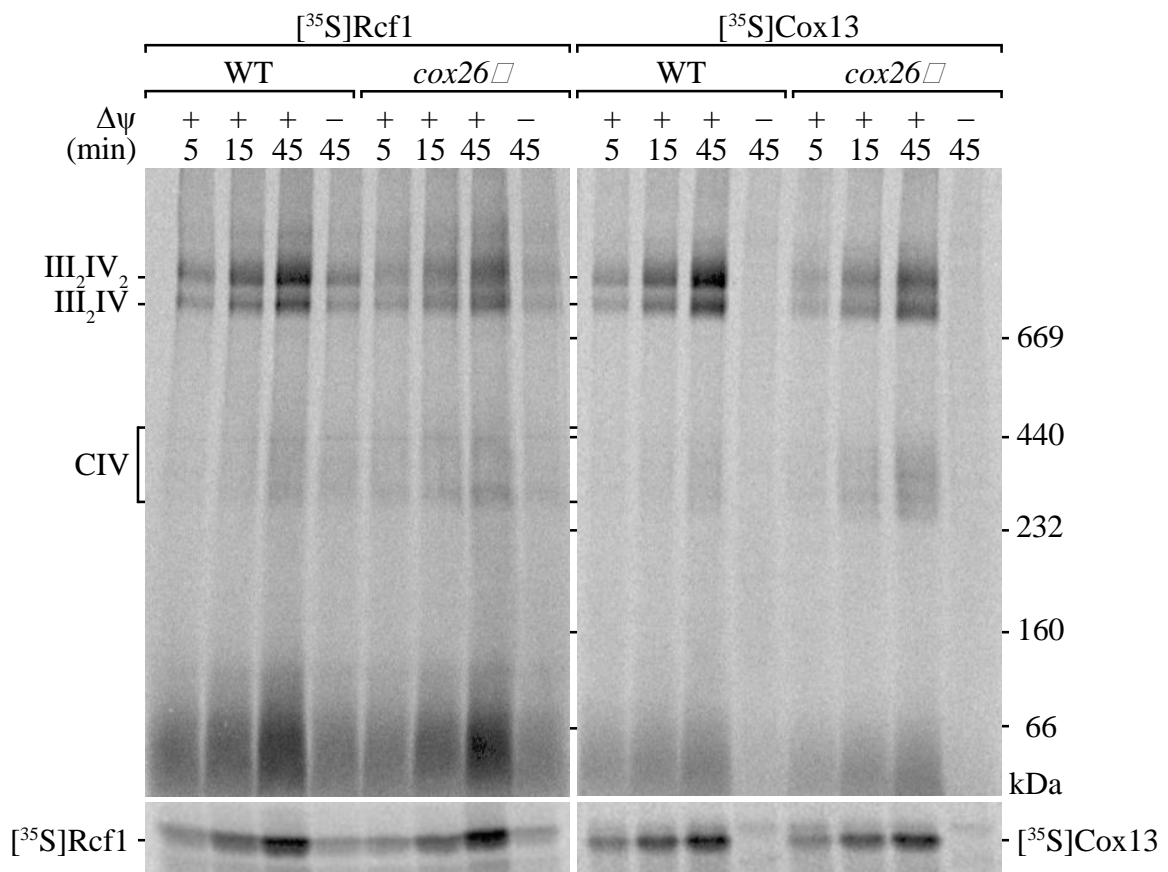
Fig. 21 COX26 deletion impairs supercomplex formation and leads to the accumulation of mature COX. Radiolabeled Rcf1 and Cox13 were assembled in isolated wild type (WT) and *cox26Δ* mitochondria in the presence or absence of membrane potential (Δψ) for the indicated times and treated with proteinase K (PK) to remove the non-imported precursors. Digitonin-lysed samples were analyzed by BN PAGE or SDS PAGE and digital autoradiography.

In conclusion, although the steady state levels of individual respiratory complexes are not affected, the absence of Cox26 clearly disturbs supercomplex formation.

3.7 COX assembly intermediates accumulate in the absence of COX26

The current model describes separate assembly lines for the mitochondria-encoded subunits Cox1, Cox2, and Cox3, which together constitute the catalytic core of COX (McStay et al., 2013). Previous studies suggest that Cox1 maturation is a starting point for COX formation, while Cox2 and Cox3 are incorporated into the enzyme at the later stages (Bestwick et al., 2010). During synthesis of the holoenzyme, these subunits progress through several intermediates, which accumulate if the downstream biogenesis step is blocked (Mick et al., 2010). Therefore, the increased levels of free complex IV observed previously (Figure 20.A and Figure 21) could result from alterations in COX biogenesis or could represent an accumulation of early assembly intermediates

Cox5a is a part of the Cox1 assembly pathway, involved in formation of an early assembly intermediate – the COA complex (Wielburski and Nelson, 1983; Herrmann and Funes, 2005; Fontanesi et al, 2006; Mick et al., 2011). To distinguish between the accumulation of early assembly intermediates and mature complex IV in *cox26Δ*, assembly of radiolabeled Cox5a after import was monitored by BN PAGE and autoradiography. While import rates were similar in the wild type and mutant mitochondria, Cox5a assembly was greatly enhanced in *cox26Δ* (Figure 22.A). Cox5a accumulated in two complexes of approximately 230 – 400 kDa that represent the COA complexes.

Prior to its association with Cox5a, Cox1 interacts with the Cox14 and Coa3 assembly factors, (Mick et al., 2010). Later on, Shy1 is included into the complex (Mick et al., 2007). To analyze the early steps of Cox1 biogenesis, COA complexes were visualized by immunodecoration for Cox1 assembly factors (Cox14, Coa3, and Shy1) after BN PAGE. Accumulation of COA complexes was observed in *cox26Δ* mitochondria, consistent with the previous result (Figure 22.B).

In summary, respirasome formation is compromised in the absence of *COX26*, leading to the accumulation of mature COX and its early assembly intermediates.
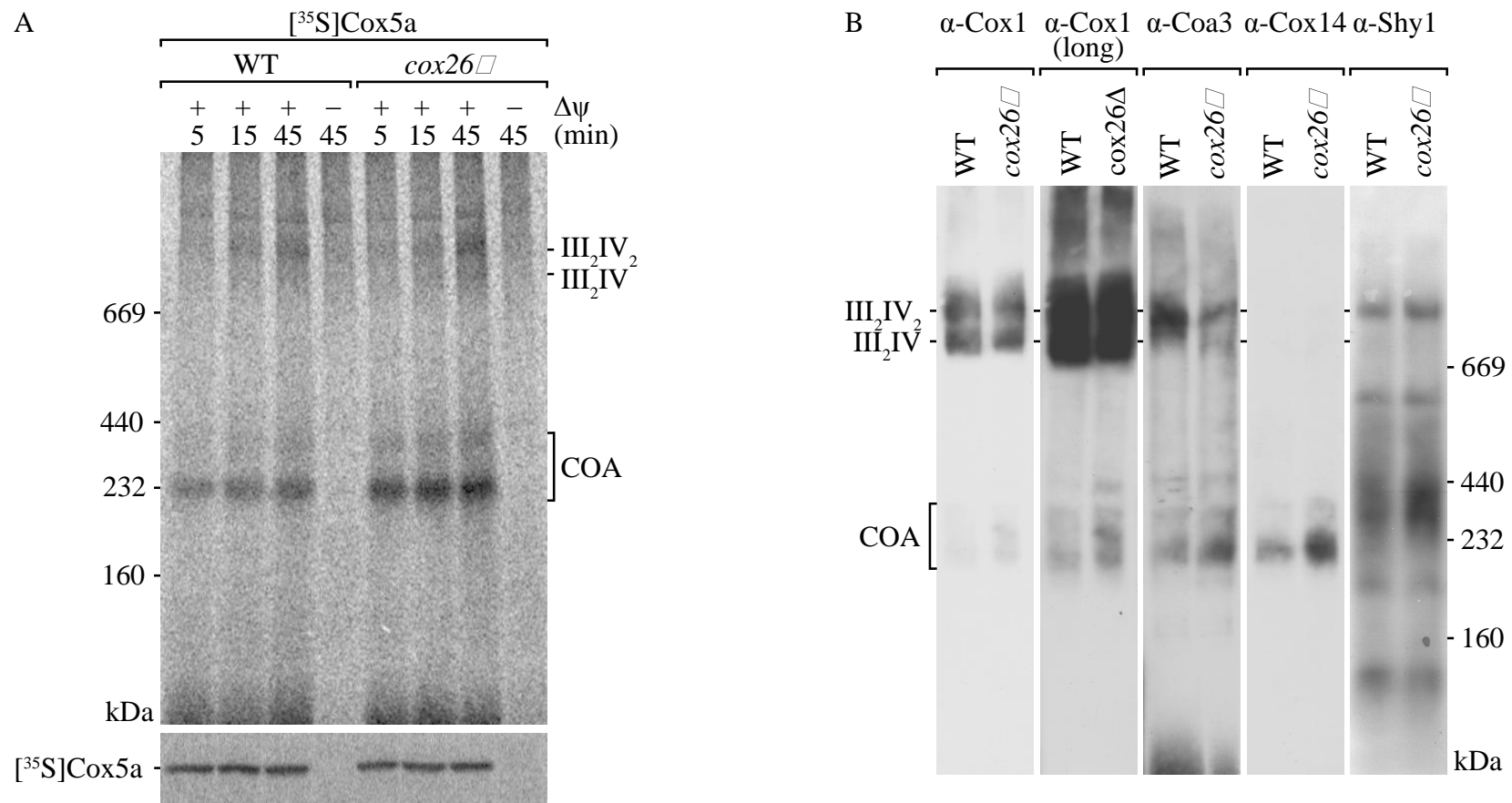
Fig. 22 Lack of Cox26 leads to an increase in COA complex levels. (A) Radiolabeled Cox5a was assembled in isolated wild type (WT) and *cox26Δ* mitochondria in the presence or absence of membrane potential (Δψ) for the indicated times and treated with proteinase K (PK) to remove the non-imported precursors. Digitonin-lysed samples were analyzed by BN PAGE or SDS PAGE and digital autoradiography. **(B)** Wild type (WT) and *cox26Δ* mitochondria were lysed in 1% digitonin buffer, subjected to BN PAGE, and analyzed by Western blotting.

3.8 Cox26 absence does not alter respiratory efficiency

3.8.1 Supercomplexes in *cox26Δ* exhibit decreased COX activity

Supercomplexes promote efficient respiration (Vukotic et al., 2012), thus a decrease in respirasome amounts can be associated with reduced enzymatic activity. To test this assumption, in-gel activity staining of OXPHOS complexes was performed. Isolated mitochondria from wild type and *cox26Δ* strains were solubilized in digitonin, and mitochondrial complexes were separated by BN PAGE. Active complexes were visualized by formation of the colored reaction products. Oxidation of the cytochrome *c* by COX is coupled to reduction of diaminobenzidine, a red-colored compound that precipitates on the active complexes. F_1F_o ATP synthase activity is reflected in the accumulation of the white-colored $Pb_3(PO)_4$, generated due to the ATP hydrolysis. To ensure equal loading, total protein amounts were compared after Coomassie staining.

COX activity staining was significantly lower in the III_2IV_2 supercomplex of *cox26Δ* mitochondria (Figure 23.A). Concurrently, the mutant showed increased amounts of active COX monomers, which appeared to be shifted in size. On the contrary, complex V activity remained unaltered in the mutant.

Both complex III and complex IV contribute to the activity of the respirasomes. Thus, activity reduction of the individual complexes could explain the observed decrease in supercomplex activity. To address this in more detail, supercomplexes were dissociated by DDM solubilization and activity staining was performed. Monomeric COX was stained with the same efficiency in the mutant and the wild type mitochondria (Figure 23.B).
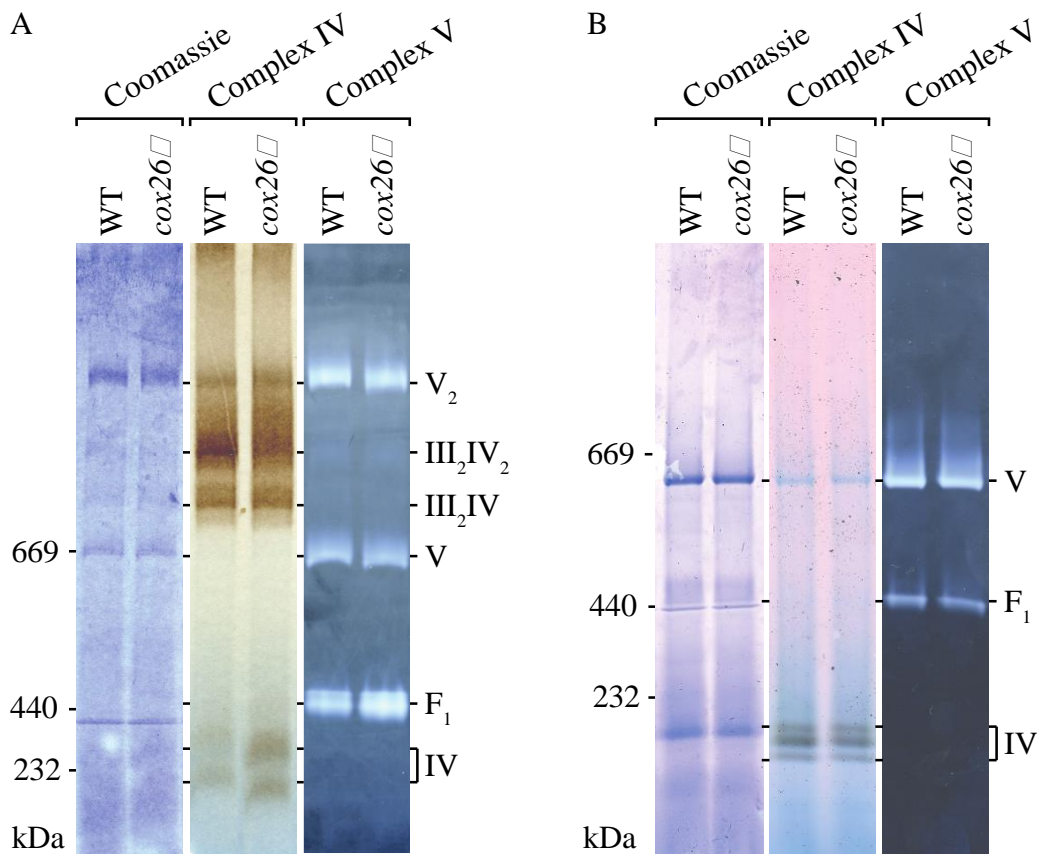
Fig. 23 Less active COX associates with the supercomplexes in the *cox26Δ* mutant. In-gel activity staining of cytochrome *c* oxidase (Complex IV) or F_1F_o ATP synthase (Complex V) in **(A)** digitonin- or **(B)** DDM-solubilized mitochondria from wild type (WT) and *cox26Δ* strains resolved by BN PAGE. Samples were stained with Coomassie as a loading control.

3.8.2 Activity of the respiratory enzymes in *cox26Δ* mitochondria is slightly reduced

Since in-gel activity staining is a semi-quantitative method, specific enzyme activities of respiratory chain complexes were determined in a spectrophotometric approach using isolated mitochondria.

Activities of complex III (cytochrome *c* reductase) and complex IV (cytochrome *c* oxidase) were identified as a change in absorbance due to cytochrome *c* reduction and oxidation, respectively. Malate dehydrogenase (MDH) was chosen as an internal control, because its activity should not be affected by alterations of the respiratory chain complexes. NADH oxidation upon conversion of oxaloacetate to malate was monitored in this assay.

Activity of the respiratory chain complexes in the *cox26Δ* mutant was slightly lower, while MDH activity was similar to the wild type (Figure 24).

77
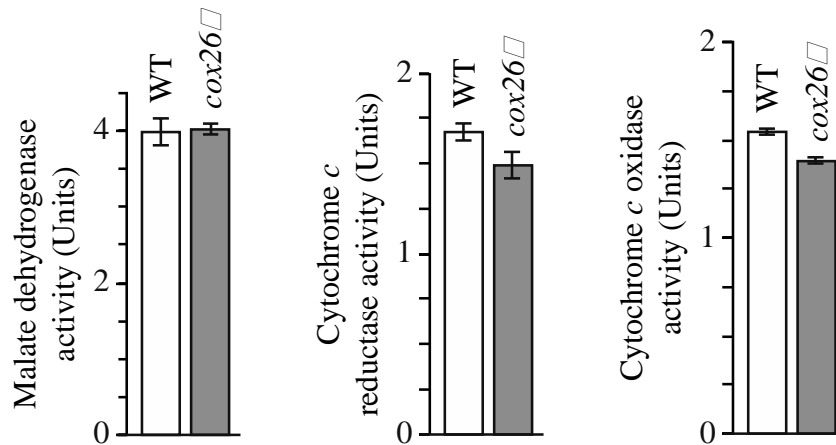
Fig. 24 Cox26-deficient respiratory complexes exhibit lower enzymatic activity. Enzyme activities of NADH-cytochrome *c* reductase, cytochrome *c* oxidase, and malate dehydrogenase were measured in the isolated wild type (WT) and *cox26Δ* mitochondria. The averages of five replicate measurements are given (SEM, n=5).

3.8.3 Reduction of the oxygen consumption rate is observed in Cox26-deficient mitochondria

The impaired supercomplex formation in *cox26Δ* observed previously (Figure 20.A and Figure 21), could affect electron transfer efficiency and have a more profound outcome on mitochondrial respiration.

To assess the respiration efficiency of the *cox26Δ* mutant its O_2 consumption rate (OCR) was compared to that of the wild type. OCR depends on respiratory chain activity since substrate oxidation is coupled to O_2 reduction by complex IV. For OCR measurements, isolated mitochondria in phosphate-containing buffer are introduced into the oxygraph chamber. After addition of the substrate (NADH) and excess ADP, mitochondria enter state 3 respiration, leading to a rapid increase in O_2 uptake (Barrientos et al., 2009). OCR of isolated wild type and *cox26Δ* mitochondria was monitored with an OROBOROS-2k oxygraph after addition of ADP and NADH. Mutant OCR was 90% of that of the wild type (Figure 25). This finding is in accordance with the mild decrease in enzymatic activity of the respiratory chain complexes.

Taken together, our results suggest that the absence of Cox26 does not have a dramatic effect on respiration and enzymatic activity of the respiratory chain despite inadequate supercomplex formation.
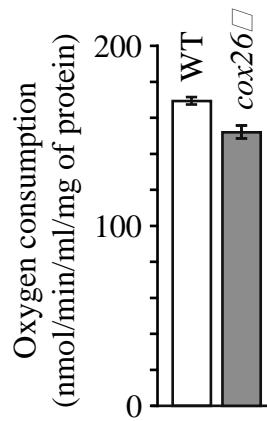
Fig. 25 Lack of Cox26 leads to a modest decrease in the oxygen consumption rate. Oxygen consumption of wild type (WT) and *cox26Δ* mitochondria was monitored with the OROBOROS oxygraph. The graph represents an average of four replicate measurements (SEM, n=4).

3.8.4 Cox26 absence leads to decreased ROS levels without affecting hydrogen peroxide-sensitivity of the cells

In the course of oxidative phosphorylation, electrons are transferred by the different complexes of the respiratory chain in a series of redox reactions. Electron leak from reduced cofactors and their subsequent interaction with molecular oxygen leads to the production of reactive oxygen species (ROS), mainly represented by the superoxide. Within the electron transport chain, complexes I and III are considered to be the major supply of superoxide anions, generating ROS during their catalytic cycles (Kowaltowski et al., 2009; Brand, 2010). Inefficient supercomplex formation can lead to increased ROS levels (Vukotic et al., 2012; Maranzana et al., 2013). Therefore mitochondrial ROS production was monitored fluorometrically using the H$_2$DCFDA (dichlorodihydrofluorescein diacetate) probe that becomes fluorescent upon oxidation.

Compared to the wild type, *cox26Δ* mitochondria had a slightly reduced rate of ROS generation (Figure 26.A). To address whether this decrease was significant for cellular function, wild type and mutant strains were treated with hydrogen peroxide and evaluated for growth. This peroxide is deleterious to mutants with high ROS production, such as *rcf1Δ* (Vukotic et al., 2012). Thus the lower ROS levels in *cox26Δ* cells could potentially lead to increased survival upon peroxide treatment. Yet, growth rates of the mutant and the wild type strains appeared to be similar (Figure 26.B). In contrast, *rcf1Δ* cells were unable to grow after peroxide exposure.
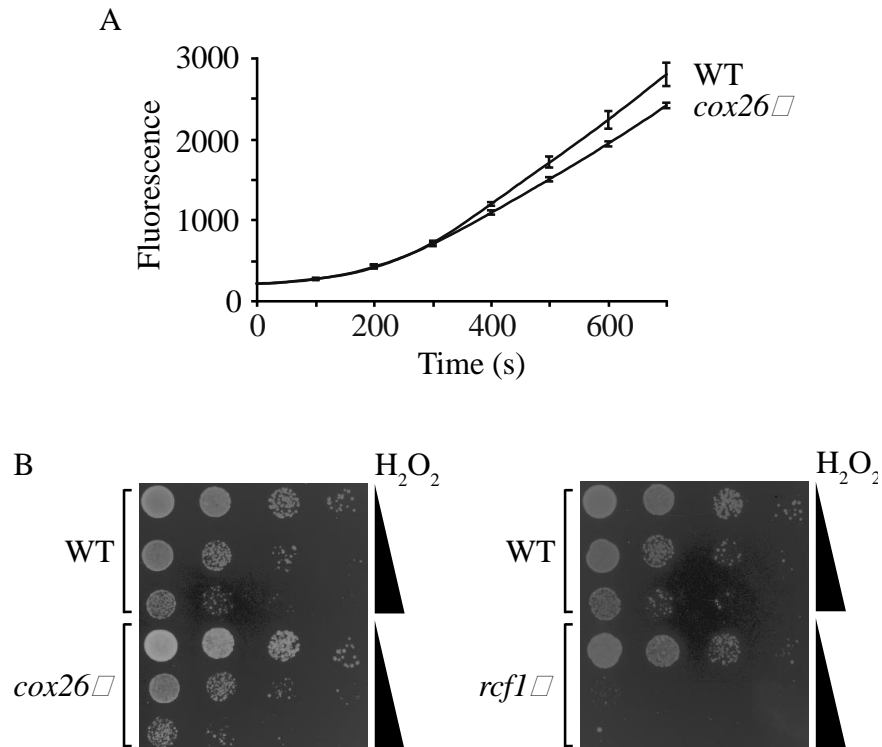
Fig. 26 *COX26* deletion is associated with a lower rate of ROS production but does not influence H₂O₂ sensitivity. (A) Mitochondrial ROS was monitored fluorometrically in wild type (WT) and *cox26Δ* mitochondria. The average of four replicate measurements is shown (SEM, n=4). **(B)** Growth test of wild type (WT), *cox26Δ*, *rcf1Δ* strains, treated with increasing concentrations of H₂O₂ (0 mM, 2.5 mM, 5 mM) for 2 hours at 30°C. Cells were plated onto YP medium supplemented with glucose and incubated for 2 days at 30°C.

These results indicate that deletion of *COX26* does not lead to increase in mitochondrial ROS levels due to supercomplex dissociation.

4 Dissecting the interaction network of the yeast mitophagy receptor Atg32

4.1 Composition of mitophagic signaling assemblies

In the yeast *S. cerevisiae*, mitophagy is known to be triggered by external stimuli, such as starvation, but the role of intra-mitochondrial pathways in mitophagy has not been addressed. It is plausible that the yeast mitophagy receptor Atg32 acts as a mitochondrial sensor, activating mitophagy in response to physiological changes within the organelle. Despite ongoing research in this area, it is not well understood, how both internal and external mitophagic cues are conveyed to the receptor and what are the major players in the mitophagic signaling cascade. To address this problem I wanted to identify Atg32 interaction partners by purification of receptor complexes, combined with mass spectrometry analysis of the complex composition.

4.2 Isolation of Atg32 receptor complexes from yeast cells

4.2.1 Establishing an Atg32 isolation procedure from cryolysed yeast powder

Atg32 is localized on the mitochondrial surface, spanning the width of the outer mitochondrial membrane. Thus it can potentially interact not only with the autophagic machinery in the cytosol, but also with mitochondrial proteins within the IMS that relay mitophagic signals from the organelle. To investigate receptor assemblies, which consist of both cytosolic and mitochondrial components, an isolation procedure from whole cells was established. For this purpose, Atg32 was chromosomally tagged with a ZZ tag. Tag addition can impede protein interactions due to steric hindrance. To account for this, two yeast strains with ZZ tag fused to either the N- or C-terminus of Atg32 (^{ZZ}Atg32 or Atg32^{ZZ}) were created for downstream applications. Additionally, a truncated Atg32 variant, lacking the cytosolic domain (^{ZZ}Atg32$_{IMS}$), was included in the analysis to specifically pull down mitochondrial interaction partners. To enable chromosomal integration of an N-terminal tag, a constitutive NOP1 promoter was introduced upstream of the protein sequence (Figure 27.A).

Signaling complexes are often transient and unstable. To shorten handling time and preserve complex integrity, a fast cell disruption method using a cryogenic mill was devised. During this procedure, samples are pulverized at liquid nitrogen temperatures, thus inhibiting proteolytic turnover. After grinding, ZZ-tagged Atg32 was purified, together with its binding partners, from digitonin-solubilized yeast powder using IgG affinity chromatography. Eluates were then analyzed by SDS PAGE and Western blotting. A wild type strain was used as a negative control for purification.

Atg32 was successfully isolated from yeast cells of all tagged strains that were tested in this experiment (Figure 27.B). Despite similar expression levels of the three constructs, the truncated Atg32 variant was much more abundant in the eluate. This could potentially be explained by different receptor degradation rates during the isolation procedure. Proteolysis is possibly prevented in the absence of Atg32 cytosolic domain, thereby resulting in higher amounts of the purified ^{ZZ}Atg32$_{IMS}$.
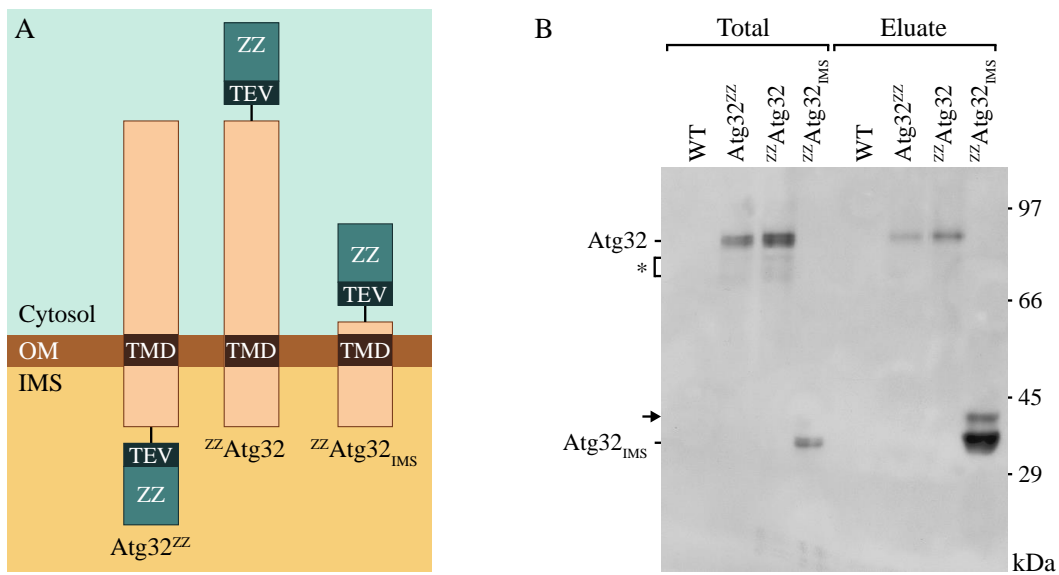
Fig. 27 Isolation of Atg32 signaling complexes. (A) Schematic representation of tagged Atg32 constructs. ZZ tag (ZZ) with a TEV protease cleavage site (TEV) was fused to a C- or N-terminus of Atg32. OM – outer membrane; IMS – intermembrane space; TMD – transmembrane domain. **(B)** Atg32 purification from yeast powder. ZZ-tagged Atg32 and its truncated version were isolated from cryolysed yeast powder by IgG chromatography. Samples were analyzed by SDS PAGE and Western blotting with the α-PAP antibody. * indicates unidentified Atg32 bands due to degradation or processing. Arrow indicates a possible modification product. Total and unbound (6%), eluate (100%).

4.2.2 Production of an anti-Atg32 antibody

To enable native elution for complex analysis, the ZZ tag can be cleaved from the protein using TEV protease. However, untagged Atg32 could not be detected due to the lack of specific antibody.

In order to generate an anti-Atg32 antibody, a corresponding antigen has to be produced for animal immunization. For this purpose, the cytosolic domain of Atg32 was cloned into a bacterial expression vector with a C-terminal His tag for downstream purification. The obtained construct ($Atg32_{CYT}$-His_{10}) was expressed in *E. coli* after IPTG induction, generating a soluble protein (Figure 28.A). His-tagged $Atg32_{CYT}$ was subsequently isolated via metal affinity chromatography and the resulting elution fractions were analyzed by SDS PAGE and Coomassie staining. In addition to the protein of interest, several other bands were detected on the gel, indicating the presence of contaminating proteins from the bacterial host (Figure 28.B). Therefore, the major elution fractions containing $Atg32_{CYT}$ were pooled together and further purified by ion exchange chromatography (Figure 28.C). The resulting sample was relatively pure and was used for immunization.

After antigen injection, serum was collected at different time points and used to prepare a primary antibody solution, which was tested for reactivity via immunoblotting. The pre-immune serum was used as a negative control. Anti-Atg32 serum recognized a protein in the expected size range in whole cell extracts from the wild type strain. The corresponding protein band was absent in the *atg32Δ* strain and was not detected by the pre-immune serum (Figure 28.D). Thus we have generated a specific antibody that is reactive against the cytosolic domain of Atg32.
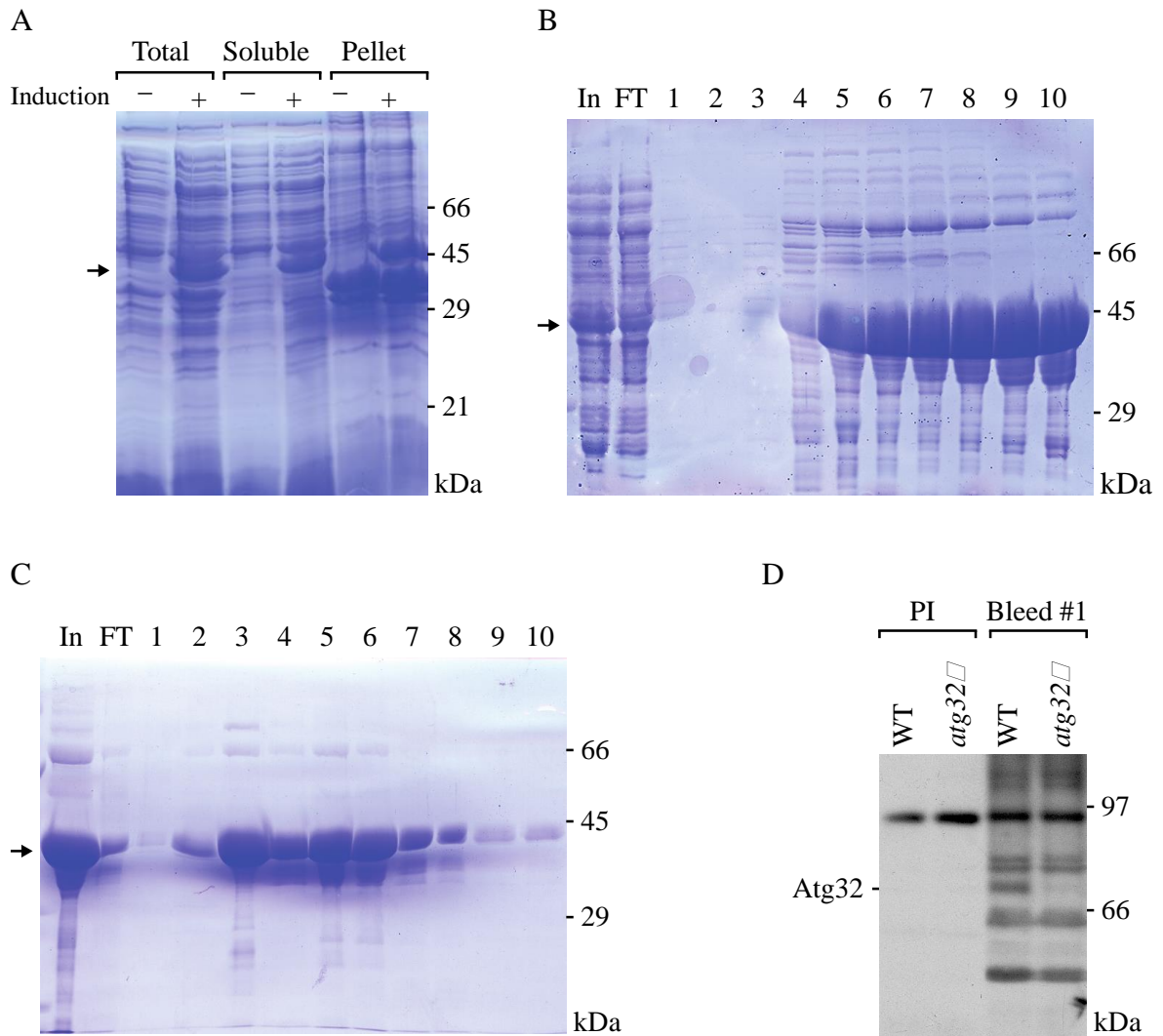
Fig. 28 Generation of Atg32-specific antibody. (A) Solubility test of the Atg32 cytosolic domain. Expression of the His_{10}-$Atg32_{CYT}$ was induced by treatment with 1 mM IPTG at 25°C. Samples were taken at 0 (−) and 4 hours (+) following induction. **(B)** Metal affinity chromatography and **(C)** ion exchange chromatography of $Atg32_{CYT}$-His_{10}. In – input, FT – flow-through. Numbers indicate elution fractions. Arrow indicates $Atg32_{CYT}$-His_{10}. **(D)** Antibody test for α-Atg32 serum. Whole cell extracts of wild type (WT) and *atg32Δ* strains decorated with α-Atg32 antibody. PI – preimmune serum.

4.2.3 Detection of Atg32 receptor complexes

The obtained anti-Atg32 antibody could now be used to visualize Atg32 assemblies and to monitor changes in their composition during the course of mitophagy. Receptor complexes were purified from cryolysed yeast cells grown under normal and mitophagy-inducing conditions. In the latter case, yeast were cultured to post-log phase, which is a known mitophagy trigger (Tal et al., 2007). Atg32^{ZZ} assemblies were isolated by IgG affinity chromatography, natively eluted via TEV protease cleavage, and analyzed by BN PAGE and immunoblotting. Atg32 could be successfully isolated together with its degradation and/or processing products (Figure 29.A). Since Atg32 could not be detected on the native gel (not shown), a second dimension (2D) SDS PAGE was performed. In this case, protein complexes resolved by BN PAGE in the first dimension were further separated using SDS PAGE in the second dimension. A complex of around 230 kDa was visible on a 2D PAGE in non-inducing conditions. When mitophagy was induced, complexes of smaller size (app. 140 kDa) could be detected, together with the free protein (around 66 kDa) (Figure 29.B). This suggests that Atg32 is part of a protein complex that dissociates upon mitophagy induction.
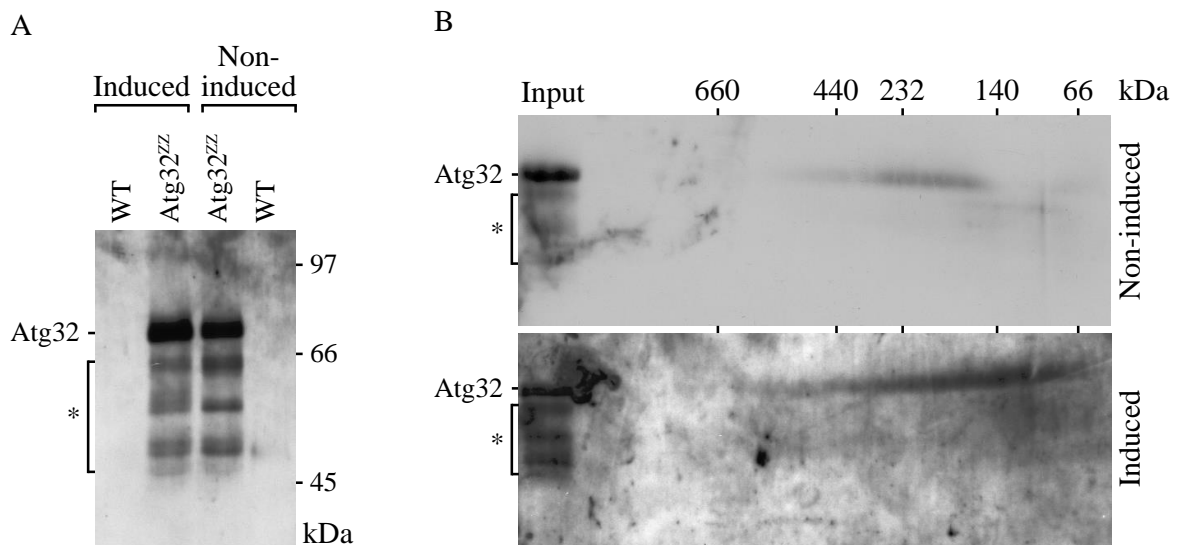
Fig. 29 Atg32 mitophagic signaling assemblies. Yeast cells were cultured in YPL medium for 12 hours (non-induced) or 72 hours (induced). Complexes containing Atg32^{ZZ} were isolated from digitonin-solubilized yeast powder using IgG chromatography and eluted natively upon cleavage with TEV protease. * indicates unidentified Atg32 bands due to degradation or processing. Immunoblots were decorated with α-Atg32 antibody. **(A)** SDS PAGE of elution fractions. **(B)** 2D BN PAGE/SDS PAGE of elution fractions. A fraction of the eluate, prior to BN PAGE, was taken as an input sample.

4.2.4 Atg32-associated assemblies in mitochondria

To further support Atg32 complex formation and to specifically focus on mitochondrial Atg32 receptor complexes, the assembly of radioactively labeled Atg32 after its import into mitochondria was analyzed. Atg32 was translated in the presence of [^{35}S] methionine using the cell-free rabbit reticulocyte lysate system and imported into isolated wild type yeast mitochondria. Protein translocation into the organelle could be monitored by visualizing an increase in radioactive signal over time. Atg32 import as expected was independent of membrane potential (Figure 30.A). After import, complexes containing radiolabeled Atg32 were resolved by BN PAGE and detected with autoradiography. Consistent with previous results (Figure 30.B), formation of a 230 kDa complex (C1) could be observed (Figure 30.B). Signal intensity of the complex declined during import, together with an increased formation of a high molecular weight complex (C2). The C2 complex was especially pronounced in mitochondria devoid of membrane potential (Figure 30.B).
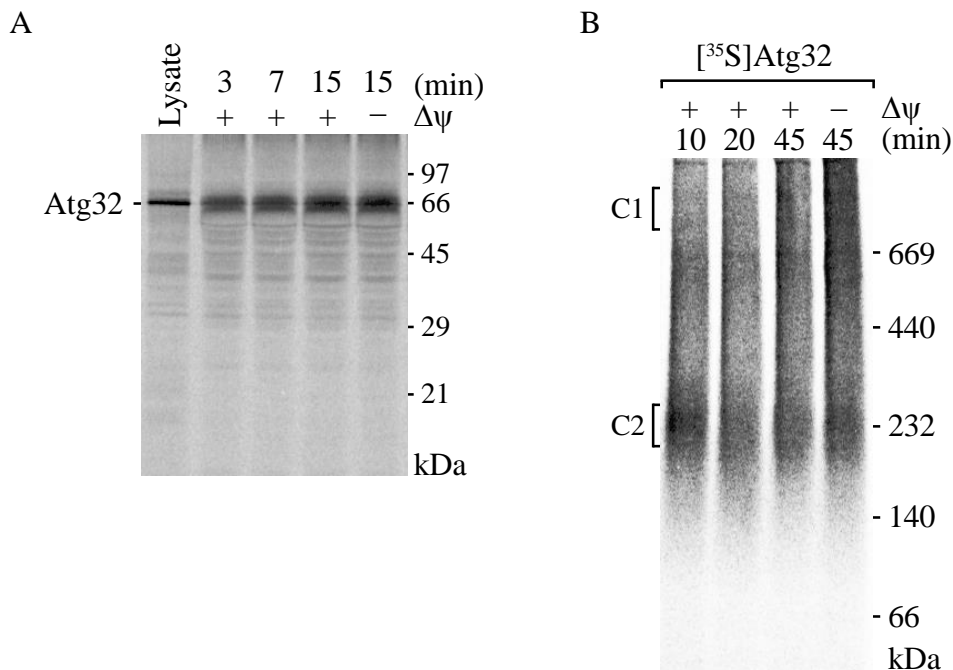
Fig. 30 Atg32 assembles into distinct complexes after mitochondrial import. Atg32 labeled with [^{35}S] methionine was imported into isolated mitochondria for the indicated times in the presence or absence of membrane potential ($\Delta\psi$). Reticulocyte lysate with radiolabelled Atg32 protein was loaded as a control. Autoradiogram of SDS PAGE **(A)** and BN PAGE **(B)** analysis. C1 and C2 indicate different complexes of Atg32.

4.2.5 Atg32 isolation specificity

These findings confirmed the presence of a mitochondrial Atg32 receptor complex, however, its composition remained unknown. To address this, the isolation specificity of Atg32 complex components was tested with the aim of further analysis by mass spectrometry. Signaling complexes, containing ZZ tagged Atg32, were purified from digitonin-solubilized yeast powder using IgG affinity chromatography. After native elution by TEV protease treatment, samples were analyzed by SDS PAGE and Western blotting. To test the specificity of the isolation procedure, part of the elution was stained with Coomassie after the gel run.

Despite successful purification, Atg32 could not be detected after Coomassie staining. Moreover, the elution contained many unspecific bands, which appeared both in the Atg32^{ZZ} and in the control samples (Figure 31). This shows that this technique does not provide sufficient isolation specificity and further optimization is required prior to mass spectrometry analysis.
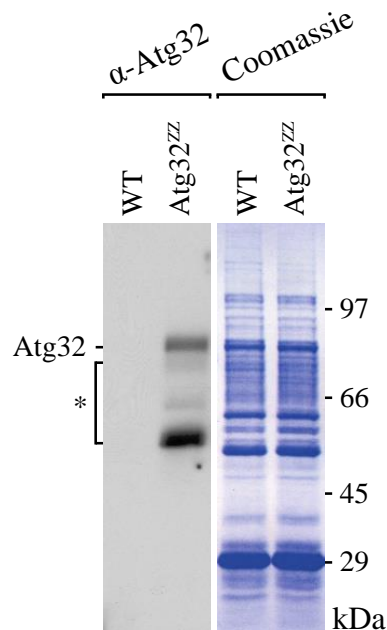
Fig. 31 Low specificity of Atg32 isolation procedure. Complexes containing Atg32^{ZZ} were isolated from digitonin-solubilized yeast powder using IgG chromatography and eluted natively upon cleavage with TEV protease. * indicates unidentified Atg32 bands due to degradation or processing.

## 4.3 Atg32 complex purification from isolated mitochondria

4.3.1 Overexpressed Atg32 is not detectable in mitochondria

Cell fractionation can decrease the high background of the isolation procedure, thus Atg32 was purified from isolated mitochondria. Since a band corresponding to the Atg32 protein was not visible following Coomassie staining of the elution fraction, it was hypothesized that the expression level of Atg32 was too low for detection. To increase expression, the endogenous promoter of ATG32 was replaced by the inducible GAL1 promoter. A triple hemagglutinin (HA) tag was chromosomally fused to the N-terminus of Atg32 for purification purposes. To address the role of the intra-mitochondrial module of Atg32, a HA-tagged construct, lacking the cytosolic domain (3HA-Atg32$_{IMS}$), was included in the analysis.

To determine sufficient levels of Atg32 expression, a time-course expression test was performed. The GAL1 promoter was induced by addition of galactose to the culture medium. Whole cell extracts were prepared from samples collected after 0, 1, 2, and 3 hours after induction and analyzed by SDS PAGE and immunoblotting. Both full-length and truncated Atg32 were successfully induced after the first hour of galactose addition (Figure 32.A). An induction period of two hours was chosen for subsequent studies.

To test the extent of Atg32 overexpression, whole cell extracts from *atg32Δ*, wild type and 3HA-Atg32 strains were probed with anti-Atg32 antibody after SDS PAGE and Western blotting. The truncated Atg32 construct was not included in this test due to the lack of the antigenic region. As can be seen from the blot, Atg32 under control of the GAL1 promoter was highly overexpressed after induction, when compared to the wild type strain (Figure 32.B).

To isolate mitochondria for receptor complex purification, yeast cells were treated with galactose and subjected to cell fractionation. The obtained mitochondrial fraction was analyzed by SDS PAGE and Western blotting. Surprisingly, and in contrast to Atg32$_{IMS}$, overexpressed full length Atg32 could not be detected, presumably due to protein degradation (Figure 32.C).
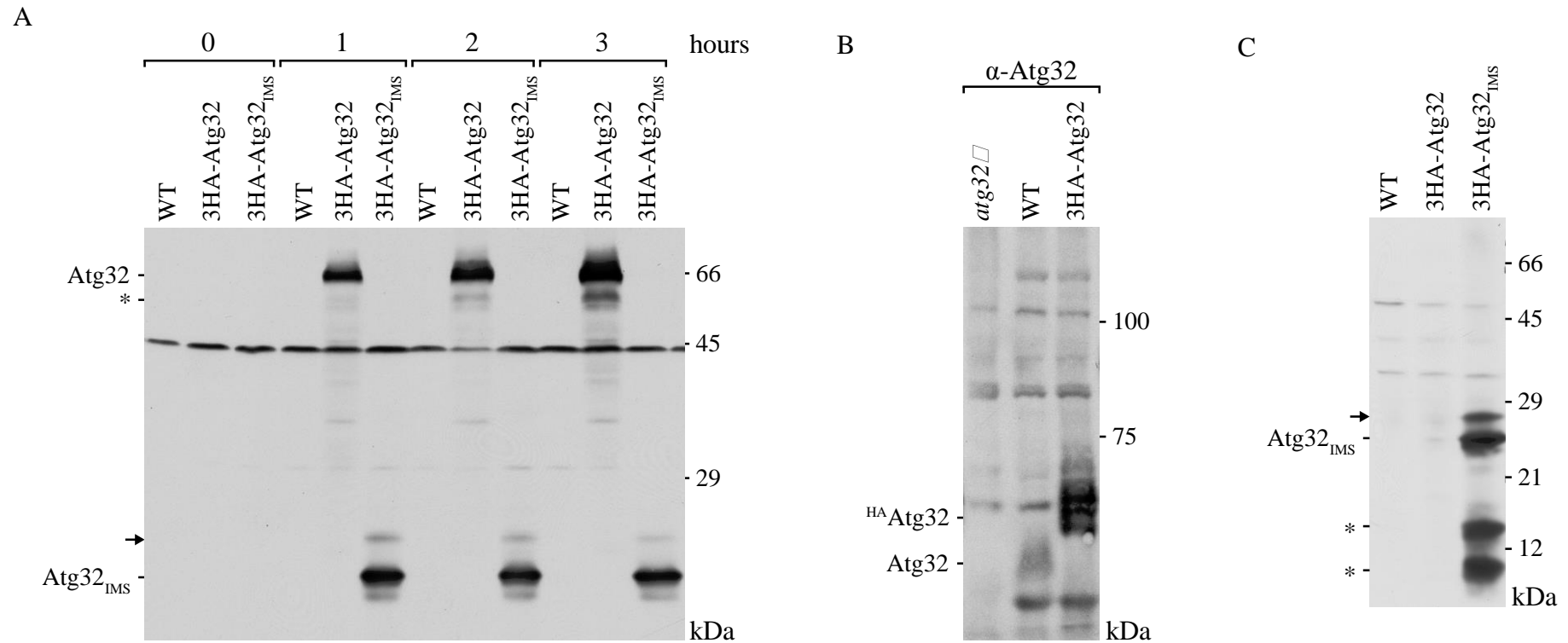
Fig. 32 Atg32 is not detectable in isolated mitochondria after overexpression. (A) Expression of HA-tagged Atg32 under control of GAL1 promoter was induced by addition of 2% galactose to the culture medium. Whole cell extracts were prepared from samples collected at the indicated times. **(B)** Whole cell extracts were prepared after 2 hours of induction with 2% galactose. **(C)** Mitochondria were isolated from corresponding strains after 2 hours of induction with 2% galactose. All samples were analyzed by SDS PAGE and Western blotting with α-HA antibody (**A** and **C**) or α-Atg32 antibody (**B**). * indicates unidentified Atg32 bands due to degradation or processing. Arrow indicates a possible modification product. WT – wild type.

4.3.2 Endogenous Atg32 is not detectable in mitochondria

The overexpression of Atg32 could be deleterious for mitochondrial function, or lead to an increased mitophagy rate. The latter would result in mitochondrial removal and receptor degradation.

Therefore, the presence of the endogenous Atg32 protein on isolated mitochondria was tested using the anti-Atg32 antibody. Whole cell extracts from wild type and *atg32Δ* cells were used as a positive control for immunoblotting. No specific band corresponding to Atg32 was observed in wild type mitochondria (Figure 33). This result could have two possible explanations; either Atg32 levels in the mitochondria were insufficient for detection, or Atg32 is degraded during mitochondrial isolation.
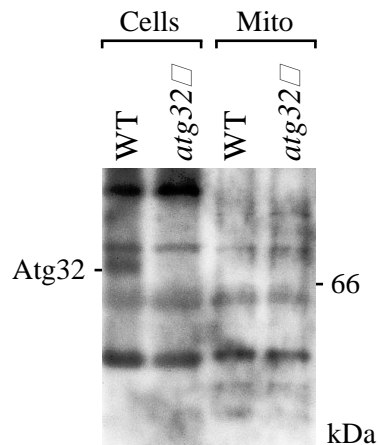
Fig. 33 No Atg32 is detected in mitochondria. Whole cell extracts (Cells) and isolated mitochondria (Mito) of the wild type (WT) and *atg32Δ* strains were analyzed by SDS PAGE and Western blotting. The blot is decorated with α-Atg32 antibody.

4.3.3 Cell fractionation causes Atg32 degradation

To test the hypothesis that Atg32 is removed from the mitochondrial surface during cell fractionation, samples were taken at each step of the procedure and analyzed by SDS PAGE and immunoblotting. The total sample was prepared prior to mitochondrial isolation from crude cell extracts. First, the cell wall was removed by enzymatic treatment and the resulting spheroplasts were re-suspended in the lysis buffer (before homogenization, BH). After homogenization (AH) and pelleting of large debris and unbroken cells (UC), cleared homogenate was obtained (CH). Finally, the enriched mitochondrial fraction was obtained by high-speed centrifugation step (Mito), while the cytosol, together with ribosomes and

small vesicles, remained in the post-mitochondrial supernatant (PMS). Each sample corresponds to the same starting amount of cells, estimated by optical density at 600 nm (OD_{600}).

Atg32, although present in whole cells, was visibly degraded in spheroplasts after cell wall lysis and homogenization (BH and AH samples). No traces of Atg32 could be detected in the homogenate (CH), while it remained stable in the unbroken cells (UC). Only a very weak signal could be seen in the gel lane with mitochondrial fraction (Figure 34). Thus, Atg32 is a highly unstable protein, sensitive to proteolysis during cell fractionation.
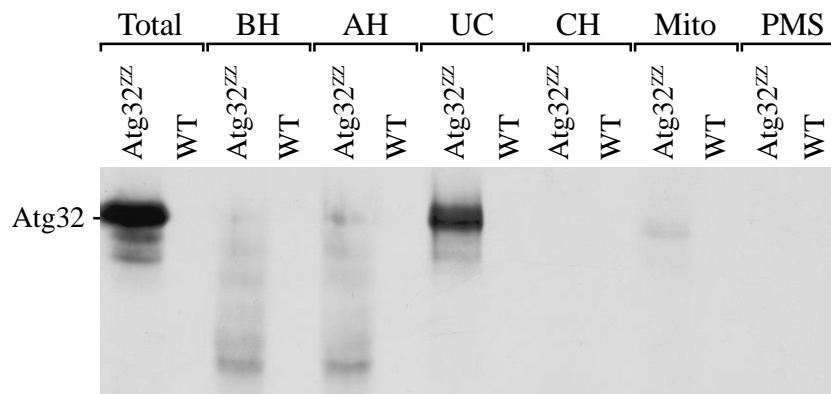
Fig. 34 Atg32 is digested during mitochondrial isolation. Samples taken at different points of the isolation procedure were analyzed by SDS PAGE and Western blotting with the α-PAP antibody. WT – wild type, BH – before homogenization, AH – after homogenization, UC – unbroken cells, CH – cleared homogenate, Mito – crude mitochondrial fraction, PMS – post-mitochondrial supernatant.

4.3.4 Search for Atg32 stabilizing mutations

In order to prevent rapid digestion of Atg32, I exploited yeast strains deficient in major cellular degradation pathways. Atg32 stability was monitored in the yeast proteasome mutant (*pre1-1 pre2-2*), and in a deletion mutant with impaired vacuolar degradation (*pep4Δ*). Pre1 and Pre2 proteasome subunits are required for chymotrypsin-like activity of the proteasome complex (Heinemeyer et al., 1991). Proteinase A, encoded by PEP4, is a major hydrolase of the yeast vacuole, responsible for maturation of other vacuolar proteases (Jones et al., 1982).

Cellular Atg32 levels were assessed after induction of mitophagy with rapamycin, which mimics the starvation response. Whole cell extracts were prepared at different time points after rapamycin treatment from the indicated yeast mutants expressing ZZ-tagged Atg32.

Upon mitophagy induction, Atg32 was almost completely degraded within the first hour of treatment, whereas another mitochondrial protein, Tim50, remained relatively stable. Atg32 degradation was not prevented in mutants with reduced proteasomal or vacuolar proteolytic activity (Figure 35).
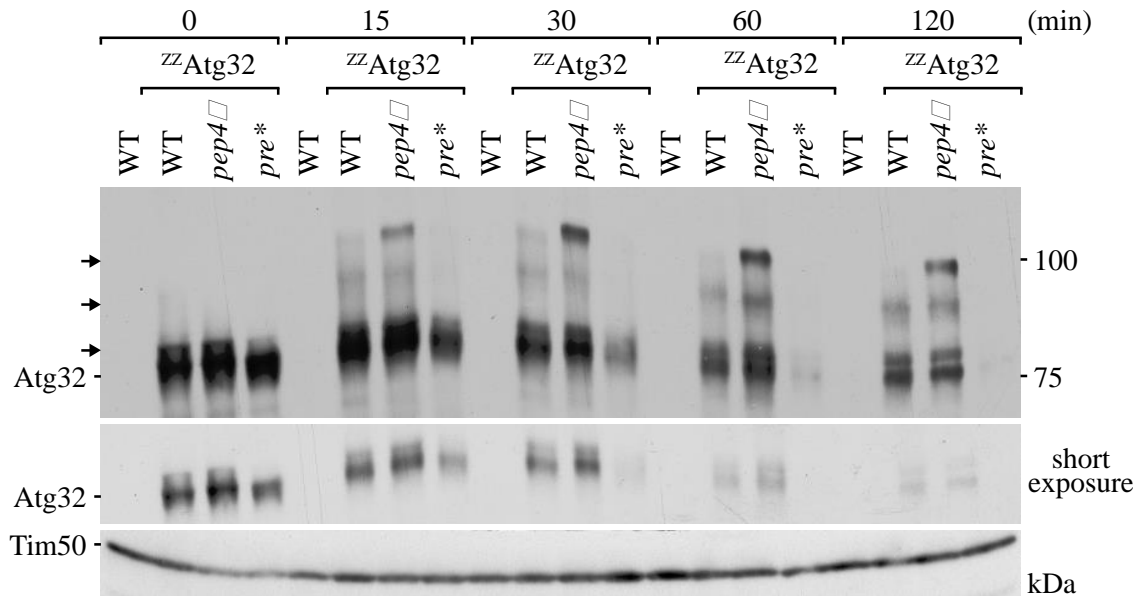
Fig. 35 Atg32 is degraded during mitophagy in mutants with impaired proteasomal and vacuolar proteolysis. Corresponding yeast strains were treated with 1 µg/ml rapamycin for the indicated time periods. Resulting whole cell extracts were analyzed by SDS PAGE and immunoblotting with the α-PAP and α-Tim50 antibody. WT – wild type, *pre* – pre1-1 pre2-2* mutant. Arrows indicate modification products.

Interestingly, Atg32 was present in several higher molecular weight bands, which potentially represent modified forms of the protein. One of these bands, with an estimated size of 100 kDa, specifically accumulated during mitophagy in the PEP4 deletion mutant. This result shows that inhibition of vacuolar proteolysis does not stabilize Atg32, but prevents degradation of its modified form.

4.4 Atg32 is modified in response to mitophagy induction

4.4.1 Atg32 modification is mitophagy specific

Rapamycin treatment, used in the previous experiment, promotes general autophagic response by inhibition of TOR signaling (Heitman et al., 1991). Accordingly, the Atg32 modification could occur independent of mitophagy.

Atg11 is an adaptor protein for selective autophagy, acting early in the mitophagic signaling cascade. To investigate whether Atg32 modification was mitophagy-specific, an Atg11-deficient mutant was included in the study. Whole cell extracts of corresponding yeast strains expressing ^{ZZ}Atg32 were prepared after rapamycin treatment and analyzed by SDS PAGE and Western blotting. No higher molecular weight band of Atg32 could be detected in the absence of Atg11. Moreover, it was missing in *pep4Δ* cells after *ATG11* deletion (Figure 36). Hence, a block in mitophagy prevents Atg32 modification.
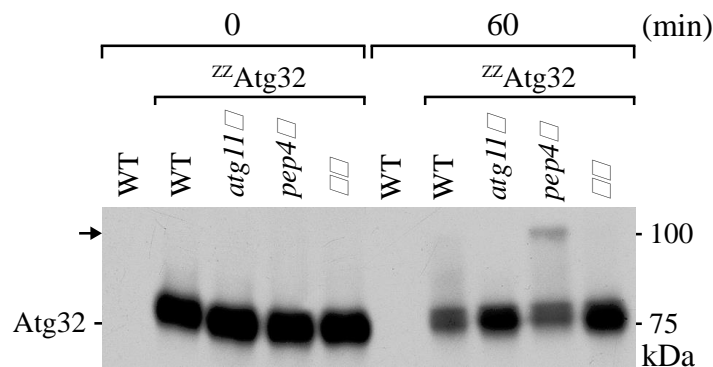
Fig. 36 Atg32 modification requires Atg11. Whole cell extracts of corresponding yeast strains were prepared after 0 or 60 min of 1 μg/ml rapamycin treatment and analyzed by SDS PAGE and immunoblotting with the α-PAP antibody. WT – wild type, ΔΔ – double deletion mutant *atg11Δ pep4Δ*. Arrow indicates a modification product.

Selective mitochondrial degradation is highly active after respiratory growth, however cells cultured on fermentable medium mostly upregulate general macroautophagy in response to starvation (Kissova et al., 2007).

To address the role of selective and non-selective autophagy in receptor modification, the Atg32 immunostaining pattern upon rapamycin treatment was compared after growth on different carbon sources. Modified forms of Atg32 were only present after rapamycin addition in glycerol-grown cells (YPG) and not in glucose-grown cells (YPD) (Figure 37).

Thus, mitochondrial proliferation due to respiratory growth is a prerequisite for receptor modification. Taken together, these results support the hypothesis that receptor modification is a part of mitophagy process.

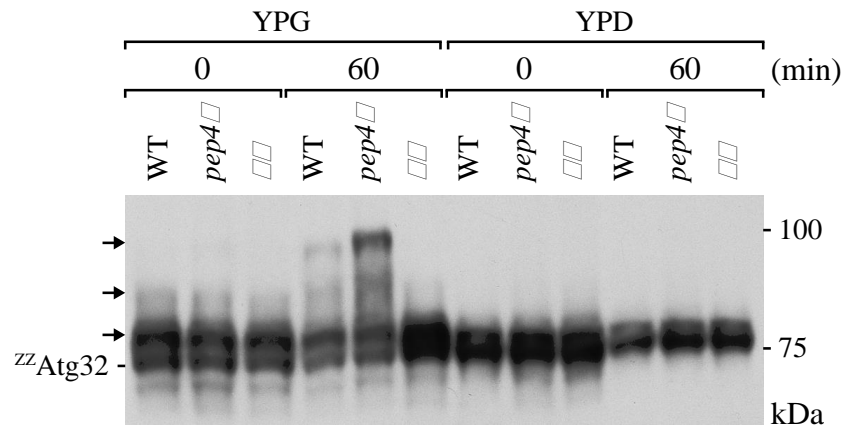**Fig. 37 Respiratory growth is a prerequisite for Atg32 modification.** Whole cell extracts of corresponding yeast strains were prepared after 0 or 60 min of 1 μg/ml rapamycin treatment and analyzed by SDS PAGE and immunoblotting with α-PAP antibody. WT – wild type, ΔΔ – double deletion mutant *atg11Δ pep4Δ*. Arrows indicate modification products.

4.4.2 Atg32 is modified in response to different mitophagy triggers

Mitophagy in yeast can be induced by different stimuli. Mitochondrial degradation occurs in respiratory medium when cells reach stationary growth phase. Alternatively, it can be triggered by nitrogen starvation after mitochondrial proliferation. Rapamycin treatment promotes a cellular response, which is similar, but non-identical, to the one occurring under starvation (Hardwick et al., 1999; Cox et al., 2004).

To test whether Atg32 modification depends on the type of mitophagy, whole cell extracts were prepared either after shifting cells from rich non-fermentable medium to starvation medium, or after culturing yeast in rich lactate medium for a prolonged period of time.

As in the case of rapamycin treatment, Atg32 formed a higher molecular weight band during starvation and in post-log phase, although in the latter case, Atg32 was modified to a lesser extent (Figure 38). In conclusion, receptor modification is independent from the mode of mitophagy induction.
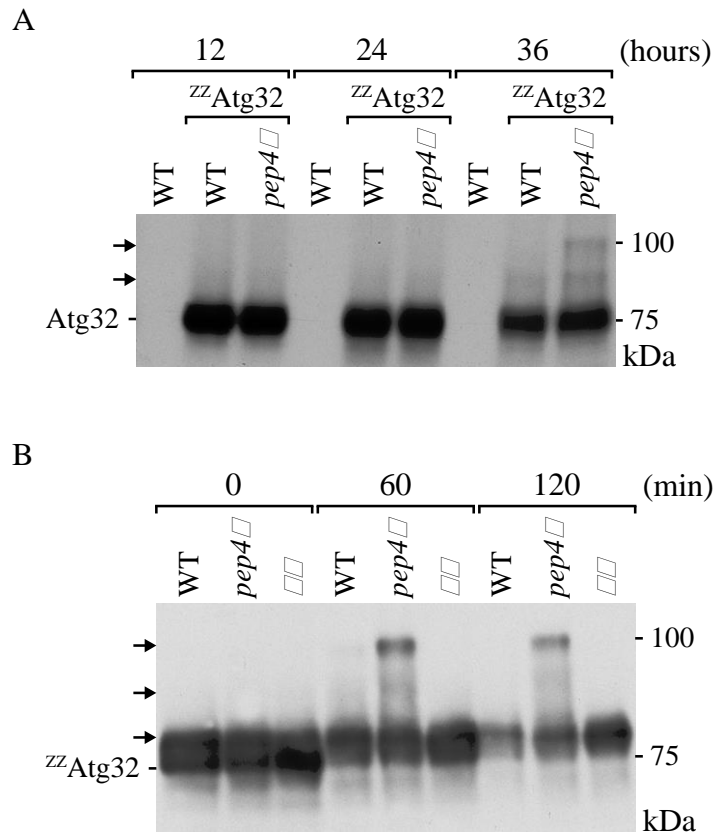
Fig. 38 Atg32 modification occurs under different modes of mitophagy induction. Whole cell extracts of corresponding yeast strains were prepared at the indicated times after **(A)** culturing yeast in YPL medium; or **(B)** after shift to SD-N starvation medium. Samples were analyzed by SDS PAGE and immunoblotting with the α-PAP antibody. WT – wild type, ΔΔ – double deletion mutant *atg11Δ pep4Δ*. Arrows indicate modification products.

4.4.3 Atg32 modification depends on autophagic machinery

Mitophagy exploits the core autophagic machinery for the generation of mitophagosomes. Components of the Atg1 kinase complex, Atg1 and Atg13, initiate the signaling cascade and recruit downstream autophagy players. Atg14 is necessary for PI3K complex targeting and thus PI3P synthesis at the site of autophagosome formation. This in turn promotes docking of other autophagy components. The morphology of the isolation membrane is determined by the covalent binding of the Atg8 protein to lipids. Atg8 conjugation machinery includes the Atg3, Atg4, Atg5, Atg7, Atg10, Atg12, and Atg16 proteins. After

the autophagic vesicle is completed, it fuses with the vacuole. Inside the vacuolar lumen the autophagosomal membrane is lysed with the help of the Atg15 lipase, while the cargo is degraded by various hydrolases, including Pep4.

To assess involvement of the autophagic machinery in Atg32 modification, deletions of various autophagic components were made in the *pep4Δ* background expressing ^{ZZ}Atg32. Whole cell extracts of resulting strains were prepared after rapamycin treatment. Atg32 modification appeared to be unperturbed in the absence of Atg15 and Atg14, while all other proteins tested were essential for the modification to occur (Figure 39).
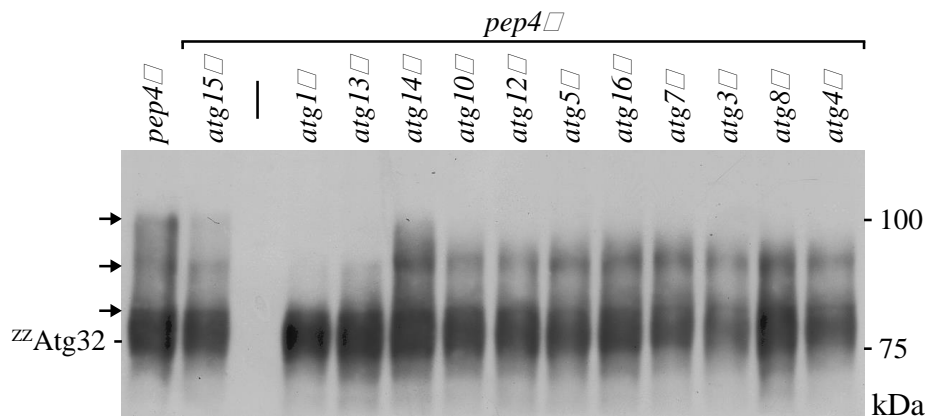
Fig. 39 Requirement of autophagy-specific genes for Atg32 modification. Whole cell extracts of corresponding yeast strains were prepared after 60 min of 1 μg/ml rapamycin treatment and analyzed by SDS PAGE and immunoblotting with the α-PAP antibody. Arrows indicate modification products.

4.4.4 The cytosolic domain of Atg32 is required for modification

The Atg32 protein contains two domains, differentially involved in the mitophagy process. The cytosolic domain of Atg32 is essential for mitophagy. It interacts with Atg8 and Atg11, and when fused to an artificial tether, initiates pexophagy in yeast (Kondo-Okamoto et al., 2012). On the other hand, the IMS domain is cleaved within the mitochondria by the Yme1 protease. This processing step is necessary for mitophagy induction, however the IMS domain itself appears to be dispensable for the process (Wang et al., 2013).

To test, whether the cytosolic domain of Atg32 is required for the modification, the *pep4Δ* strain expressing ZZ-tagged Atg32$_{IMS}$ was used to prepare whole cell extracts after

mitophagy induction with rapamycin. The double mutant, lacking both Pep4 and Atg11, was used as a negative control.

Immunostaining of Atg32$_{IMS}$ revealed several higher molecular weight bands, potentially representing the modification. One of the bands was stabilized in the absence of the Pep4 protease. However, this band was also present when mitophagy was blocked by *ATG11* deletion (Figure 40). Thus the IMS domain of Atg32 is not sufficient for the mitophagy-specific modification. This suggests that the modification takes place on the cytosolic domain of Atg32, or that the cytosolic domain is required for the modification to occur.

Fig. 40 The cytosolic domain of Atg32 is essential for modification. Whole cell extracts of corresponding yeast strains were prepared after 0 or 60 min of 1 μg/ml rapamycin treatment and analyzed by SDS PAGE and immunoblotting with the α-PAP antibody. Arrows indicate modification products.
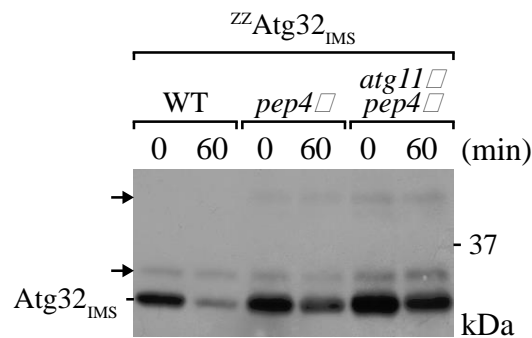
In conclusion, Atg32 is modified during the course of mitophagy. This modified version of the receptor is delivered to the vacuole, where it is degraded by Pep4. Meanwhile, the unmodified form is removed from the mitochondrial surface by a Pep4-independent mechanism. The nature of this modification remains elusive and further studies are required to identify the modification and the modifier.

5 Discussion

5.1 Cox26 is a novel subunit of the cytochrome *c* oxidase

The cytochrome *c* oxidase (COX) is the terminal enzyme of the respiratory chain, transferring electrons from ferrocytochrome *c* to molecular oxygen. It is functionally conserved in pro- and eukaryotes, however its composition became more complex throughout evolution. The oxidase monomer is composed of three mitochondria-encoded subunits involved in catalysis and proton pumping, as well as several nuclear-encoded subunits, varying between different species (Pierron et al., 2012). The role of these supplementary subunits is still a matter of ongoing research. They are involved in multiple processes, from complex assembly and stability, to regulation of its enzymatic activity. Novel components of the cytochrome c oxidase have been described in recent years, adding yet another function to this array. In the mitochondria the cytochrome c oxidase does not act as a single entity. Together with other complexes of the ETC it forms higher oligomer structures – supercomplexes. This oligomerization requires specific factors, such as Rcf1, a conserved subunit of complex IV (Vukotic et al., 2012). While the impact of lipid environment on supercomplexes is well established (Zhang et al., 2002; Pfeiffer et al., 2003; Zhang et al., 2005; Brandner et al., 2005; McKenzie et al., 2006), Rcf1 is so far the only known protein factor in yeast that specifically affects supercomplex formation. Thus a mechanistic basis of respiratory chain oligomerization remains ill defined.

In this study I have identified Cox26 protein as a novel cytochrome *c* oxidase subunit, and characterized its function in cytochrome *c* oxidase and supercomplex biogenesis. Cox26 was previously suggested to associate with respiratory chain supercomplexes (Helbig et al., 2009; Vukotic et al., 2012). Therefore the first goal of this thesis was to confirm this interaction.

Cox26 association with respiratory chain supercomplexes was supported both by BN PAGE analysis as well as by immunoprecipitation of the tagged Cox26. Further investigation assigned Cox26 as a complex IV component. Cox26 is associated with the cytochrome *c* oxidase in the absence of complex III, and co-isolates the COX monomer but not the complex III dimer. Thus Cox26 is not a supercomplex-specific subunit, but rather interacts with the supercomplexes via the complex IV.

The observation that Cox26 co-purifies COX subunits in amounts similar to Cox4 isolation let us to conclude that Cox26 is a stoichiometric subunit of the complex. Moreover, mobility shift of supercomplexes in Cox26^{ZZ} mitochondria visible on the BN PAGE indicates that Cox26 is present in every respiratory chain supercomplex, rather than a specific sub-population of respirasomes. The fact that Cox26 was not identified as a cytochrome c oxidase component in previous studies is probably due to the labile association of Cox26 with the complex IV, illustrated by its loss upon DDM treatment (Taanman and Capaldi, 1992). Besides Cox26 does not appear to have homologues in higher eukaryotes, explaining the lack of Cox26 in the homology model of the yeast cytochrome c oxidase (Marechal et al., 2012). However, one should note that the amino acid sequence among the nuclear-encoded COX subunits is relatively low conserved, in some cases comprising as little as 10% between mammals and yeast species (Das et al., 2004). For such cases the homology is mostly supported by the common function, or the presence of conserved domains, which are difficult to predict for small proteins like Cox26.

5.2 Cox26 facilitates assembly of supercomplexes and cytochrome *c* oxidase

Further studies suggested that Cox26 is required for efficient formation of respirasomes. The absence of Cox26 led to a decrease in supercomplex amounts and conversely to accumulation of free complex IV and complex III dimer. This decrease was supercomplex-specific, as levels of individual complexes were not affected. Partial reduction of supercomplexes, rather than their complete loss, suggests that Cox26 is important but not essential for supercomplex assembly, and that other factors may be involved in this process.

Observed loss of supercomplexes was mainly caused by a defect in biogenesis, opposite to dissociation due to reduced stability. In favor of this hypothesis assembly of several COX subunits into the supercomplexes was compromised. Moreover, if supercomplexes fall apart in the absence of Cox26, one would expect an upturn of mature complex IV. However, not only the mature form of the cytochrome c oxidase, but also its early assembly intermediates (COA) accumulate in Cox26-deficient cells. These assemblies depict Cox1-containing subcomplexes of the COX biogenesis pathway, rather than

dissociation products (Mick et al., 2007). One could envisage a model, where loss of Cox26 detains supercomplex formation, shifting the kinetic equilibrium of COX assembly. The COX is produced faster than it can be included into the supercomplexes, therefore it accumulates together with its early assembly intermediates. Enhanced formation of COA complexes upon deletion of *COX26* suggests that it influences not only respirasomes, but also complex IV maturation. However its exact role in this process remains unclear. Cox26 was only present in the mature oxidase, but not in the COA complexes (data not shown). Moreover, no interaction of Cox26 with Cox1 assembly factors, acting in the first steps of COX biogenesis, could be observed. Thus it is unlikely that Cox26 would directly affect early stages of complex IV formation. Often the block in assembly leads to increased turnover of unassembled proteins in order to prevent their aggregation (Nakai et al., 1994; Nijtmans et al., 1995). However the steady state levels of all tested complex IV constituents remained unaltered in *cox26Δ* cells.

Few possible mechanism of Cox26 function can be assumed. The influence of Cox26 on Cox2 or Cox3 assembly lines was not tested in this thesis. Alternatively, Cox26 deficiency could compromise late steps of COX biosynthesis, leading to accumulation of a preceding COA complex. To dissect which point of the COX assembly line is affected in the absence of Cox26, it would be important to know when it is incorporated into the maturing enzyme. Cox26 retained its interaction with the complex IV in the absence of late subunits, such as Rcf1, Cox13, and Rcf2. On the other hand, despite decreased efficiency, Rcf1 and Cox13 were integrated into the COX in *cox26Δ* strain. This suggests that their assembly is reciprocally independent, leaving the exact stage of Cox26 addition undetermined. Thus further studies are required to determine Cox26 function in the respiratory chain biogenesis.

5.3   Cox26 is not essential for respiratory chain activity

Despite Cox26 role in the supercomplex formation, it had relatively minor impact on respiration-related processes. *cox26Δ* cells appeared to be respiratory proficient, and displayed a 10% reduction of mitochondrial oxygen consumption rate (OCR). Lower OCR was consistent with a mild decrease of enzymatic activity of the respiratory chain complexes. Thus Cox26 appeared to be non-essential for the cytochrome *c* oxidase activity despite affecting its biogenesis. There could be several reasons for this discrepancy. One

possibility is occurrence of a suppressor mutation in *cox26Δ* background that alleviates Cox26-mediated phenotypes. To verify this hypothesis a suppressor screen can be performed, searching for genes that have a synthetic defect together with *COX26* deletion. Another option is that Cox26 is a regulatory subunit of the cytochrome *c* oxidase, which modulates its activity in response to environmental changes. It was proposed that the addition of nuclear-encoded subunits in the course of evolution was not to create a more efficient COX. It apparently imposes a higher level of control on the mitochondria-encoded components, based on cellular energy demand (Pierron et al., 2012). Thus Cox26 could have a more profound outcome on mitochondrial respiration only under certain conditions. For example, Cox13-deficient cells display a COX activity defect only at high ionic strength and perform even better than the wild type, if the ionic strength is low (Taanman and Capaldi, 1993). In this case it would be interesting to see whether various environmental stresses could have a different impact on *cox26Δ* cells and their respiration efficiency. Finally, some nuclear subunits seem to function specifically in assembly. For instance, Cox12 is required for efficient COX formation, but can be removed from the mature enzyme without any effect on activity (LaMarche et al., 1992). Regulation of assembly pathway and complex stability is an important control mechanism, which acts through increasing or limiting the amount of COX. Cox26 could be responsible for fine-tuning the rate of complex IV biogenesis or its inclusion into the respiratory chain supercomplexes, thus adjusting the organization of the respiratory chain to the current cellular requirements.

It has been postulated that supercomplexes play a role in optimizing mitochondrial respiration by substrate channeling (Bianchi et al., 2003; Bianchi et al., 2004). However, several other conflicting reports disprove this notion (Lenaz and Genova, 2007; Trouillard et al., 2011; Blaza et al., 2014). Results presented in this thesis argue along the same lines and suggest that supercomplex organization of the respiratory complexes does not affect catalytic activity of individual assemblies, but rather influences their formation and stability.

In conclusion, Cox26 is a novel constituent of the yeast cytochrome *c* oxidase, necessary for its assembly and subsequent supercomplex formation, but dispensable for mitochondrial respiration. Its discovery broadens the arsenal of accessory COX subunits. Nonetheless, further investigation is required to understand the physiological significance of Cox26 function.

5.4 Mitophagic signaling complexes in mitochondria

OXPHOS function in energy metabolism is important for the cell. However, besides ATP mitochondria also produce ROS and heat, while consuming oxygen and nutrients. Imbalance between substrates and products favors generation of ROS over antioxidant defense mechanisms and thus can lead to oxidative stress, toxic for cells and mitochondria themselves. Such imbalance is especially pronounced under harsh conditions, such as starvation, when cells cannot efficiently cope with increased ROS levels because of limited biosynthetic capacity (Deffieu et al., 2009). Damage induced by ROS decreases the efficiency of the respiratory chain, generating a positive feedback loop of enhanced mitochondrial ROS production and resulting mitochondrial malfunction. In this case mitochondrial network has to be trimmed by mitophagy to selectively remove impaired organelles. Yet the mechanistic details of "healthy versus damaged" differentiation remain unknown. PINK1-Parkin pathway represents one example of mitochondrial damage sensor. It discriminates defective mitochondria based on membrane potential reduction, (Koh and Chung, 2012). However, mitochondrial depolarization is not the only cellular cue leading to mitochondrial degradation. Mitochondrial calcium overload, unfolded protein response, increased ROS levels, iron depletion, and hypoxia can trigger mitophagy (Byrne et al., 1999; Kim and Lemasters, 2011; Liu et al., 2012; Allen et al., 2013; Jin and Youle, 2013). In some cases mitophagy happens even without membrane potential loss in the targeted mitochondria, and it is not clear whether significant mitochondrial depolarization regularly occurs *in vivo* (Jin and Youle, 2013). Moreover, in contrast to mammalian systems, CCCP-induced membrane potential loss does not result in mitophagy in yeast (Kissova et al., 2004; Kanki et al., 2009a; Mendl et al., 2011). Damage-induced mitophagy has been described for S. cerevisiae, however how mitochondrial defects trigger mitophagic response is not known. Thus, despite extensive research in this area, exact pathways involved in mitochondrial damage sensing and mitophagy signaling are not fully characterized. In yeast *S. cerevisiae* Atg32 protein fulfills mitophagy receptor function. It was shown to bind components of the autophagy machinery, such as Atg8 and Atg11, however its mitochondrial interaction partners remain to be discovered. Our initial hypothesis proposed formation of mitochondrial signaling complexes in response to mitophagy. Therefore, the first aim of this project was to isolate Atg32-associated receptor assemblies and determine their composition.

Analysis of Atg32 receptor complexes showed that it was present in a 230 kDa assembly (Atg32$^{230\text{ kDa}}$). Post-log phase mitophagy promoted Atg32$^{230\text{ kDa}}$ dissociation, and as a consequence a smaller complex of 140 kDa could be observed. One explanation is that Atg32 is negatively regulated in physiological conditions, to prevent excessive mitochondrial degradation. When yeast age, they progressively increase ROS production and accumulate mitochondrial damage (Laun et al., 2001; Lam et al., 2011). This presumably induces mitophagy and leads to de-repression of Atg32, allowing its interaction with downstream autophagy components. A similar 230 kDa complex could be seen after import of Atg32 into isolated mitochondria, supporting the initial observation. Interestingly, Atg32 shifted from the Atg32$^{230\text{ kDa}}$ complex towards a high molecular weight assembly (Atg32$^{700\text{ kDa}}$) with increasing import times. This Atg32$^{700\text{ kDa}}$ complex was not detected in the previous experiment presumably due to a different setup. Considering that formation of the 700 kDa complex was greatly enhanced upon membrane potential loss, it could provide a physiological link between mitochondrial damage and mitophagy signaling. It is tempting to speculate that once mitochondria become depolarized, mitophagy receptor is shifted to another signaling complex, allowing mitophagy induction. Although, according to the literature, mitochondrial membrane potential loss does not trigger mitophagy in yeast, the CCCP treatment commonly used to dissipate the $\Delta\psi$ impairs mitophagy and vacuolar protein turnover (Padman et al., 2013). Alternatively, Atg32 engages into this 700 kDa complex to perform a mitophagy-independent function. One cannot exclude that observed complexes result from protein aggregation during import procedure. Established protocol requires protease treatment to remove non-imported protein, which otherwise could form aggregates. Since Atg32 is an outer membrane protein it would be at least partially digested by protease treatment, which therefore had to be omitted. However, the fact that a complex of comparable size was detected after Atg32 isolation argues against this hypothesis and in favor of a specific complex formation.

It would be interesting to know if other mitophagy cues, such as nitrogen starvation and rapamycin treatment, result in similar complex formation. Another question is whether receptor complexes detected after mitochondrial import would differ between mitophagy-induced and non-induced samples. This would let us compare the impact of cytosolic effectors on Atg32 assemblies. Of course, the most intriguing issue is the complex composition. However, I was unable to address this question due to technical difficulties,

such as receptor instability and low isolation specificity. It is however conceivable that the Atg32$^{230 \text{ kDa}}$ complex could be stabilized in the absence of autophagic machinery components, such as Atg8 or Atg11, allowing its purification. It remains to be tested whether deletion of these proteins would thus influence Atg32 complex formation, and its dissociation upon mitophagy induction. Atg33 was described as a mitophagy sensor specific for stationary phase mitophagy (Kanki et al., 2009a). It is one of the possible candidates to associate with Atg32 to trigger mitophagy under these conditions. Its requirement for Atg32 complex formation can thus be evaluated in future experiments.

5.5 Atg32 is a highly unstable protein

As already mentioned, Atg32 has proven to be profoundly unstable even under conditions, which do not induce mitochondrial degradation. Proteolysis of Atg32 seemingly depends on the presence of its cytosolic domain, since the Atg32$_{IMS}$ construct was not digested during isolation procedure and remained stable during cell fractionation.

Two major degradation pathways exist in the cell. Both the proteasome and the lysosome (vacuole in yeast) mediate cellular proteolysis. Surprisingly, inhibition of either pathway did not prevent rapid digestion of Atg32 upon mitophagy induction. Moreover, Atg32 was degraded even more rapidly when proteasomal activity was decreased. This could be attributed to enhanced autophagy in proteasomal mutants. Such compensatory increase was previously reported for quiescent yeast cells (Takeda et al., 2010). Unexpectedly, also deletion of *PEP4*, a major vacuolar peptidase essential for degradation of autophagic cargoes (Takeshige et al., 1992), did not stabilize Atg32. This result suggests that Atg32 is digested by a yet unknown protease, which specifically recognizes its cytosolic domain. A screen for an increase in receptor stability among protease deletion mutants could help to identify the enzyme responsible for Atg32 proteolysis. This would broaden our understanding of the mitophagic pathway and provide a useful tool for future studies.

Atg32 is removed from mitochondrial surface rather quickly, within the first hour of rapamycin treatment, while other mitophagy cargos take several hours to be broken down (Eiyama et al., 2013). This could represent a safety mechanism, which prevents an overactivation of the mitochondrial degradation pathway. Mitochondria are essential for the cell, and only a portion of them is targeted to the vacuole during mitophagy (Kanki et

al., 2009b). The downregulation of mitophagy receptor on certain organelles could provide a mechanism to selectively trim mitochondrial network without detrimental consequences.

5.6 Mitophagy leads to modification of Atg32 receptor

Interestingly, the absence of Pep4 stabilized a high molecular weight form of Atg32, which potentially represents covalent protein modification. This form appeared only upon induction of mitophagy, and thus could serve as a regulatory mechanism in mitophagic signaling. This is a robust response, occurring under different mitophagy triggers. The most baffling question is the nature of the modifying moiety. Atg32 is known to be phosphorylated (Aoki et al., 2011), however phosphorylation usually produces only a minor shift in protein SDS PAGE mobility. Thus an increase of 25 kDa, observed for Atg32, is possibly due to a different modification type. This statement, however, had to be supported by experimental evidence. Atg32 was tested for several possible modifications, including phosphorylation and ubiquitination (not shown). Nonetheless, obtained results remained inconclusive. Due to receptor instability, purification of its modified form for mass spectrometry analysis was of insufficient quality. It remains to be elucidated whether observed modification occurs within the cytosolic or within the IMS domain of Atg32. My results strongly suggest that the cytosolic domain of Atg32 is modified in the course of mitophagy. First, it is essential for modification; second, autophagic machinery required for modification is localized in the cytosol; third, the IMS domain was shown to be dispensable for mitophagy (Wang et al., 2013). However, we cannot exclude that the cytosolic domain recruits a modifying agent, while the IMS domain itself gets modified. To differentiate between these possibilities one should test the presence of modification in the absence of Atg32 IMS domain.

Respiratory growth and mitochondrial proliferation are a prerequisite for Atg32 modification, since rapamycin treatment of glucose-grown cells did not produce a mobility shift for Atg32. It is noteworthy that the degradation of mitochondria is inhibited under mitophagy-inducing conditions if mitochondria are essential for metabolism of the available carbon source (Kanki and Klionsky, 2008). It thus remains to be tested whether Atg32 modification occurs during starvation on non-fermentable medium.

The modified form of Atg32 accumulated in the first 15 min of rapamycin treatment. Therefore it is a fast reaction, possibly modulating receptor activity. Since modified Atg32

was only stabilized in the absence of Pep4, it is logical to assume that in wild type cells it is degraded by a Pep4-dependent mechanism within the vacuole. The unmodified Atg32 was quickly degraded, while the levels of the modified version increased during the first hour. It seems that the receptor is modified in response to the mitophagy stimuli and recruited along with its cargo to the vacuole. Meanwhile, mitochondria that are spared from degradation remove Atg32 from their membranes. It is interesting whether mitochondrial malfunction could lead to receptor modification, and whether defects in mitochondrial physiology could stabilize Atg32 in a manner similar to PINK1 stabilization.

The requirement of autophagic machinery for Atg32 receptor modification was also addressed in this thesis. The initial aim was to dissect at which point of the autophagy pathway Atg32 gets modified. As Atg32 modification is unperturbed in the absence of the vacuolar lipase Atg15, it should happen prior to vacuolar fusion. On account of Atg11 being essential for the modification, one would expect that the modification occurs really early in the signaling cascade. Nevertheless, this assumption does not fit very well with the requirement of Atg8 conjugation machinery, which acts downstream from Atg11. Most unexpected finding was however dispensability of Atg14. In the absence of Atg14 PAS recruitment of autophagy components, including Atg8, is disturbed. Taken together these results can be justified by autophagy-independent role of Atg8 at the mitochondria. Interestingly, Atg32 is capable of binding free Atg8, not conjugated to the lipids of autophagic membrane (Kondo-Okamoto et al., 2012). This interaction could provide a mechanism for Atg8 recruitment to mitochondrial surface independent from Atg14. However it would not explain why the rest of conjugation machinery is required for Atg32 modification. It would be thus compelling to test, whether the cytosolic terminus of Atg32 is actually fused to one of the ubiquitin-like proteins during mitophagy.

Based on the data presented in this thesis, I suggest a revised model of mitophagic process in yeast. Under physiological conditions Atg32 is sequestered in a mitochondrial complex, preventing it from mitophagy initiation. Upon specific trigger Atg32 is discharged from this inhibitory complex and modified by a yet unknown mechanism. I expect receptor modification to be the cue for mitophagic degradation of selected organelles, unable to remove the unmodified receptor from their surface. Results of this study uncover novel aspects of mitophagy pathway and provide direction for future research.

Bibliography

Abeliovich, H., Zhang, C., Dunn, W. A., Jr., Shokat, K. M. and Klionsky, D. J. (2003). Chemical genetic analysis of Apg1 reveals a non-kinase role in the induction of autophagy. Mol Biol Cell 14, 477-90.

Acin-Perez, R., Bayona-Bafaluy, M. P., Fernandez-Silva, P., Moreno-Loshuertos, R., Perez-Martos, A., Bruno, C., Moraes, C. T. and Enriquez, J. A. (2004). Respiratory complex III is required to maintain complex I in mammalian mitochondria. Mol Cell 13, 805-15.

Acin-Perez, R., Fernandez-Silva, P., Peleato, M. L., Perez-Martos, A. and Enriquez, J. A. (2008). Respiratory active mitochondrial supercomplexes. Mol Cell 32, 529-39.

Adams, K. L. and Palmer, J. D. (2003). Evolution of mitochondrial gene content: gene loss and transfer to the nucleus. Mol Phylogenet Evol 29, 380-95.

Aggeler, R. and Capaldi, R. A. (1990). Yeast cytochrome c oxidase subunit VII is essential for assembly of an active enzyme. Cloning, sequencing, and characterization of the nuclear-encoded gene. J Biol Chem 265, 16389-93.

Alkhaja, A. K., Jans, D. C., Nikolov, M., Vukotic, M., Lytovchenko, O., Ludewig, F., Schliebs, W., Riedel, D., Urlaub, H., Jakobs, S. et al. (2012). MINOS1 is a conserved component of mitofilin complexes and required for mitochondrial function and cristae organization. Mol Biol Cell 23, 247-57.

Allen, G. F., Toth, R., James, J. and Ganley, I. G. (2013). Loss of iron triggers PINK1/Parkin-independent mitophagy. EMBO Rep 14, 1127-35.

Altamura, N., Capitanio, N., Bonnefoy, N., Papa, S. and Dujardin, G. (1996). The Saccharomyces cerevisiae OXA1 gene is required for the correct assembly of cytochrome c oxidase and oligomycin-sensitive ATP synthase. FEBS Lett 382, 111-5.

Althoff, T., Mills, D. J., Popot, J. L. and Kuhlbrandt, W. (2011). Arrangement of electron transport chain components in bovine mitochondrial supercomplex I1III2IV1. EMBO J 30, 4652-64.

Altschul, S. F., Gish, W., Miller, W., Myers, E. W. and Lipman, D. J. (1990). Basic local alignment search tool. J Mol Biol 215, 403-10.

Aoki, Y., Kanki, T., Hirota, Y., Kurihara, Y., Saigusa, T., Uchiumi, T. and Kang, D. (2011). Phosphorylation of Serine 114 on Atg32 mediates mitophagy. Mol Biol Cell 22, 3206-17.

Area-Gomez, E. and Schon, E. A. (2014). Mitochondrial genetics and disease. J Child Neurol 29, 1208-15.

Arnold, I., Pfeiffer, K., Neupert, W., Stuart, R. A. and Schagger, H. (1998). Yeast mitochondrial F1F0-ATP synthase exists as a dimer: identification of three dimer-specific subunits. EMBO J 17, 7170-8.

Barja, G. (2014). The mitochondrial free radical theory of aging. Prog Mol Biol Transl Sci 127, 1-27.

Barrientos, A., Fontanesi, F. and Diaz, F. (2009). Evaluation of the mitochondrial respiratory chain and oxidative phosphorylation system using polarography and spectrophotometric enzyme assays. Curr Protoc Hum Genet Chapter 19, Unit19 3.

Barrientos, A., Zambrano, A. and Tzagoloff, A. (2004). Mss51p and Cox14p jointly regulate mitochondrial Cox1p expression in Saccharomyces cerevisiae. EMBO J 23, 3472-82.

Barros, M. H. and Tzagoloff, A. (2002). Regulation of the heme A biosynthetic pathway in Saccharomyces cerevisiae. FEBS Lett 516, 119-23.

Baxter, B. K., Abeliovich, H., Zhang, X., Stirling, A. G., Burlingame, A. L. and Goldfarb, D. S. (2005). Atg19p ubiquitination and the cytoplasm to vacuole trafficking pathway in yeast. J Biol Chem 280, 39067-76.

Bellot, G., Garcia-Medina, R., Gounon, P., Chiche, J., Roux, D., Pouyssegur, J. and Mazure, N. M. (2009). Hypoxia-induced autophagy is mediated through hypoxia-inducible factor induction of BNIP3 and BNIP3L via their BH3 domains. Mol Cell Biol 29, 2570-81.

Bernhardt, D., Muller, M., Reichert, A. S. and Osiewacz, H. D. (2015). Simultaneous impairment of mitochondrial fission and fusion reduces mitophagy and shortens replicative lifespan. Sci Rep 5, 7885.

Berry, E. A. and Trumpower, B. L. (1985). Isolation of ubiquinol oxidase from Paracoccus denitrificans and resolution into cytochrome bc1 and cytochrome c-aa3 complexes. J Biol Chem 260, 2458-67.

Bestwick, M., Jeong, M. Y., Khalimonchuk, O., Kim, H. and Winge, D. R. (2010). Analysis of Leigh syndrome mutations in the yeast SURF1 homolog reveals a new member of the cytochrome oxidase assembly factor family. Mol Cell Biol 30, 4480-91.

Bianchi, C., Fato, R., Genova, M. L., Parenti Castelli, G. and Lenaz, G. (2003). Structural and functional organization of Complex I in the mitochondrial respiratory chain. Biofactors 18, 3-9.

Bianchi, C., Genova, M. L., Parenti Castelli, G. and Lenaz, G. (2004). The mitochondrial respiratory chain is partially organized in a supercomplex assembly: kinetic evidence using flux control analysis. J Biol Chem 279, 36562-9.

Blaza, J. N., Serreli, R., Jones, A. J., Mohammed, K. and Hirst, J. (2014). Kinetic evidence against partitioning of the ubiquinone pool and the catalytic relevance of respiratory-chain supercomplexes. Proc Natl Acad Sci U S A 111, 15735-40.

Bockler, S. and Westermann, B. (2014). Mitochondrial ER contacts are crucial for mitophagy in yeast. Dev Cell 28, 450-8.

Bonnefoy, N., Chalvet, F., Hamel, P., Slonimski, P. P. and Dujardin, G. (1994). OXA1, a Saccharomyces cerevisiae nuclear gene whose sequence is conserved from prokaryotes to eukaryotes controls cytochrome oxidase biogenesis. J Mol Biol 239, 201-12.

Boumans, H., Grivell, L. A. and Berden, J. A. (1998). The respiratory chain in yeast behaves as a single functional unit. J Biol Chem 273, 4872-7.

Bowles, E. J., Campbell, K. H. and St John, J. C. (2007). Nuclear transfer: preservation of a nuclear genome at the expense of its associated mtDNA genome(s). Curr Top Dev Biol 77, 251-90.

Bradford, M. M. (1976). A rapid and sensitive method for the quantitation of microgram quantities of protein utilizing the principle of protein-dye binding. Anal Biochem 72, 248-54.

Brand, M. D. (2010). The sites and topology of mitochondrial superoxide production. Exp Gerontol 45, 466-72.

Brandner, K., Mick, D. U., Frazier, A. E., Taylor, R. D., Meisinger, C. and Rehling, P. (2005). Taz1, an outer mitochondrial membrane protein, affects stability and assembly of inner membrane protein complexes: implications for Barth Syndrome. Mol Biol Cell 16, 5202-14.

Brunori, M., Antonini, G., Malatesta, F., Sarti, P. and Wilson, M. T. (1987). Cytochrome-c oxidase. Subunit structure and proton pumping. Eur J Biochem 169, 1-8.

Burman, C. and Ktistakis, N. T. (2010). Regulation of autophagy by phosphatidylinositol 3-phosphate. FEBS Lett 584, 1302-12.

Byrne, A. M., Lemasters, J. J. and Nieminen, A. L. (1999). Contribution of increased mitochondrial free Ca2+ to the mitochondrial permeability transition induced by tert-butylhydroperoxide in rat hepatocytes. Hepatology 29, 1523-31.

Campbell, C. L. and Thorsness, P. E. (1998). Escape of mitochondrial DNA to the nucleus in yme1 yeast is mediated by vacuolar-dependent turnover of abnormal mitochondrial compartments. J Cell Sci 111 (Pt 16), 2455-64.

Castresana, J., Lubben, M., Saraste, M. and Higgins, D. G. (1994). Evolution of cytochrome oxidase, an enzyme older than atmospheric oxygen. EMBO J 13, 2516-25.

Caulfield, T. R., Fiesel, F. C. and Springer, W. (2015). Activation of the E3 ubiquitin ligase Parkin. Biochem Soc Trans 43, 269-74.

Chakavarti, B. and Chakavarti, D. (2008). Electrophoretic separation of proteins. J Vis Exp.

Chan, D. C. (2012). Fusion and fission: interlinked processes critical for mitochondrial health. Annu Rev Genet 46, 265-87.

Chan, N. C., Salazar, A. M., Pham, A. H., Sweredoski, M. J., Kolawa, N. J., Graham, R. L., Hess, S. and Chan, D. C. (2011). Broad activation of the ubiquitin-proteasome system by Parkin is critical for mitophagy. Hum Mol Genet 20, 1726-37.

Chen, C., Huang, Q. L., Jiang, S. H., Pan, X. and Hua, Z. C. (2006). Immobilized protein ZZ, an affinity tool for immunoglobulin isolation and immunological experimentation. Biotechnol Appl Biochem 45, 87-92.

Chen, Y. C., Taylor, E. B., Dephoure, N., Heo, J. M., Tonhato, A., Papandreou, I., Nath, N., Denko, N. C., Gygi, S. P. and Rutter, J. (2012). Identification of a protein mediating respiratory supercomplex stability. Cell Metab 15, 348-60.

Cheong, H., Nair, U., Geng, J. and Klionsky, D. J. (2008). The Atg1 kinase complex is involved in the regulation of protein recruitment to initiate sequestering vesicle formation for nonspecific autophagy in Saccharomyces cerevisiae. Mol Biol Cell 19, 668-81.

Church, C., Goehring, B., Forsha, D., Wazny, P. and Poyton, R. O. (2005). A role for Pet100p in the assembly of yeast cytochrome c oxidase: interaction with a subassembly that accumulates in a pet100 mutant. J Biol Chem 280, 1854-63.

Claros, M. G. and Vincens, P. (1996). Computational method to predict mitochondrially imported proteins and their targeting sequences. Eur J Biochem 241, 779-86.

Cory, S. and Adams, J. M. (2002). The Bcl2 family: regulators of the cellular life-or-death switch. Nat Rev Cancer 2, 647-56.

Cox, K. H., Kulkarni, A., Tate, J. J. and Cooper, T. G. (2004). Gln3 phosphorylation and intracellular localization in nutrient limitation and starvation differ from those generated by rapamycin inhibition of Tor1/2 in Saccharomyces cerevisiae. J Biol Chem 279, 10270-8.

Cruciat, C. M., Brunner, S., Baumann, F., Neupert, W. and Stuart, R. A. (2000). The cytochrome bc1 and cytochrome c oxidase complexes associate to form a single supracomplex in yeast mitochondria. J Biol Chem 275, 18093-8.

Cunningham, C. N., Baughman, J. M., Phu, L., Tea, J. S., Yu, C., Coons, M., Kirkpatrick, D. S., Bingol, B. and Corn, J. E. (2015). USP30 and parkin homeostatically regulate atypical ubiquitin chains on mitochondria. Nat Cell Biol 17, 160-9.

Curran, B. P. and Bugeja, V. (2006). Basic investigations in Saccharomyces cerevisiae. Methods Mol Biol 313, 1-13.

Das, J., Miller, S. T. and Stern, D. L. (2004). Comparison of diverse protein sequences of the nuclear-encoded subunits of cytochrome C oxidase suggests conservation of structure underlies evolving functional sites. Mol Biol Evol 21, 1572-82.

Davis, R. L. and Sue, C. M. (2011). The genetics of mitochondrial disease. Semin Neurol 31, 519-30.

Deas, E., Plun-Favreau, H., Gandhi, S., Desmond, H., Kjaer, S., Loh, S. H., Renton, A. E., Harvey, R. J., Whitworth, A. J., Martins, L. M. et al. (2011). PINK1 cleavage at position A103 by the mitochondrial protease PARL. Hum Mol Genet 20, 867-79.

Decoster, E., Simon, M., Hatat, D. and Faye, G. (1990). The MSS51 gene product is required for the translation of the COX1 mRNA in yeast mitochondria. Mol Gen Genet 224, 111-8.

Deffieu, M., Bhatia-Kissova, I., Salin, B., Galinier, A., Manon, S. and Camougrand, N. (2009). Glutathione participates in the regulation of mitophagy in yeast. J Biol Chem 284, 14828-37.

Dekker, P. J., Martin, F., Maarse, A. C., Bomer, U., Muller, H., Guiard, B., Meijer, M., Rassow, J. and Pfanner, N. (1997). The Tim core complex defines the number of mitochondrial translocation contact sites and can hold arrested preproteins in the absence of matrix Hsp70-Tim44. EMBO J 16, 5408-19.

Diaz, F., Fukui, H., Garcia, S. and Moraes, C. T. (2006). Cytochrome c oxidase is required for the assembly/stability of respiratory complex I in mouse fibroblasts. Mol Cell Biol 26, 4872-81.

Diaz, F., Kotarsky, H., Fellman, V. and Moraes, C. T. (2011). Mitochondrial disorders caused by mutations in respiratory chain assembly factors. Semin Fetal Neonatal Med 16, 197-204.

Dimauro, S. and Davidzon, G. (2005). Mitochondrial DNA and disease. Ann Med 37, 222-32.

DiMauro, S. and Schon, E. A. (2008). Mitochondrial disorders in the nervous system. Annu Rev Neurosci 31, 91-123.

Ding, W. X., Ni, H. M., Li, M., Liao, Y., Chen, X., Stolz, D. B., Dorn, G. W., 2nd and Yin, X. M. (2010). Nix is critical to two distinct phases of mitophagy, reactive oxygen species-mediated autophagy induction and Parkin-ubiquitin-p62-mediated mitochondrial priming. J Biol Chem 285, 27879-90.

Dowhan, W., Bibus, C. R. and Schatz, G. (1985). The cytoplasmically-made subunit IV is necessary for assembly of cytochrome c oxidase in yeast. EMBO J 4, 179-84.

Dudek, J., Rehling, P. and van der Laan, M. (2013). Mitochondrial protein import: common principles and physiological networks. Biochim Biophys Acta 1833, 274-85.

Dudkina, N. V., Eubel, H., Keegstra, W., Boekema, E. J. and Braun, H. P. (2005). Structure of a mitochondrial supercomplex formed by respiratory-chain complexes I and III. Proc Natl Acad Sci U S A 102, 3225-9.

Eiyama, A., Kondo-Okamoto, N. and Okamoto, K. (2013). Mitochondrial degradation during starvation is selective and temporally distinct from bulk autophagy in yeast. FEBS Lett 587, 1787-92.

Endo, T. and Yamano, K. (2010). Transport of proteins across or into the mitochondrial outer membrane. Biochim Biophys Acta 1803, 706-14.

Epple, U. D., Suriapranata, I., Eskelinen, E. L. and Thumm, M. (2001). Aut5/Cvt17p, a putative lipase essential for disintegration of autophagic bodies inside the vacuole. J Bacteriol 183, 5942-55.

Eubel, H., Heinemeyer, J. and Braun, H. P. (2004). Identification and characterization of respirasomes in potato mitochondria. Plant Physiol 134, 1450-9.

Eubel, H., Jansch, L. and Braun, H. P. (2003). New insights into the respiratory chain of plant mitochondria. Supercomplexes and a unique composition of complex II. Plant Physiol 133, 274-86.

Finkel, T., Menazza, S., Holmstrom, K. M., Parks, R. J., Liu, J., Sun, J., Liu, J., Pan, X. and Murphy, E. (2015). The ins and outs of mitochondrial calcium. Circ Res 116, 1810-9.

Fontanesi, F., Soto, I. C., Horn, D. and Barrientos, A. (2006). Assembly of mitochondrial cytochrome c-oxidase, a complicated and highly regulated cellular process. Am J Physiol Cell Physiol 291, C1129-47.

Forsburg, S. L. and Guarente, L. (1989). Communication between mitochondria and the nucleus in regulation of cytochrome genes in the yeast Saccharomyces cerevisiae. Annu Rev Cell Biol 5, 153-80.

Frazier, A. E., Taylor, R. D., Mick, D. U., Warscheid, B., Stoepel, N., Meyer, H. E., Ryan, M. T., Guiard, B. and Rehling, P. (2006). Mdm38 interacts with ribosomes and is a component of the mitochondrial protein export machinery. J Cell Biol 172, 553-64.

Fujiki, Y., Hubbard, A. L., Fowler, S. and Lazarow, P. B. (1982). Isolation of intracellular membranes by means of sodium carbonate treatment: application to endoplasmic reticulum. J Cell Biol 93, 97-102.

Funakoshi, T., Matsuura, A., Noda, T. and Ohsumi, Y. (1997). Analyses of APG13 gene involved in autophagy in yeast, Saccharomyces cerevisiae. Gene 192, 207-13.

Gallagher, S., Winston, S. E., Fuller, S. A. and Hurrell, J. G. (2004). Immunoblotting and immunodetection. Curr Protoc Mol Biol Chapter 10, Unit 10 8.

Geisler, S., Holmstrom, K. M., Skujat, D., Fiesel, F. C., Rothfuss, O. C., Kahle, P. J. and Springer, W. (2010). PINK1/Parkin-mediated mitophagy is dependent on VDAC1 and p62/SQSTM1. Nat Cell Biol 12, 119-31.

Ghelli, A., Tropeano, C. V., Calvaruso, M. A., Marchesini, A., Iommarini, L., Porcelli, A. M., Zanna, C., De Nardo, V., Martinuzzi, A., Wibrand, F. et al. (2013). The cytochrome b p.278Y>C mutation causative of a multisystem disorder enhances superoxide production and alters supramolecular interactions of respiratory chain complexes. Hum Mol Genet 22, 2141-51.

Gietz, R. D. and Schiestl, R. H. (2007). Quick and easy yeast transformation using the LiAc/SS carrier DNA/PEG method. Nat Protoc 2, 35-7.

Gilkerson, R. W., Schon, E. A., Hernandez, E. and Davidson, M. M. (2008). Mitochondrial nucleoids maintain genetic autonomy but allow for functional complementation. J Cell Biol 181, 1117-28.

Giorgio, M., Migliaccio, E., Orsini, F., Paolucci, D., Moroni, M., Contursi, C., Pelliccia, G., Luzi, L., Minucci, S., Marcaccio, M. et al. (2005). Electron transfer between cytochrome c and p66Shc generates reactive oxygen species that trigger mitochondrial apoptosis. Cell 122, 221-33.

Glerum, D. M., Koerner, T. J. and Tzagoloff, A. (1995). Cloning and characterization of COX14, whose product is required for assembly of yeast cytochrome oxidase. J Biol Chem 270, 15585-90.

Glick, B. S., Brandt, A., Cunningham, K., Muller, S., Hallberg, R. L. and Schatz, G. (1992). Cytochromes c1 and b2 are sorted to the intermembrane space of yeast mitochondria by a stop-transfer mechanism. Cell 69, 809-22.

Graef, M. and Nunnari, J. (2011). Mitochondria regulate autophagy by conserved signalling pathways. EMBO J 30, 2101-14.

Guldener, U., Heck, S., Fielder, T., Beinhauer, J. and Hegemann, J. H. (1996). A new efficient gene disruption cassette for repeated use in budding yeast. Nucleic Acids Res 24, 2519-24.

Hanada, T., Noda, N. N., Satomi, Y., Ichimura, Y., Fujioka, Y., Takao, T., Inagaki, F. and Ohsumi, Y. (2007). The Atg12-Atg5 conjugate has a novel E3-like activity for protein lipidation in autophagy. J Biol Chem 282, 37298-302.

Hanahan, D. (1983). Studies on transformation of Escherichia coli with plasmids. J Mol Biol 166, 557-80.

Haque, M. E., Elmore, K. B., Tripathy, A., Koc, H., Koc, E. C. and Spremulli, L. L. (2010). Properties of the C-terminal tail of human mitochondrial inner membrane protein Oxa1L and its interactions with mammalian mitochondrial ribosomes. J Biol Chem 285, 28353-62.

Hardwick, J. S., Kuruvilla, F. G., Tong, J. K., Shamji, A. F. and Schreiber, S. L. (1999). Rapamycin-modulated transcription defines the subset of nutrient-sensitive signaling pathways directly controlled by the Tor proteins. Proc Natl Acad Sci U S A 96, 14866-70.

Harman, D. (1972). The biologic clock: the mitochondria? J Am Geriatr Soc 20, 145-7.

He, S. and Fox, T. D. (1997). Membrane translocation of mitochondrially coded Cox2p: distinct requirements for export of N and C termini and dependence on the conserved protein Oxa1p. Mol Biol Cell 8, 1449-60.

Heijne, G. (1986). The distribution of positively charged residues in bacterial inner membrane proteins correlates with the trans-membrane topology. EMBO J 5, 3021-7.

Heinemeyer, W., Kleinschmidt, J. A., Saidowsky, J., Escher, C. and Wolf, D. H. (1991). Proteinase yscE, the yeast proteasome/multicatalytic-multifunctional proteinase: mutants unravel its function in stress induced proteolysis and uncover its necessity for cell survival. EMBO J 10, 555-62.

Heitman, J., Movva, N. R. and Hall, M. N. (1991). Targets for cell cycle arrest by the immunosuppressant rapamycin in yeast. Science 253, 905-9.

Helbig, A. O., de Groot, M. J., van Gestel, R. A., Mohammed, S., de Hulster, E. A., Luttik, M. A., Daran-Lapujade, P., Pronk, J. T., Heck, A. J. and Slijper, M. (2009). A three-way proteomics strategy allows differential analysis of yeast mitochondrial membrane protein complexes under anaerobic and aerobic conditions. Proteomics 9, 4787-98.

Hell, K., Herrmann, J., Pratje, E., Neupert, W. and Stuart, R. A. (1997). Oxa1p mediates the export of the N- and C-termini of pCoxII from the mitochondrial matrix to the intermembrane space. FEBS Lett 418, 367-70.

Hell, K., Neupert, W. and Stuart, R. A. (2001). Oxa1p acts as a general membrane insertion machinery for proteins encoded by mitochondrial DNA. EMBO J 20, 1281-8.

Hell, K., Tzagoloff, A., Neupert, W. and Stuart, R. A. (2000). Identification of Cox20p, a novel protein involved in the maturation and assembly of cytochrome oxidase subunit 2. J Biol Chem 275, 4571-8.

Herlan, M., Bornhovd, C., Hell, K., Neupert, W. and Reichert, A. S. (2004). Alternative topogenesis of Mgm1 and mitochondrial morphology depend on ATP and a functional import motor. J Cell Biol 165, 167-73.

Herrmann, J. M. and Funes, S. (2005). Biogenesis of cytochrome oxidase-sophisticated assembly lines in the mitochondrial inner membrane. Gene 354, 43-52.

Herrmann, J. M., Koll, H., Cook, R. A., Neupert, W. and Stuart, R. A. (1995). Topogenesis of cytochrome oxidase subunit II. Mechanisms of protein export from the mitochondrial matrix. J Biol Chem 270, 27079-86.

Hilt, W., Enenkel, C., Gruhler, A., Singer, T. and Wolf, D. H. (1993). The PRE4 gene codes for a subunit of the yeast proteasome necessary for peptidylglutamyl-peptide-hydrolyzing activity. Mutations link the proteasome to stress- and ubiquitin-dependent proteolysis. J Biol Chem 268, 3479-86.

Hofmann, K. and Stoffel, W. (1993). TMbase-a database of membrane spanning proteins segments. Biol. Chem. Hoppe-Seyler 347, 166.

Horan, S., Bourges, I., Taanman, J. W. and Meunier, B. (2005). Analysis of COX2 mutants reveals cytochrome oxidase subassemblies in yeast. Biochem J 390, 703-8.

Hosler, J. P. (2004). The influence of subunit III of cytochrome c oxidase on the D pathway, the proton exit pathway and mechanism-based inactivation in subunit I. Biochim Biophys Acta 1655, 332-9.

Ichimura, Y., Kirisako, T., Takao, T., Satomi, Y., Shimonishi, Y., Ishihara, N., Mizushima, N., Tanida, I., Kominami, E., Ohsumi, M. et al. (2000). A ubiquitin-like system mediates protein lipidation. Nature 408, 488-92.

Ishihara, N., Jofuku, A., Eura, Y. and Mihara, K. (2003). Regulation of mitochondrial morphology by membrane potential, and DRP1-dependent division and FZO1-dependent fusion reaction in mammalian cells. Biochem Biophys Res Commun 301, 891-8.

Jan, P. S., Esser, K., Pratje, E. and Michaelis, G. (2000). Som1, a third component of the yeast mitochondrial inner membrane peptidase complex that contains Imp1 and Imp2. Mol Gen Genet 263, 483-91.

Janke, C., Magiera, M. M., Rathfelder, N., Taxis, C., Reber, S., Maekawa, H., Moreno-Borchart, A., Doenges, G., Schwob, E., Schiebel, E. et al. (2004). A versatile toolbox for PCR-based tagging of yeast genes: new fluorescent proteins, more markers and promoter substitution cassettes. Yeast 21, 947-62.

Jia, L., Dienhart, M., Schramp, M., McCauley, M., Hell, K. and Stuart, R. A. (2003). Yeast Oxa1 interacts with mitochondrial ribosomes: the importance of the C-terminal region of Oxa1. EMBO J 22, 6438-47.

Jia, L., Kaur, J. and Stuart, R. A. (2009). Mapping of the Saccharomyces cerevisiae Oxa1-mitochondrial ribosome interface and identification of MrpL40, a ribosomal protein in close proximity to Oxa1 and critical for oxidative phosphorylation complex assembly. Eukaryot Cell 8, 1792-802.

Jin, S. M., Lazarou, M., Wang, C., Kane, L. A., Narendra, D. P. and Youle, R. J. (2010). Mitochondrial membrane potential regulates PINK1 import and proteolytic destabilization by PARL. J Cell Biol 191, 933-42.

Jin, S. M. and Youle, R. J. (2013). The accumulation of misfolded proteins in the mitochondrial matrix is sensed by PINK1 to induce PARK2/Parkin-mediated mitophagy of polarized mitochondria. Autophagy 9, 1750-7.

Johannsen, D. L. and Ravussin, E. (2009). The role of mitochondria in health and disease. Curr Opin Pharmacol 9, 780-6.

Johansen, T. and Lamark, T. (2011). Selective autophagy mediated by autophagic adapter proteins. Autophagy 7, 279-96.

Jones, E. W., Zubenko, G. S. and Parker, R. R. (1982). PEP4 gene function is required for expression of several vacuolar hydrolases in Saccharomyces cerevisiae. Genetics 102, 665-77.

Journo, D., Mor, A. and Abeliovich, H. (2009). Aup1-mediated regulation of Rtg3 during mitophagy. J Biol Chem 284, 35885-95.

Jurgensmeier, J. M., Xie, Z., Deveraux, Q., Ellerby, L., Bredesen, D. and Reed, J. C. (1998). Bax directly induces release of cytochrome c from isolated mitochondria. Proc Natl Acad Sci U S A 95, 4997-5002.

Kabeya, Y., Kamada, Y., Baba, M., Takikawa, H., Sasaki, M. and Ohsumi, Y. (2005). Atg17 functions in cooperation with Atg1 and Atg13 in yeast autophagy. Mol Biol Cell 16, 2544-53.

Kamada, Y., Funakoshi, T., Shintani, T., Nagano, K., Ohsumi, M. and Ohsumi, Y. (2000). Tor-mediated induction of autophagy via an Apg1 protein kinase complex. J Cell Biol 150, 1507-13.

Kametaka, S., Okano, T., Ohsumi, M. and Ohsumi, Y. (1998). Apg14p and Apg6/Vps30p form a protein complex essential for autophagy in the yeast, Saccharomyces cerevisiae. J Biol Chem 273, 22284-91.

Kanki, T. and Klionsky, D. J. (2008). Mitophagy in yeast occurs through a selective mechanism. J Biol Chem 283, 32386-93.

Kanki, T., Kurihara, Y., Jin, X., Goda, T., Ono, Y., Aihara, M., Hirota, Y., Saigusa, T., Aoki, Y., Uchiumi, T. et al. (2013). Casein kinase 2 is essential for mitophagy. EMBO Rep 14, 788-94.

Kanki, T., Wang, K., Baba, M., Bartholomew, C. R., Lynch-Day, M. A., Du, Z., Geng, J., Mao, K., Yang, Z., Yen, W. L. et al. (2009a). A genomic screen for yeast mutants defective in selective mitochondria autophagy. Mol Biol Cell 20, 4730-8.

Kanki, T., Wang, K., Cao, Y., Baba, M. and Klionsky, D. J. (2009b). Atg32 is a mitochondrial protein that confers selectivity during mitophagy. Dev Cell 17, 98-109.

Karbowski, M. and Youle, R. J. (2011). Regulating mitochondrial outer membrane proteins by ubiquitination and proteasomal degradation. Curr Opin Cell Biol 23, 476-82.

Kerr, J. F., Wyllie, A. H. and Currie, A. R. (1972). Apoptosis: a basic biological phenomenon with wide-ranging implications in tissue kinetics. Br J Cancer 26, 239-57.

Khalimonchuk, O., Bird, A. and Winge, D. R. (2007). Evidence for a pro-oxidant intermediate in the assembly of cytochrome oxidase. J Biol Chem 282, 17442-9.

Kihara, A., Noda, T., Ishihara, N. and Ohsumi, Y. (2001). Two distinct Vps34 phosphatidylinositol 3-kinase complexes function in autophagy and carboxypeptidase Y sorting in Saccharomyces cerevisiae. J Cell Biol 152, 519-30.

Kim, I. and Lemasters, J. J. (2011). Mitophagy selectively degrades individual damaged mitochondria after photoirradiation. Antioxid Redox Signal 14, 1919-28.

Kim, J., Huang, W. P. and Klionsky, D. J. (2001). Membrane recruitment of Aut7p in the autophagy and cytoplasm to vacuole targeting pathways requires Aut1p, Aut2p, and the autophagy conjugation complex. J Cell Biol 152, 51-64.

Kirisako, T., Ichimura, Y., Okada, H., Kabeya, Y., Mizushima, N., Yoshimori, T., Ohsumi, M., Takao, T., Noda, T. and Ohsumi, Y. (2000). The reversible modification regulates the membrane-binding state of Apg8/Aut7 essential for autophagy and the cytoplasm to vacuole targeting pathway. J Cell Biol 151, 263-76.

Kissova, I., Deffieu, M., Manon, S. and Camougrand, N. (2004). Uth1p is involved in the autophagic degradation of mitochondria. J Biol Chem 279, 39068-74.

Kissova, I., Salin, B., Schaeffer, J., Bhatia, S., Manon, S. and Camougrand, N. (2007). Selective and non-selective autophagic degradation of mitochondria in yeast. Autophagy 3, 329-36.

Kissova, I. B. and Camougrand, N. (2009). Glutathione participates in the regulation of mitophagy in yeast. Autophagy 5, 872-3.

Kitada, T., Asakawa, S., Hattori, N., Matsumine, H., Yamamura, Y., Minoshima, S., Yokochi, M., Mizuno, Y. and Shimizu, N. (1998). Mutations in the parkin gene cause autosomal recessive juvenile parkinsonism. Nature 392, 605-8.

Klecker, T., Bockler, S. and Westermann, B. (2014). Making connections: interorganelle contacts orchestrate mitochondrial behavior. Trends Cell Biol 24, 537-45.

Klecker, T. and Westermann, B. (2014). Mitochondria are clamped to vacuoles for lipid transport. Dev Cell 30, 1-2.

Klionsky, D. J. and Codogno, P. (2013). The mechanism and physiological function of macroautophagy. J Innate Immun 5, 427-33.

Klionsky, D. J., Cregg, J. M., Dunn, W. A., Jr., Emr, S. D., Sakai, Y., Sandoval, I. V., Sibirny, A., Subramani, S., Thumm, M., Veenhuis, M. et al. (2003). A unified nomenclature for yeast autophagy-related genes. Dev Cell 5, 539-45.

Knop, M., Siegers, K., Pereira, G., Zachariae, W., Winsor, B., Nasmyth, K. and Schiebel, E. (1999). Epitope tagging of yeast genes using a PCR-based strategy: more tags and improved practical routines. Yeast 15, 963-72.

Knorr, R. L., Dimova, R. and Lipowsky, R. (2012). Curvature of double-membrane organelles generated by changes in membrane size and composition. PLoS One 7, e32753.

Knorr, R. L., Nakatogawa, H., Ohsumi, Y., Lipowsky, R., Baumgart, T. and Dimova, R. (2014). Membrane morphology is actively transformed by covalent binding of the protein Atg8 to PE-lipids. PLoS One 9, e115357.

Koh, H. and Chung, J. (2012). PINK1 as a molecular checkpoint in the maintenance of mitochondrial function and integrity. Mol Cells 34, 7-13.

Kon, M. and Cuervo, A. M. (2010). Chaperone-mediated autophagy in health and disease. FEBS Lett 584, 1399-404.

Kondapalli, C., Kazlauskaite, A., Zhang, N., Woodroof, H. I., Campbell, D. G., Gourlay, R., Burchell, L., Walden, H., Macartney, T. J., Deak, M. et al. (2012). PINK1 is activated by mitochondrial membrane potential depolarization and stimulates Parkin E3 ligase activity by phosphorylating Serine 65. Open Biol 2, 120080.

Kondo-Okamoto, N., Noda, N. N., Suzuki, S. W., Nakatogawa, H., Takahashi, I., Matsunami, M., Hashimoto, A., Inagaki, F., Ohsumi, Y. and Okamoto, K. (2012). Autophagy-related protein 32 acts as autophagic degron and directly initiates mitophagy. J Biol Chem 287, 10631-8.

Kowaltowski, A. J., de Souza-Pinto, N. C., Castilho, R. F. and Vercesi, A. E. (2009). Mitochondria and reactive oxygen species. Free Radic Biol Med 47, 333-43.

Kraft, C., Deplazes, A., Sohrmann, M. and Peter, M. (2008). Mature ribosomes are selectively degraded upon starvation by an autophagy pathway requiring the Ubp3p/Bre5p ubiquitin protease. Nat Cell Biol 10, 602-10.

Krick, R., Henke, S., Tolstrup, J. and Thumm, M. (2008). Dissecting the localization and function of Atg18, Atg21 and Ygr223c. Autophagy 4, 896-910.

Kuma, A., Mizushima, N., Ishihara, N. and Ohsumi, Y. (2002). Formation of the approximately 350-kDa Apg12-Apg5.Apg16 multimeric complex, mediated by Apg16 oligomerization, is essential for autophagy in yeast. J Biol Chem 277, 18619-25.

Kurihara, Y., Kanki, T., Aoki, Y., Hirota, Y., Saigusa, T., Uchiumi, T. and Kang, D. (2012). Mitophagy plays an essential role in reducing mitochondrial production of reactive oxygen species and mutation of mitochondrial DNA by maintaining mitochondrial quantity and quality in yeast. J Biol Chem 287, 3265-72.

Lackner, L. L. (2014). Shaping the dynamic mitochondrial network. BMC Biol 12, 35.

Laemmli, U. K. (1970). Cleavage of structural proteins during the assembly of the head of bacteriophage T4. Nature 227, 680-5.

Lam, Y. T., Aung-Htut, M. T., Lim, Y. L., Yang, H. and Dawes, I. W. (2011). Changes in reactive oxygen species begin early during replicative aging of Saccharomyces cerevisiae cells. Free Radic Biol Med 50, 963-70.

LaMarche, A. E., Abate, M. I., Chan, S. H. and Trumpower, B. L. (1992). Isolation and characterization of COX12, the nuclear gene for a previously unrecognized subunit of Saccharomyces cerevisiae cytochrome c oxidase. J Biol Chem 267, 22473-80.

Lapuente-Brun, E., Moreno-Loshuertos, R., Acin-Perez, R., Latorre-Pellicer, A., Colas, C., Balsa, E., Perales-Clemente, E., Quiros, P. M., Calvo, E., Rodriguez-Hernandez, M. A. et al. (2013). Supercomplex assembly determines electron flux in the mitochondrial electron transport chain. Science 340, 1567-70.

Laun, P., Pichova, A., Madeo, F., Fuchs, J., Ellinger, A., Kohlwein, S., Dawes, I., Frohlich, K. U. and Breitenbach, M. (2001). Aged mother cells of Saccharomyces cerevisiae show markers of oxidative stress and apoptosis. Mol Microbiol 39, 1166-73.

Lenaz, G. and Genova, M. L. (2007). Kinetics of integrated electron transfer in the mitochondrial respiratory chain: random collisions vs. solid state electron channeling. Am J Physiol Cell Physiol 292, C1221-39.

Lenaz, G. and Genova, M. L. (2010). Structure and organization of mitochondrial respiratory complexes: a new understanding of an old subject. Antioxid Redox Signal 12, 961-1008.

Li, M. X. and Dewson, G. (2015). Mitochondria and apoptosis: emerging concepts. F1000Prime Rep 7, 42.

Li, W. W., Li, J. and Bao, J. K. (2012). Microautophagy: lesser-known self-eating. Cell Mol Life Sci 69, 1125-36.

Li, X. and Chang, Y. H. (1995). Amino-terminal protein processing in Saccharomyces cerevisiae is an essential function that requires two distinct methionine aminopeptidases. Proc Natl Acad Sci U S A 92, 12357-61.

Li, Y., D'Aurelio, M., Deng, J. H., Park, J. S., Manfredi, G., Hu, P., Lu, J. and Bai, Y. (2007). An assembled complex IV maintains the stability and activity of complex I in mammalian mitochondria. J Biol Chem 282, 17557-62.

Lill, R. and Muhlenhoff, U. (2008). Maturation of iron-sulfur proteins in eukaryotes: mechanisms, connected processes, and diseases. Annu Rev Biochem 77, 669-700.

Liu, L., Feng, D., Chen, G., Chen, M., Zheng, Q., Song, P., Ma, Q., Zhu, C., Wang, R., Qi, W. et al. (2012). Mitochondrial outer-membrane protein FUNDC1 mediates hypoxia-induced mitophagy in mammalian cells. Nat Cell Biol 14, 177-85.

Livnat-Levanon, N. and Glickman, M. H. (2011). Ubiquitin-proteasome system and mitochondria - reciprocity. Biochim Biophys Acta 1809, 80-7.

Longtine, M. S., McKenzie, A., 3rd, Demarini, D. J., Shah, N. G., Wach, A., Brachat, A., Philippsen, P. and Pringle, J. R. (1998). Additional modules for versatile and economical PCR-based gene deletion and modification in Saccharomyces cerevisiae. Yeast 14, 953-61.

Looke, M., Kristjuhan, K. and Kristjuhan, A. (2011). Extraction of genomic DNA from yeasts for PCR-based applications. Biotechniques 50, 325-8.

Luciano, P. and Geli, V. (1996). The mitochondrial processing peptidase: function and specificity. Experientia 52, 1077-82.

Lupo, D., Vollmer, C., Deckers, M., Mick, D. U., Tews, I., Sinning, I. and Rehling, P. (2011). Mdm38 is a 14-3-3-like receptor and associates with the protein synthesis machinery at the inner mitochondrial membrane. Traffic 12, 1457-66.

Luttik, M. A., Overkamp, K. M., Kotter, P., de Vries, S., van Dijken, J. P. and Pronk, J. T. (1998). The Saccharomyces cerevisiae NDE1 and NDE2 genes encode separate mitochondrial NADH dehydrogenases catalyzing the oxidation of cytosolic NADH. J Biol Chem 273, 24529-34.

Manthey, G. M. and McEwen, J. E. (1995). The product of the nuclear gene PET309 is required for translation of mature mRNA and stability or production of intron-containing RNAs derived from the mitochondrial COX1 locus of Saccharomyces cerevisiae. EMBO J 14, 4031-43.

Mao, K., Wang, K., Liu, X. and Klionsky, D. J. (2013). The scaffold protein Atg11 recruits fission machinery to drive selective mitochondria degradation by autophagy. Dev Cell 26, 9-18.

Mao, K., Wang, K., Zhao, M., Xu, T. and Klionsky, D. J. (2011). Two MAPK-signaling pathways are required for mitophagy in Saccharomyces cerevisiae. J Cell Biol 193, 755-67.

Maranzana, E., Barbero, G., Falasca, A. I., Lenaz, G. and Genova, M. L. (2013). Mitochondrial respiratory supercomplex association limits production of reactive oxygen species from complex I. Antioxid Redox Signal 19, 1469-80.

Marechal, A., Meunier, B., Lee, D., Orengo, C. and Rich, P. R. (2012). Yeast cytochrome c oxidase: a model system to study mitochondrial forms of the haem-copper oxidase superfamily. Biochim Biophys Acta 1817, 620-8.

Margulis, L. (1975). Symbiotic theory of the origin of eukaryotic organelles; criteria for proof. Symp Soc Exp Biol, 21-38.

Martin, J., Mahlke, K. and Pfanner, N. (1991). Role of an energized inner membrane in mitochondrial protein import. Delta psi drives the movement of presequences. J Biol Chem 266, 18051-7.

Matsuura, A., Tsukada, M., Wada, Y. and Ohsumi, Y. (1997). Apg1p, a novel protein kinase required for the autophagic process in Saccharomyces cerevisiae. Gene 192, 245-50.

Mattiazzi Usaj, M., Brloznik, M., Kaferle, P., Zitnik, M., Wolinski, H., Leitner, F., Kohlwein, S. D., Zupan, B. and Petrovic, U. (2015). Genome-Wide Localization Study of Yeast Pex11 Identifies Peroxisome-Mitochondria Interactions through the ERMES Complex. J Mol Biol 427, 2072-87.

McKenzie, M., Lazarou, M., Thorburn, D. R. and Ryan, M. T. (2006). Mitochondrial respiratory chain supercomplexes are destabilized in Barth Syndrome patients. J Mol Biol 361, 462-9.

McStay, G. P., Su, C. H. and Tzagoloff, A. (2013). Modular assembly of yeast cytochrome oxidase. Mol Biol Cell 24, 440-52.

Meisinger, C., Pfanner, N. and Truscott, K. N. (2006). Isolation of yeast mitochondria. Methods Mol Biol 313, 33-9.

Meissner, C., Lorenz, H., Weihofen, A., Selkoe, D. J. and Lemberg, M. K. (2011). The mitochondrial intramembrane protease PARL cleaves human Pink1 to regulate Pink1 trafficking. J Neurochem 117, 856-67.

Mendl, N., Occhipinti, A., Muller, M., Wild, P., Dikic, I. and Reichert, A. S. (2011). Mitophagy in yeast is independent of mitochondrial fission and requires the stress response gene WHI2. J Cell Sci 124, 1339-50.

Mick, D. U., Fox, T. D. and Rehling, P. (2011). Inventory control: cytochrome c oxidase assembly regulates mitochondrial translation. Nat Rev Mol Cell Biol 12, 14-20.

Mick, D. U., Vukotic, M., Piechura, H., Meyer, H. E., Warscheid, B., Deckers, M. and Rehling, P. (2010). Coa3 and Cox14 are essential for negative feedback regulation of COX1 translation in mitochondria. J Cell Biol 191, 141-54.

Mick, D. U., Wagner, K., van der Laan, M., Frazier, A. E., Perschil, I., Pawlas, M., Meyer, H. E., Warscheid, B. and Rehling, P. (2007). Shy1 couples Cox1 translational regulation to cytochrome c oxidase assembly. EMBO J 26, 4347-58.

Mitchell, P. and Moyle, J. (1968). Proton translocation coupled to ATP hydrolysis in rat liver mitochondria. Eur J Biochem 4, 530-9.

Mizushima, N. (2005). The pleiotropic role of autophagy: from protein metabolism to bactericide. Cell Death Differ 12 Suppl 2, 1535-41.

Mizushima, N., Noda, T. and Ohsumi, Y. (1999). Apg16p is required for the function of the Apg12p-Apg5p conjugate in the yeast autophagy pathway. EMBO J 18, 3888-96.

Mizushima, N., Noda, T., Yoshimori, T., Tanaka, Y., Ishii, T., George, M. D., Klionsky, D. J., Ohsumi, M. and Ohsumi, Y. (1998). A protein conjugation system essential for autophagy. Nature 395, 395-8.

Mizushima, N., Yoshimori, T. and Ohsumi, Y. (2011). The role of Atg proteins in autophagosome formation. Annu Rev Cell Dev Biol 27, 107-32.

Moreno-Lastres, D., Fontanesi, F., Garcia-Consuegra, I., Martin, M. A., Arenas, J., Barrientos, A. and Ugalde, C. (2012). Mitochondrial complex I plays an essential role in human respirasome assembly. Cell Metab 15, 324-35.

Muller, M., Kotter, P., Behrendt, C., Walter, E., Scheckhuber, C. Q., Entian, K. D. and Reichert, A. S. (2015). Synthetic quantitative array technology identifies the Ubp3-Bre5 deubiquitinase complex as a negative regulator of mitophagy. Cell Rep 10, 1215-25.

Murakawa, T., Yamaguchi, O., Hashimoto, A., Hikoso, S., Takeda, T., Oka, T., Yasui, H., Ueda, H., Akazawa, Y., Nakayama, H. et al. (2015). Bcl-2-like protein 13 is a mammalian Atg32 homologue that mediates mitophagy and mitochondrial fragmentation. Nat Commun 6, 7527.

Nakai, T., Mera, Y., Yasuhara, T. and Ohashi, A. (1994). Divalent metal ion-dependent mitochondrial degradation of unassembled subunits 2 and 3 of cytochrome c oxidase. J Biochem 116, 752-8.

Nakatogawa, H. (2013). Two ubiquitin-like conjugation systems that mediate membrane formation during autophagy. Essays Biochem 55, 39-50.

Nakatogawa, H., Ichimura, Y. and Ohsumi, Y. (2007). Atg8, a ubiquitin-like protein required for autophagosome formation, mediates membrane tethering and hemifusion. Cell 130, 165-78.

Nakatogawa, H., Suzuki, K., Kamada, Y. and Ohsumi, Y. (2009). Dynamics and diversity in autophagy mechanisms: lessons from yeast. Nat Rev Mol Cell Biol 10, 458-67.

Narendra, D., Tanaka, A., Suen, D. F. and Youle, R. J. (2008). Parkin is recruited selectively to impaired mitochondria and promotes their autophagy. J Cell Biol 183, 795-803.

Narendra, D. P., Jin, S. M., Tanaka, A., Suen, D. F., Gautier, C. A., Shen, J., Cookson, M. R. and Youle, R. J. (2010). PINK1 is selectively stabilized on impaired mitochondria to activate Parkin. PLoS Biol 8, e1000298.

Narita, M., Shimizu, S., Ito, T., Chittenden, T., Lutz, R. J., Matsuda, H. and Tsujimoto, Y. (1998). Bax interacts with the permeability transition pore to induce permeability transition and cytochrome c release in isolated mitochondria. Proc Natl Acad Sci U S A 95, 14681-6.

Ney, P. A. (2015). Mitochondrial autophagy: Origins, significance, and role of BNIP3 and NIX. Biochim Biophys Acta 1853, 2775-83.

Nijtmans, L. G., Spelbrink, J. N., Van Galen, M. J., Zwaan, M., Klement, P. and Van den Bogert, C. (1995). Expression and fate of the nuclearly encoded subunits of cytochrome-c oxidase in cultured human cells depleted of mitochondrial gene products. Biochim Biophys Acta 1265, 117-26.

Nijtmans, L. G., Taanman, J. W., Muijsers, A. O., Speijer, D. and Van den Bogert, C. (1998). Assembly of cytochrome-c oxidase in cultured human cells. Eur J Biochem 254, 389-94.

Nilsson, B., Moks, T., Jansson, B., Abrahmsen, L., Elmblad, A., Holmgren, E., Henrichson, C., Jones, T. A. and Uhlen, M. (1987). A synthetic IgG-binding domain based on staphylococcal protein A. Protein Eng 1, 107-13.

Noda, N. N., Fujioka, Y., Hanada, T., Ohsumi, Y. and Inagaki, F. (2013). Structure of the Atg12-Atg5 conjugate reveals a platform for stimulating Atg8-PE conjugation. EMBO Rep 14, 206-11.

Noda, N. N., Kumeta, H., Nakatogawa, H., Satoo, K., Adachi, W., Ishii, J., Fujioka, Y., Ohsumi, Y. and Inagaki, F. (2008). Structural basis of target recognition by Atg8/LC3 during selective autophagy. Genes Cells 13, 1211-8.

Noda, T. and Ohsumi, Y. (1998). Tor, a phosphatidylinositol kinase homologue, controls autophagy in yeast. J Biol Chem 273, 3963-6.

Novak, I., Kirkin, V., McEwan, D. G., Zhang, J., Wild, P., Rozenknop, A., Rogov, V., Lohr, F., Popovic, D., Occhipinti, A. et al. (2010). Nix is a selective autophagy receptor for mitochondrial clearance. EMBO Rep 11, 45-51.

Nowikovsky, K., Reipert, S., Devenish, R. J. and Schweyen, R. J. (2007). Mdm38 protein depletion causes loss of mitochondrial K+/H+ exchange activity, osmotic swelling and mitophagy. Cell Death Differ 14, 1647-56.

Nunnari, J., Fox, T. D. and Walter, P. (1993). A mitochondrial protease with two catalytic subunits of nonoverlapping specificities. Science 262, 1997-2004.

Obara, K., Sekito, T. and Ohsumi, Y. (2006). Assortment of phosphatidylinositol 3-kinase complexes--Atg14p directs association of complex I to the pre-autophagosomal structure in Saccharomyces cerevisiae. Mol Biol Cell 17, 1527-39.

Okamoto, K., Kondo-Okamoto, N. and Ohsumi, Y. (2009). Mitochondria-anchored receptor Atg32 mediates degradation of mitochondria via selective autophagy. Dev Cell 17, 87-97.

Okatsu, K., Saisho, K., Shimanuki, M., Nakada, K., Shitara, H., Sou, Y. S., Kimura, M., Sato, S., Hattori, N., Komatsu, M. et al. (2010). p62/SQSTM1 cooperates with Parkin for perinuclear clustering of depolarized mitochondria. Genes Cells 15, 887-900.

Ordureau, A., Sarraf, S. A., Duda, D. M., Heo, J. M., Jedrychowski, M. P., Sviderskiy, V. O., Olszewski, J. L., Koerber, J. T., Xie, T., Beausoleil, S. A. et al. (2014). Quantitative

proteomics reveal a feedforward mechanism for mitochondrial PARKIN translocation and ubiquitin chain synthesis. Mol Cell 56, 360-75.

Ott, M. and Herrmann, J. M. (2010). Co-translational membrane insertion of mitochondrially encoded proteins. Biochim Biophys Acta 1803, 767-75.

Ott, M., Prestele, M., Bauerschmitt, H., Funes, S., Bonnefoy, N. and Herrmann, J. M. (2006). Mba1, a membrane-associated ribosome receptor in mitochondria. EMBO J 25, 1603-10.

Padman, B. S., Bach, M., Lucarelli, G., Prescott, M. and Ramm, G. (2013). The protonophore CCCP interferes with lysosomal degradation of autophagic cargo in yeast and mammalian cells. Autophagy 9, 1862-75.

Paumard, P., Vaillier, J., Coulary, B., Schaeffer, J., Soubannier, V., Mueller, D. M., Brethes, D., di Rago, J. P. and Velours, J. (2002). The ATP synthase is involved in generating mitochondrial cristae morphology. EMBO J 21, 221-30.

Pavlakis, S. G., Phillips, P. C., DiMauro, S., De Vivo, D. C. and Rowland, L. P. (1984). Mitochondrial myopathy, encephalopathy, lactic acidosis, and strokelike episodes: a distinctive clinical syndrome. Ann Neurol 16, 481-8.

Pequignot, M. O., Dey, R., Zeviani, M., Tiranti, V., Godinot, C., Poyau, A., Sue, C., Di Mauro, S., Abitbol, M. and Marsac, C. (2001). Mutations in the SURF1 gene associated with Leigh syndrome and cytochrome C oxidase deficiency. Hum Mutat 17, 374-81.

Perez-Martinez, X., Broadley, S. A. and Fox, T. D. (2003). Mss51p promotes mitochondrial Cox1p synthesis and interacts with newly synthesized Cox1p. EMBO J 22, 5951-61.

Perez-Martinez, X., Butler, C. A., Shingu-Vazquez, M. and Fox, T. D. (2009). Dual functions of Mss51 couple synthesis of Cox1 to assembly of cytochrome c oxidase in Saccharomyces cerevisiae mitochondria. Mol Biol Cell 20, 4371-80.

Pfeiffer, K., Gohil, V., Stuart, R. A., Hunte, C., Brandt, U., Greenberg, M. L. and Schagger, H. (2003). Cardiolipin stabilizes respiratory chain supercomplexes. J Biol Chem 278, 52873-80.

Pierrel, F., Bestwick, M. L., Cobine, P. A., Khalimonchuk, O., Cricco, J. A. and Winge, D. R. (2007). Coa1 links the Mss51 post-translational function to Cox1 cofactor insertion in cytochrome c oxidase assembly. EMBO J 26, 4335-46.

Pierron, D., Wildman, D. E., Huttemann, M., Markondapatnaikuni, G. C., Aras, S. and Grossman, L. I. (2012). Cytochrome c oxidase: evolution of control via nuclear subunit addition. Biochim Biophys Acta 1817, 590-7.

Poole, A. M. and Gribaldo, S. (2014). Eukaryotic origins: How and when was the mitochondrion acquired? Cold Spring Harb Perspect Biol 6, a015990.

Preuss, M., Leonhard, K., Hell, K., Stuart, R. A., Neupert, W. and Herrmann, J. M. (2001). Mba1, a novel component of the mitochondrial protein export machinery of the yeast Saccharomyces cerevisiae. J Cell Biol 153, 1085-96.

Priault, M., Salin, B., Schaeffer, J., Vallette, F. M., di Rago, J. P. and Martinou, J. C. (2005). Impairing the bioenergetic status and the biogenesis of mitochondria triggers mitophagy in yeast. Cell Death Differ 12, 1613-21.

Quiros, P. M., Langer, T. and Lopez-Otin, C. (2015). New roles for mitochondrial proteases in health, ageing and disease. Nat Rev Mol Cell Biol 16, 345-59.

Radke, S., Chander, H., Schafer, P., Meiss, G., Kruger, R., Schulz, J. B. and Germain, D. (2008). Mitochondrial protein quality control by the proteasome involves ubiquitination and the protease Omi. J Biol Chem 283, 12681-5.

Rehling, P., Model, K., Brandner, K., Kovermann, P., Sickmann, A., Meyer, H. E., Kuhlbrandt, W., Wagner, R., Truscott, K. N. and Pfanner, N. (2003). Protein insertion into the mitochondrial inner membrane by a twin-pore translocase. Science 299, 1747-51.

Rentzsch, A., Krummeck-Weiss, G., Hofer, A., Bartuschka, A., Ostermann, K. and Rodel, G. (1999). Mitochondrial copper metabolism in yeast: mutational analysis of Sco1p involved in the biogenesis of cytochrome c oxidase. Curr Genet 35, 103-8.

Riistama, S., Puustinen, A., Garcia-Horsman, A., Iwata, S., Michel, H. and Wikstrom, M. (1996). Channelling of dioxygen into the respiratory enzyme. Biochim Biophys Acta 1275, 1-4.

Sakoh-Nakatogawa, M., Matoba, K., Asai, E., Kirisako, H., Ishii, J., Noda, N. N., Inagaki, F., Nakatogawa, H. and Ohsumi, Y. (2013). Atg12-Atg5 conjugate enhances E2 activity of Atg3 by rearranging its catalytic site. Nat Struct Mol Biol 20, 433-9.

Sambrook, J. and Russel, D. W. (2001). Molecular Cloning: A laboratory manual. 3rd ed. New York: Cold Spring Harbor Laboratory Press.

Sarraf, S. A., Raman, M., Guarani-Pereira, V., Sowa, M. E., Huttlin, E. L., Gygi, S. P. and Harper, J. W. (2013). Landscape of the PARKIN-dependent ubiquitylome in response to mitochondrial depolarization. Nature 496, 372-6.

Sathananthan, A. H. and Trounson, A. O. (2000). Mitochondrial morphology during preimplantational human embryogenesis. Hum Reprod 15 Suppl 2, 148-59.

Schagger, H. (2001). Respiratory chain supercomplexes. IUBMB Life 52, 119-28.

Schagger, H., de Coo, R., Bauer, M. F., Hofmann, S., Godinot, C. and Brandt, U. (2004). Significance of respirasomes for the assembly/stability of human respiratory chain complex I. J Biol Chem 279, 36349-53.

Schagger, H. and Pfeiffer, K. (2000). Supercomplexes in the respiratory chains of yeast and mammalian mitochondria. EMBO J 19, 1777-83.

Schagger, H. and von Jagow, G. (1991). Blue native electrophoresis for isolation of membrane protein complexes in enzymatically active form. Anal Biochem 199, 223-31.

Schneider, A., Behrens, M., Scherer, P., Pratje, E., Michaelis, G. and Schatz, G. (1991). Inner membrane protease I, an enzyme mediating intramitochondrial protein sorting in yeast. EMBO J 10, 247-54.

Schulz, C., Schendzielorz, A. and Rehling, P. (2015). Unlocking the presequence import pathway. Trends Cell Biol 25, 265-75.

Schweers, R. L., Zhang, J., Randall, M. S., Loyd, M. R., Li, W., Dorsey, F. C., Kundu, M., Opferman, J. T., Cleveland, J. L., Miller, J. L. et al. (2007). NIX is required for programmed mitochondrial clearance during reticulocyte maturation. Proc Natl Acad Sci U S A 104, 19500-5.

Shimizu, S., Eguchi, Y., Kamiike, W., Funahashi, Y., Mignon, A., Lacronique, V., Matsuda, H. and Tsujimoto, Y. (1998). Bcl-2 prevents apoptotic mitochondrial dysfunction by regulating proton flux. Proc Natl Acad Sci U S A 95, 1455-9.

Sickmann, A., Reinders, J., Wagner, Y., Joppich, C., Zahedi, R., Meyer, H. E., Schonfisch, B., Perschil, I., Chacinska, A., Guiard, B. et al. (2003). The proteome of Saccharomyces cerevisiae mitochondria. Proc Natl Acad Sci U S A 100, 13207-12.

Sikorski, R. S. and Hieter, P. (1989). A system of shuttle vectors and yeast host strains designed for efficient manipulation of DNA in Saccharomyces cerevisiae. Genetics 122, 19-27.

Silvestri, L., Caputo, V., Bellacchio, E., Atorino, L., Dallapiccola, B., Valente, E. M. and Casari, G. (2005). Mitochondrial import and enzymatic activity of PINK1 mutants associated to recessive parkinsonism. Hum Mol Genet 14, 3477-92.

Small, W. C. and McAlister-Henn, L. (1998). Identification of a cytosolically directed NADH dehydrogenase in mitochondria of Saccharomyces cerevisiae. J Bacteriol 180, 4051-5.

Stiburek, L., Vesela, K., Hansikova, H., Pecina, P., Tesarova, M., Cerna, L., Houstek, J. and Zeman, J. (2005). Tissue-specific cytochrome c oxidase assembly defects due to mutations in SCO2 and SURF1. Biochem J 392, 625-32.

Straub, M., Bredschneider, M. and Thumm, M. (1997). AUT3, a serine/threonine kinase gene, is essential for autophagocytosis in Saccharomyces cerevisiae. J Bacteriol 179, 3875-83.

Strogolova, V., Furness, A., Robb-McGrath, M., Garlich, J. and Stuart, R. A. (2012). Rcf1 and Rcf2, members of the hypoxia-induced gene 1 protein family, are critical components of the mitochondrial cytochrome bc1-cytochrome c oxidase supercomplex. Mol Cell Biol 32, 1363-73.

Stroh, A., Anderka, O., Pfeiffer, K., Yagi, T., Finel, M., Ludwig, B. and Schagger, H. (2004). Assembly of respiratory complexes I, III, and IV into NADH oxidase supercomplex stabilizes complex I in Paracoccus denitrificans. J Biol Chem 279, 5000-7.

Su, C. H., McStay, G. P. and Tzagoloff, A. (2014). The Cox3p assembly module of yeast cytochrome oxidase. Mol Biol Cell 25, 965-76.

Summer, H., Gramer, R. and Droge, P. (2009). Denaturing urea polyacrylamide gel electrophoresis (Urea PAGE). J Vis Exp.

Suzuki, K. (2013). Selective autophagy in budding yeast. Cell Death Differ 20, 43-8.

Suzuki, S. W., Onodera, J. and Ohsumi, Y. (2011). Starvation induced cell death in autophagy-defective yeast mutants is caused by mitochondria dysfunction. PLoS One 6, e17412.

Szyrach, G., Ott, M., Bonnefoy, N., Neupert, W. and Herrmann, J. M. (2003). Ribosome binding to the Oxa1 complex facilitates co-translational protein insertion in mitochondria. EMBO J 22, 6448-57.

Taanman, J. W. and Capaldi, R. A. (1992). Purification of yeast cytochrome c oxidase with a subunit composition resembling the mammalian enzyme. J Biol Chem 267, 22481-5.

Taanman, J. W. and Capaldi, R. A. (1993). Subunit VIa of yeast cytochrome c oxidase is not necessary for assembly of the enzyme complex but modulates the enzyme activity. Isolation and characterization of the nuclear-coded gene. J Biol Chem 268, 18754-61.

Takeda, K. and Yanagida, M. (2010). In quiescence of fission yeast, autophagy and the proteasome collaborate for mitochondrial maintenance and longevity. Autophagy 6, 564-5.

Takeshige, K., Baba, M., Tsuboi, S., Noda, T. and Ohsumi, Y. (1992). Autophagy in yeast demonstrated with proteinase-deficient mutants and conditions for its induction. J Cell Biol 119, 301-11.

Tal, R., Winter, G., Ecker, N., Klionsky, D. J. and Abeliovich, H. (2007). Aup1p, a yeast mitochondrial protein phosphatase homolog, is required for efficient stationary phase mitophagy and cell survival. J Biol Chem 282, 5617-24.

Tatsuta, T. and Langer, T. (2008). Quality control of mitochondria: protection against neurodegeneration and ageing. EMBO J 27, 306-14.

Teter, S. A., Eggerton, K. P., Scott, S. V., Kim, J., Fischer, A. M. and Klionsky, D. J. (2001). Degradation of lipid vesicles in the yeast vacuole requires function of Cvt17, a putative lipase. J Biol Chem 276, 2083-7.

Thornberry, N. A. (1997). The caspase family of cysteine proteases. Br Med Bull 53, 478-90.

Thumm, M., Egner, R., Koch, B., Schlumpberger, M., Straub, M., Veenhuis, M. and Wolf, D. H. (1994). Isolation of autophagocytosis mutants of Saccharomyces cerevisiae. FEBS Lett 349, 275-80.

Tiranti, V., Corona, P., Greco, M., Taanman, J. W., Carrara, F., Lamantea, E., Nijtmans, L., Uziel, G. and Zeviani, M. (2000). A novel frameshift mutation of the mtDNA COIII gene leads to impaired assembly of cytochrome c oxidase in a patient affected by Leigh-like syndrome. Hum Mol Genet 9, 2733-42.

Tiranti, V., Hoertnagel, K., Carrozzo, R., Galimberti, C., Munaro, M., Granatiero, M., Zelante, L., Gasparini, P., Marzella, R., Rocchi, M. et al. (1998). Mutations of SURF-1 in Leigh disease associated with cytochrome c oxidase deficiency. Am J Hum Genet 63, 1609-21.

Towpik, J. (2005). Regulation of mitochondrial translation in yeast. Cell Mol Biol Lett 10, 571-94.

Trouillard, M., Meunier, B. and Rappaport, F. (2011). Questioning the functional relevance of mitochondrial supercomplexes by time-resolved analysis of the respiratory chain. Proc Natl Acad Sci U S A 108, E1027-34.

Tsukada, M. and Ohsumi, Y. (1993). Isolation and characterization of autophagy-defective mutants of Saccharomyces cerevisiae. FEBS Lett 333, 169-74.

Tsukihara, T., Aoyama, H., Yamashita, E., Tomizaki, T., Yamaguchi, H., Shinzawa-Itoh, K., Nakashima, R., Yaono, R. and Yoshikawa, S. (1995). Structures of metal sites of oxidized bovine heart cytochrome c oxidase at 2.8 A. Science 269, 1069-74.

Tsukihara, T., Aoyama, H., Yamashita, E., Tomizaki, T., Yamaguchi, H., Shinzawa-Itoh, K., Nakashima, R., Yaono, R. and Yoshikawa, S. (1996). The whole structure of the 13-subunit oxidized cytochrome c oxidase at 2.8 A. Science 272, 1136-44.

Valente, E. M., Abou-Sleiman, P. M., Caputo, V., Muqit, M. M., Harvey, K., Gispert, S., Ali, Z., Del Turco, D., Bentivoglio, A. R., Healy, D. G. et al. (2004). Hereditary early-onset Parkinson's disease caused by mutations in PINK1. Science 304, 1158-60.

van Loon, A. P. and Schatz, G. (1987). Transport of proteins to the mitochondrial intermembrane space: the 'sorting' domain of the cytochrome c1 presequence is a stop-transfer sequence specific for the mitochondrial inner membrane. EMBO J 6, 2441-8.

Velazquez, I. and Pardo, J. P. (2001). Kinetic characterization of the rotenone-insensitive internal NADH: ubiquinone oxidoreductase of mitochondria from Saccharomyces cerevisiae. Arch Biochem Biophys 389, 7-14.

Venditti, P., Di Stefano, L. and Di Meo, S. (2013). Mitochondrial metabolism of reactive oxygen species. Mitochondrion 13, 71-82.

Vergne, I. and Deretic, V. (2010). The role of PI3P phosphatases in the regulation of autophagy. FEBS Lett 584, 1313-8.

Vevea, J. D., Swayne, T. C., Boldogh, I. R. and Pon, L. A. (2014). Inheritance of the fittest mitochondria in yeast. Trends Cell Biol 24, 53-60.

Vogel, F., Bornhovd, C., Neupert, W. and Reichert, A. S. (2006). Dynamic subcompartmentalization of the mitochondrial inner membrane. J Cell Biol 175, 237-47.

Vogtle, F. N., Wortelkamp, S., Zahedi, R. P., Becker, D., Leidhold, C., Gevaert, K., Kellermann, J., Voos, W., Sickmann, A., Pfanner, N. et al. (2009). Global analysis of the mitochondrial N-proteome identifies a processing peptidase critical for protein stability. Cell 139, 428-39.

Vukotic, M., Oeljeklaus, S., Wiese, S., Vogtle, F. N., Meisinger, C., Meyer, H. E., Zieseniss, A., Katschinski, D. M., Jans, D. C., Jakobs, S. et al. (2012). Rcf1 mediates cytochrome oxidase assembly and respirasome formation, revealing heterogeneity of the enzyme complex. Cell Metab 15, 336-47.

Wallace, D. C. (2007). Why do we still have a maternally inherited mitochondrial DNA? Insights from evolutionary medicine. Annu Rev Biochem 76, 781-821.

Wang, K., Jin, M., Liu, X. and Klionsky, D. J. (2013). Proteolytic processing of Atg32 by the mitochondrial i-AAA protease Yme1 regulates mitophagy. Autophagy 9, 1828-36.

Watson, K. (1972). The organization of ribosomal granules within mitochondrial structures of aerobic and anaerobic cells of Saccharomyces cerevisae. J Cell Biol 55, 721-6.

Wei, H., Liu, L. and Chen, Q. (2015). Selective removal of mitochondria via mitophagy: distinct pathways for different mitochondrial stresses. Biochim Biophys Acta 1853, 2784-90.

Welter, E., Montino, M., Reinhold, R., Schlotterhose, P., Krick, R., Dudek, J., Rehling, P. and Thumm, M. (2013). Uth1 is a mitochondrial inner membrane protein dispensable for post-log-phase and rapamycin-induced mitophagy. FEBS J 280, 4970-82.

Wiedemann, N., Pfanner, N. and Rehling, P. (2006). Import of precursor proteins into isolated yeast mitochondria. Methods Mol Biol 313, 373-83.

Wielburski, A. and Nelson, B. D. (1983). Evidence for the sequential assembly of cytochrome oxidase subunits in rat liver mitochondria. Biochem J 212, 829-34.

Wittig, I., Braun, H. P. and Schagger, H. (2006). Blue native PAGE. Nat Protoc 1, 418-28.

Wittig, I., Karas, M. and Schagger, H. (2007). High resolution clear native electrophoresis for in-gel functional assays and fluorescence studies of membrane protein complexes. Mol Cell Proteomics 6, 1215-25.

Wittig, I. and Schagger, H. (2008). Structural organization of mitochondrial ATP synthase. Biochim Biophys Acta 1777, 592-8.

Wright, R. M., Dircks, L. K. and Poyton, R. O. (1986). Characterization of COX9, the nuclear gene encoding the yeast mitochondrial protein cytochrome c oxidase subunit VIIa. Subunit VIIa lacks a leader peptide and is an essential component of the holoenzyme. J Biol Chem 261, 17183-91.

Wrobel, L., Trojanowska, A., Sztolsztener, M. E. and Chacinska, A. (2013). Mitochondrial protein import: Mia40 facilitates Tim22 translocation into the inner membrane of mitochondria. Mol Biol Cell 24, 543-54.

Xie, Z., Nair, U. and Klionsky, D. J. (2008). Atg8 controls phagophore expansion during autophagosome formation. Mol Biol Cell 19, 3290-8.

Yaffe, M. P. and Schatz, G. (1984). Two nuclear mutations that block mitochondrial protein import in yeast. Proc Natl Acad Sci U S A 81, 4819-23.

Yamano, K. and Youle, R. J. (2013). PINK1 is degraded through the N-end rule pathway. Autophagy 9, 1758-69.

Yang, M., Jensen, R. E., Yaffe, M. P., Oppliger, W. and Schatz, G. (1988). Import of proteins into yeast mitochondria: the purified matrix processing protease contains two subunits which are encoded by the nuclear MAS1 and MAS2 genes. EMBO J 7, 3857-62.

Zerbes, R. M., van der Klei, I. J., Veenhuis, M., Pfanner, N., van der Laan, M. and Bohnert, M. (2012). Mitofilin complexes: conserved organizers of mitochondrial membrane architecture. Biol Chem 393, 1247-61.

Zhang, J. and Ney, P. A. (2008). NIX induces mitochondrial autophagy in reticulocytes. Autophagy 4, 354-6.

Zhang, M., Mileykovskaya, E. and Dowhan, W. (2002). Gluing the respiratory chain together. Cardiolipin is required for supercomplex formation in the inner mitochondrial membrane. J Biol Chem 277, 43553-6.

Zhang, M., Mileykovskaya, E. and Dowhan, W. (2005). Cardiolipin is essential for organization of complexes III and IV into a supercomplex in intact yeast mitochondria. J Biol Chem 280, 29403-8.

Zhang, Y., Qi, H., Taylor, R., Xu, W., Liu, L. F. and Jin, S. (2007b). The role of autophagy in mitochondria maintenance: characterization of mitochondrial functions in autophagy-deficient S. cerevisiae strains. Autophagy 3, 337-46.

Zhang, Y., Yang, Y. L., Sun, F., Cai, X., Qian, N., Yuan, Y., Wang, Z. X., Qi, Y., Xiao, J. X., Wang, X. Y. et al. (2007a). Clinical and molecular survey in 124 Chinese patients with Leigh or Leigh-like syndrome. J Inherit Metab Dis 30, 265.

Zhu, Z., Yao, J., Johns, T., Fu, K., De Bie, I., Macmillan, C., Cuthbert, A. P., Newbold, R. F., Wang, J., Chevrette, M. et al. (1998). SURF1, encoding a factor involved in the biogenesis of cytochrome c oxidase, is mutated in Leigh syndrome. Nat Genet 20, 337-43.

Zick, M., Rabl, R. and Reichert, A. S. (2009). Cristae formation-linking ultrastructure and function of mitochondria. Biochim Biophys Acta 1793, 5-19.

Acknowledgements

Curriculum vitae

PERSONAL INFORMATION

Name	Mariia Levchenko
Date of birth	01.11.1988
Place of birth	Kyiv, Ukraine

EDUCATION

PhD thesis at the Georg-August-University Göttingen, Germany Institute for Cellular Biochemistry. Supervisor Prof. Dr. Rehling	10/2011 – 12/2015
Master studies at the International Max Planck Research School International MSc/PhD Molecular Biology Program Georg-August-University Göttingen, Germany	10/2010 – 09/2011
BSc in Biology at the National Taras Shevchenko University, Kiev, Ukraine	09/2006 – 08/2010
Kyiv-Pechersk Lyceum № 171 "Leader", Kyiv, Ukraine	09/2002 - 08/2006

RESEARCH EXPERIENCE

PhD project at the Institute for Cellular Biochemistry, Göttingen, Germany. Supervisor Prof. Dr. Rehling. "Mitochondrial protein assemblies: Biogenesis of the cytochrome c oxidase and mitophagic signaling complexes"	10/2011 – 12/2015
Research internship at the Institute for Cellular Biochemistry. Supervisor Prof. Dr. Rehling. "Interaction of Tim21 and Tim50 at the mitochondrial presequence translocase".	05/2011 – 07/2011
Research internship at the Institute of Molecular Oncology. Supervisor Prof. Dr. Johnsen. "Histone H2B ubiquitination in DNA damage responce"	03/2011 – 05/2011

Research internship at the Institute of Microbiology and Genetics. Supervisor Prof. Dr. Braus. "α-Synuclein degradation in yeast model system of Parkinson's disease"	01/2011 – 03/2011
Research internship at the Middle East Technical University (METU), Ankara, Turkey. Supervisor Prof. Dr. Kurç. "Use of zeolites in glyceroloxidase amperometric biosensors"	02/2010 – 04/2010
Research internship at the Institute for Molecular Biology, Kiev, Ukraine. Supervisor Prof. Dr. Soldatkin. "Testing amperometric biosensors for industrial wine production"	09/2009 – 06/2010
Research internship at the Institute for Molecular Biology, Kiev, Ukraine. Supervisor Prof. Dr. Kordium "Microsatellite markers for PCR analysis of post-transplantation chimerism"	02/2009 – 09/2009
Research internship at the Institute for Molecular Biology, Kiev, Ukraine. Supervisor Prof. Dr. Telegeev. "Influence of BCR/Abl fusion proteins on course of Ph' leukemias"	09/2007 – 12/2008

SCIENTIFIC COMMUNICATION

FEBS-EMBO Symposium, Paris, France. Travel award from GGNB	2014
Biogenesis of Cellular Organelles Symposium, Bochum, Germany	2012 and 2014
Life Science Open Day, Weizmann Institute of Science, Rehovot, Israel	2012

SCHOLARSHIPS AND AWARDS

Boehringer-Ingelheim Fonds (BIF) fellow	2012-2014
Selected participant of the 64th Lindau Nobel Laureate meeting	2014
Stipend of the Excellence Foundation for the Promotion of the Max Planck Society	2010-2011
2nd award at the National Ukrainian Biology Olympiad	2006